1-1-2019

Groundwater transfer and injection pilot project: construction of a three dimensional groundwater flow model

Wesley Bluvstein

GROUNDWATER TRANSFER AND INJECTION PILOT PROJECT:

CONSTRUCTION OF A THREE DIMENSIONAL GROUNDWATER FLOW MODEL

A Thesis
Presented in partial fulfillment of requirements
for the degree of Master of Science
in the Department of Geology and Geological Engineering
The University of Mississippi

by

WESLEY J. BLUVSTEIN

August 2019

ABSTRACT

The Mississippi River Valley Alluvial Aquifer has experienced substantial groundwater declines in eastern Arkansas and northwest Mississippi due largely to irrigation for rice, corn, soybeans, and other water intensive crops. To alleviate groundwater decline and ensure future sustainability of water resources, the U.S. Department of Agriculture has, in conjunction with the U.S. Geological Survey and the University of Mississippi, initiated studies to determine potential avenues of remediation. Options include improved irrigation efficiency, installation of surface weirs, inter-basin transfers, and groundwater transfer and injection. This study develops a three-dimensional groundwater flow model of a withdrawal well adjacent to a river for a groundwater transfer and injection project. The numerical model is developed using Modflow Flex Visual 5.0 and utilized to assess the effect of varying hydrologic and geologic parameters on the local potentiometric surface. Assessing the potential for drawdown of the potentiometric surface and reduction of storage in the aquifer surrounding the withdrawal well is of particular importance. According to the model results, drawdown and reduction of storage are minimal in all cases. Changes in the river conductance and aquifer conductivity are the most substantial factors affecting the water table and resulting changes in storage.

LIST OF ABBREVIATIONS AND SYMBOLS

MRVAA	Mississippi River Valley Alluvial Aquifer
AMSL	Above mean sea level
GPM	Gallons per minute
GTIP	Groundwater Transfer and Injection Project
MAP	Mississippi Alluvial Plain
MAR	Managed Aquifer Recharge
ME	Mississippi Embayment
MERAS	Mississippi Embayment Regional Aquifer Study
USGS	United States Geological Survey
USDA	United States Department of Agriculture
ACE	Army Corps of Engineers

TABLE OF CONTENTS

LIST OF TABLES

LIST OF FIGURES

I. INTRODUCTION

Groundwater withdrawal in the Mississippi River Valley Alluvial Aquifer now exceeds that of the California Central Valley and is second in the United States only to the Ogallala Aquifer. Before 1988, maximum withdrawal was estimated to be 5,000 MGal/d (Ackerman, 1996), as of 2000 that figure has increased to 9,290 Mgal/d (Maupin and Barber, 2001). Resulting water level declines have been substantial, particularly in eastern Arkansas and northwest Mississippi where agriculture is most intensive. Twenty-year net change in groundwater levels show a roughly 0.3 - 0.5 meters per year (1 - 1.5 feet per year) decline in the Mississippi Delta region. Owing to the economic importance of agriculture in the Delta, groundwater withdrawals are expected to increase in the future. The USDA, with support from the USGS, Army Corps of Engineers (ACE), and UM, is studying potential alleviation of aquifer decline in the MRVAA (Barlow, 2011). Since changes in aquifer storage reflect the difference between inflows and outflows, this necessarily involves decreasing outflows (conservation) or increasing inflows (enhanced recharge). For the MRVAA, increasing recharge shows the most promise for alleviating groundwater level decline.

The USDA Agricultural Research Service, under National Program 211 (NP211), provides for a multitude of research projects investigating water availability and watershed management. The goal of the program is not only to examine the physical processes dictating water availability, but to develop novel or improved technologies for managing agricultural water resources. Under NP 211, the National Sedimentation Laboratory in Oxford, MS, is

conducting a groundwater withdrawal, transfer, and injection project (GTIP) in conjunction with the University of Mississippi (UM). The goal of the GTIP is to mitigate groundwater decline by injecting surface water directly to the water table, with the added caveat that the surface water is obtained from wells that induce flow through riverbank sediments, thus reducing cost and the need for treatment before injection. This is the first managed aquifer recharge (MAR) project of its kind and presents a potentially technologically efficient and economical solution to groundwater decline in the MRVAA.

While the goal is to maximize surface water capture through riverbank sediments, groundwater will also inevitably be withdrawn from storage in the surrounding aquifer. If 100% of the groundwater pumped is removed from storage to be piped some distance away and reinjected, then no enhancement of groundwater via surface water has truly occurred; that is to say groundwater has simply been moved from one area to another. To assess the likelihood or magnitude of this scenario, we develop a three-dimensional groundwater flow model of a withdrawal well adjacent to a major river. The model is constructed using observed geologic conditions near the withdrawal well and is calibrated using steady-state groundwater heads. Streambed conductance and aquifer properties are varied and the sensitivity of the overall source of the pumped water and the impact of pumping on the surrounding groundwater table are evaluated; the decrease in storage across the river from the pumping well and maximum head declines are determined for a variety of scenarios. This information is used to infer the ultimate source of the water and relative effectiveness of the well at inducing surface water through the riverbed bottom to be used for injection elsewhere.

II. BACKGROUND

1 Purpose and Scope

The overall goal of the GTIP is to assess the potential for direct injection wells to alleviate piezometric decline in the MRVAA. Other methods such as increased irrigation efficiency, low-head weirs, or inter-basin transfers may be viable in the Mississippi Delta as well but groundwater transfer and injection shows the most promise for reducing water level decline according to research that is pending publication by the USGS and USDA.

Withdrawal of source water from the banks of a river provides many advantages over the use of traditional surface water. Pre-filtration by the riverbank sediments reduces turbidity and sediment load, minimizing the need for treatment at the surface and clogging issues at the injection interface. However, excessive abstraction from the withdrawal well could lower the groundwater surface across the river, negatively impacting users and property owners. The purpose of constructing a three-dimensional groundwater flow model of a withdrawal site is to evaluate this potential impact and quantify allowable pumping rates and durations.

2 Managed Aquifer Recharge

The practice of enhancing recharge has been performed across the world (Maliva, 2014; Prathapar, 2015; Sprenger, 2017) with varying degrees of success, depending on political and social support and proper system design and hydrogeologic understanding. There are multiple existing methods to enhance infiltration of water through the subsurface. Drainage basins, such

as the one shown on the left-hand side of Figure 1, are the simplest and cheapest option. Due to that, they are by far the most common systems utilized (Bouwer, 2002). They function by impounding surface water in order to increase percolation time. These systems can be built on or off of existing stream channels and work best where sediments between the surface and the water table are highly transmissive. Occasionally, mounding of the local water table (Figure 1) can occur to the degree where it reduces the head difference between the surface impoundment and the groundwater table and reduces infiltration. Recharge trenches and vadose zone wells, displayed on the right-hand side of Figure 1, can be used when fine-grained sediments in the shallow subsurface (up to 5 meters or 16.5 feet) impede the flow of water downward. The trench or shallow well is constructed to a depth beyond the confining layer (the hatched area at the surface of the well picture in Figure 1) where sediments are more transmissive and flow is not impeded. Both systems will eventually clog with sediments as the suspended sediment load of the infiltration water is filtered and trapped by the subsurface media (Bouwer, 2002).

Where suitable sediments or sufficient land area are not available, direct injection wells can be used. Whereas vadose zone wells are screened in the unsaturated portion of the subsurface, direct injection wells are screened in saturated intervals to allow injection of water directly into aquifer storage. In the MRVAA, where there are extensive fine-grained deposits that inhibit downward percolation of surface water, direction aquifer injection is a favorable solution. Unlike vadose zone wells, direct injection wells can be backwashed to prevent or reduce clogging. However, they require a sufficiently transmissive aquifer to prevent excess pressure buildup or mounding of the groundwater surface and do not provide any pretreatment of injected water in the vadose zone (Bouwer, 2002). Clogging of the subsurface interface in basins, trenches, and wells is the bane of any MAR system (Bouwer, 2002).

Infiltration of surface water through riverbank sediments does pose its own unique management challenges. Depending on the hydrogeologic parameters of the riverbank sediments, surrounding aquifer material, and the surface water flow dynamics, a multitude of flow conditions can be observed at bank filtration sites. Figure 2 illustrates some of the various hydraulic situations encountered. Groundwater flow beneath the river is typically neglected at most sites depending on the well construction and is usually not desirable according to the project goals.

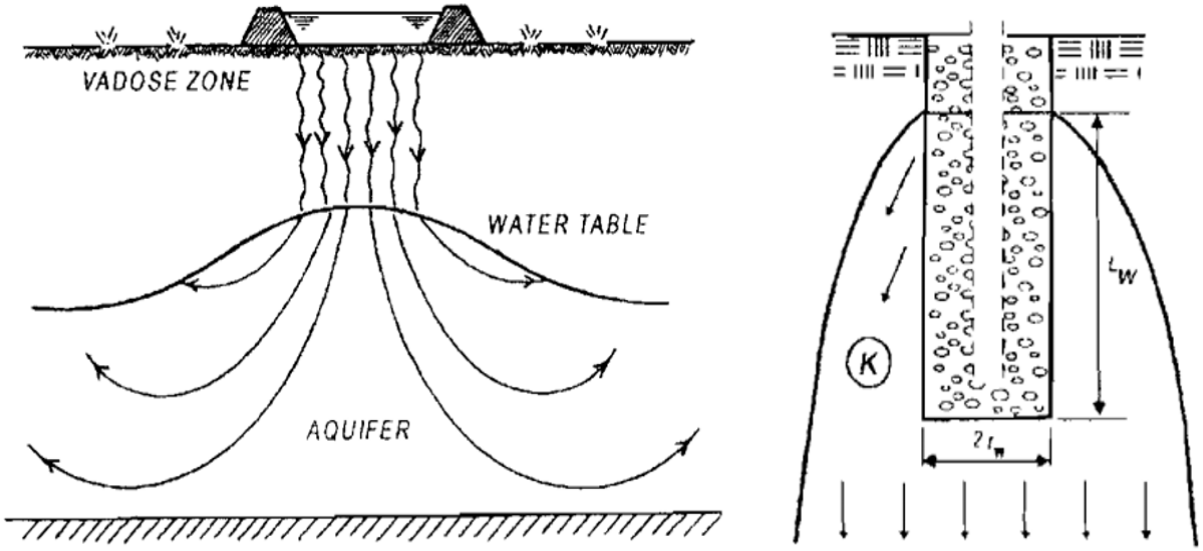

Figure 1: Managed Aquifer Recharge. Left, cross sectional view of a surface infiltration recharge system with corresponding groundwater mound in the underlying water table. Right, a vadose-zone recharge well, where arrows represent direction of groundwater flow. From Bouwer, 2002.

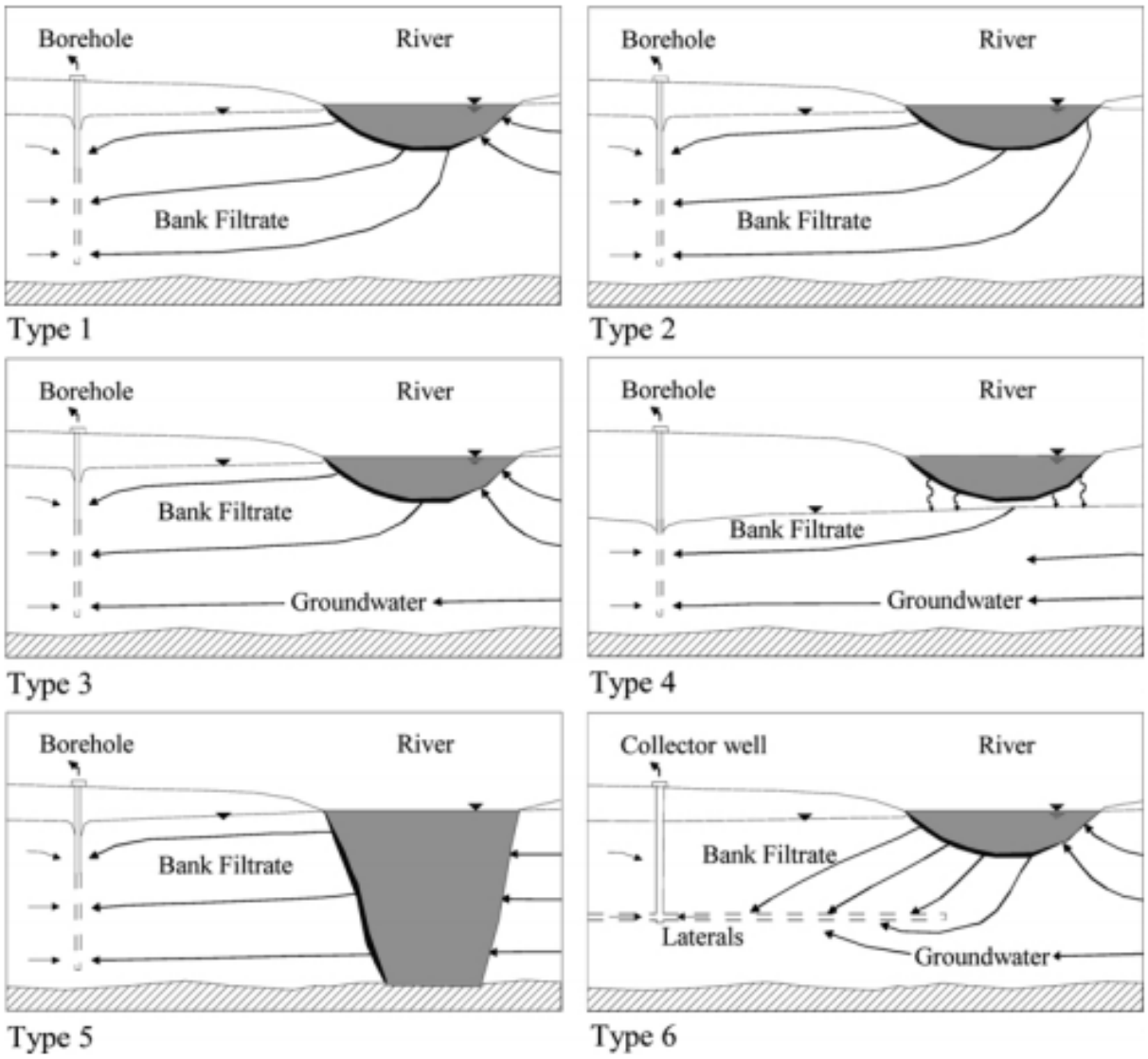

Figure 2: Bank Filtration Site Types. Cross sectional representation of various flow regimes for a bank filtration well. From Hiscock and Grischek, 2002.

The majority of bank filtration wells are Type 1 conditions (Figure 2) (Hoscock and Grischek, 2002). Discharged water is sourced from bank storage and induced surface water filtration with a colmation layer predominately facing the portion of the streambed with the abstraction well. Formation of a colmation layer in the river bed can reduce hydraulic conductivity due to filtration of sediments, formation of gases, and geochemical

precipitation (Hiscock and Grischek, 2002). Ideally the areal extent and thickness of any colmation layer is minimized, and Type 2 conditions (Figure 2) can contribute negatively to the surface ecology via reduction of streamflow. In a Type 4 situation (Figure 2), excessive drawdown creates an unsaturated zone between the bottom of the hyporheic zone (where surface water and groundwater mix) and the water table, lowering infiltration rates and potentially inducing groundwater decline on the bank adjacent to the withdrawal well. Type 5 conditions (Figure 2) are only observed when the surface water body incises into impermeable material, and Type 6 (Figure 2) involves a well construction using horizontal collectors.

The overall amount of water available to a withdrawal well is thus dependent on the dynamics of the colmation layer as well as the catchment and infiltration zones, flow paths, and flow velocities of the filtrate. Water level measurements are commonly used to interpret these conditions for the purposes of numerical modelling.

3 Geologic Setting

A substantial amount of previous research on the MRVAA and the Mississippi Embayment (ME) has been performed to date. Initial large-scale studies by Ackerman and Sumner have been performed to investigate its geologic history, lithology, and hydraulic properties.

The Mississippi Embayment is a structural syncline plunging southward from an apex at the southern tip of Illinois, with a hinge line approximately parallel to the Mississippi River (Van Arsdale, 2002). It contains roughly 1.5 kilometers (0.9 miles) of sediments that began depositing in the mid-cretaceous. Underlying these strata is the early Paleozoic Mississippi Valley graben fault complex (Van Arsdale, 2002).

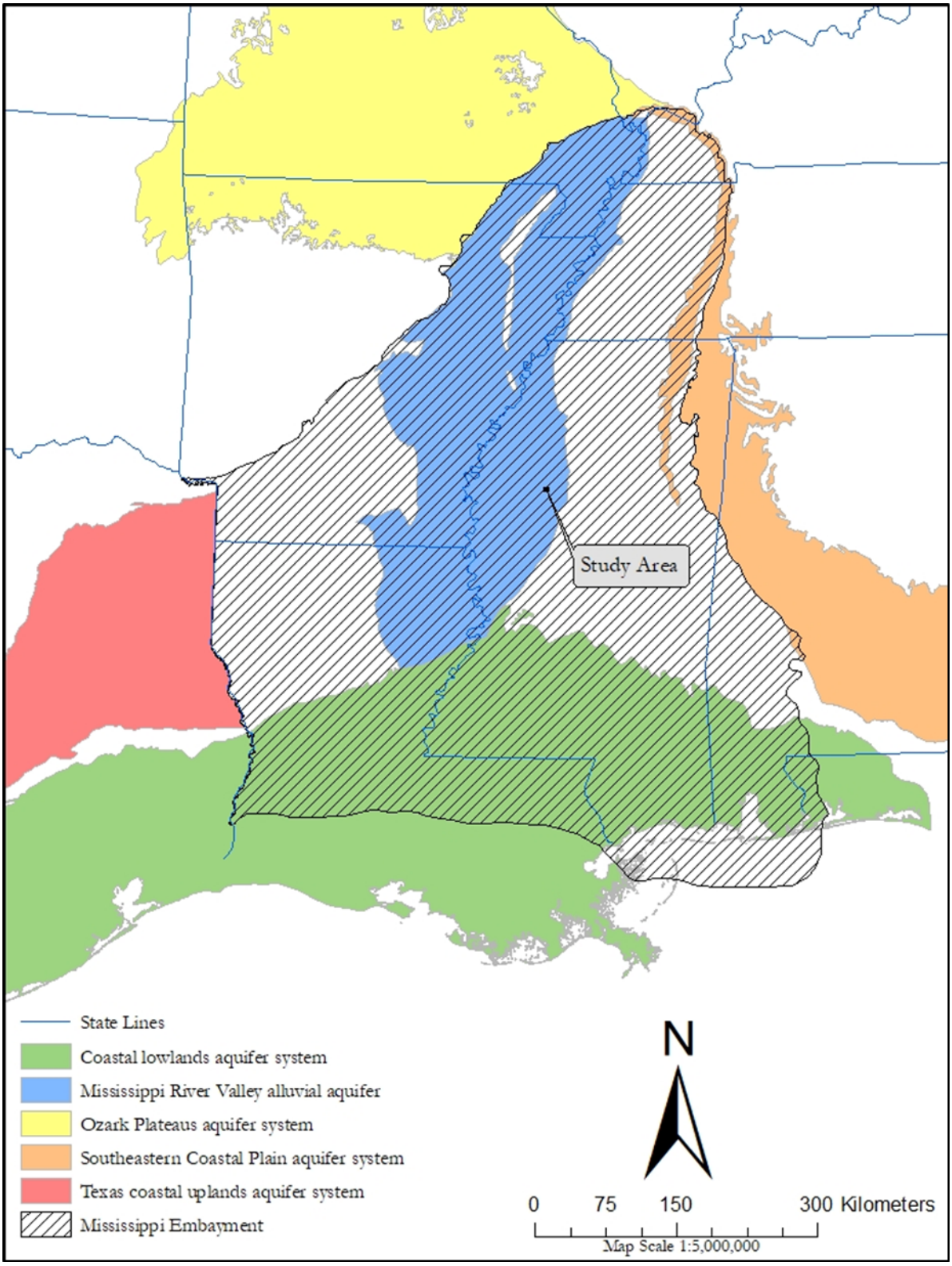

Figure 3: Mississippi Embayment and Regional Aquifers.

The embayment, delineated by the hatched area in Figure 3, likely formed as a result of subsidence after crustal uplifting of the weakened Mississippi Valley graben due to passage over the Bermuda hotspot mantle plume in the mid-Cretaceous (Van Arsdale, 2002). The land was uplifted roughly 1 - 3 kilometers (0.6 - 1.9 miles) and eroded. After passing the mantle plume, the crust subsided and the eroded land became a trough which filled with sediment sequences from marine and deltaic depositional environments that were emplaced by repeated transgression and regression of the coastline throughout the Cretaceous and Tertiary Periods (Clark and Hart, 2009). The Quaternary MRVAA alluvial sediments are fluvial in origin and lie unconformably on the formations of the underlying ME (Van Arsdale, 2002; Clark & Hart, 2009).

The infilling fluvial sediments of the ME were deposited by the Mississippi River via erosional and depositional processes related to glaciation, forming a coarse grained base for the current day MRVAA that fines upward as the glaciers waned and the ancestral Mississippi changed from a braided to a meandering river (Renken, 1998).

The uppermost fine-grained cap to the MRVAA ranges from 8 - 45 meters (25 - 150 feet) thick but is locally absent in places (Figure 4). The total thickness of the Quaternary-aged MRVAA sediments is observed to be roughly 18 - 43 meters (60 - 140 feet), thinning towards the western and eastern margins where the formations of the ME dip upwards and form the lateral boundaries of the aquifer. The southward portion of the aquifer merges with the Coastal Lowlands Aquifer System along low-lying areas of the Gulf (Renken, 1998), where it extends into the bird-foot delta of southern Louisiana (Figure 3).

The USDA Groundwater and Transfer Injection Project will take place in the alluvial floodplain sediments of the Mississippi River in northwest Mississippi, known locally as the Delta. The MRVAA in the region extends from the Mississippi-Tennessee border southwards to

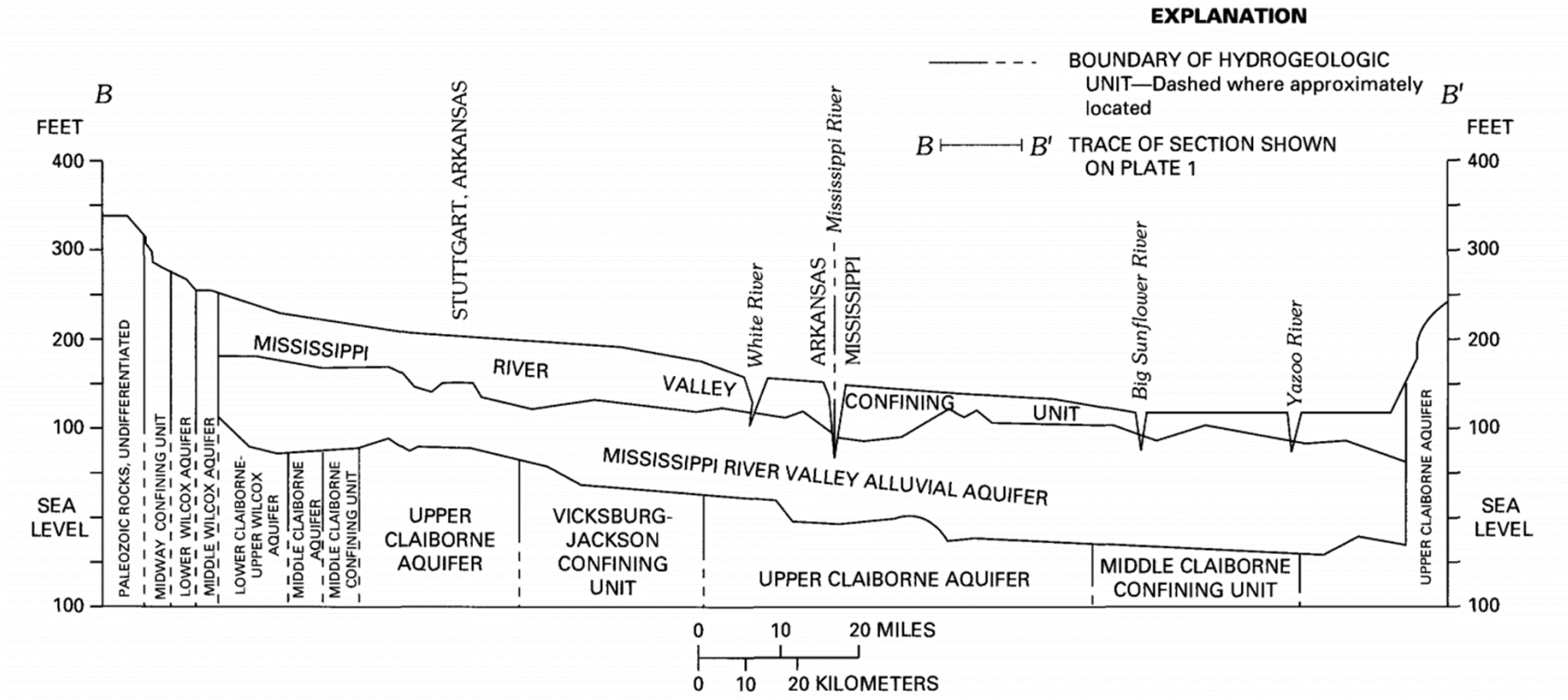

Figure 4: General stratigraphy of the MRVAA. Shows incision by major rivers through the confining unit as well as topographical variation of the top and base of the aquifer (From Ackerman, 1996). Vertical relief is greatly exaggerated.

Vicksburg, a distance of roughly 320 kilometers (200 miles), and from the Mississippi River in the west to the loessial Bluff Hills in the East.

The surface topography is relatively flat with a slope of 10 centimeters per kilometer (0.5 feet per mile) trending north-south (Renken, 1998) and east-west towards the Sunflower River basin in the central Delta, which is shown in Figure 4. The transition to the Bluff Hills in the east is dramatic and represents a significant transition in geology as well as a 30 - 60 meter (100 - 200-feet) rise in land surface (Ackerman, 1996).

Aquifer thickness in the delta averages 40 meters (135 feet) (Figure 4) although it has been observed to be greater than 60 meters (200 feet) in places (Fisk, 1951). The coarse-grained base of the alluvium locally tends to be thickest where the total aquifer thickness is greatest and these locations likely represent the infilling of Tertiary aged river valley systems (Arthur, 2001). Except where influenced by ancient topography, the alluvium generally thickens towards the center of the MRVAA and underlying ME syncline.

The topstratum of the MRVAA (Mississipi River Valley Confining Unit of Figure 4) is a combination of finer-grained silts and clays that were deposited by the Mississippi after its transition to a meandering river. Within the topstratum are found numerous remnants of historic river activity such as clay plugs and lenses, backwater deposits, natural levees, point bars, and crevasse splays (Ackerman, 1996; Arthur, 2001). The topstratum serves as a hydraulic confining unit for the aquifer and is present over roughly 99% of the MRVAA surface area (Arthur, 2001).

4 Hydrogeologic Overview

Groundwater resources are found in several surficial aquifers of the MAP as well as the underlying Mississippi Embayment (Clark, 2011). The most prolific of these surficial aquifers is the Mississippi River Valley Alluvial Aquifer, but the Arkansas, Red, and Ouachita-Saline River Alluvial Aquifers produce locally important sources of groundwater (Renken, 1998). The nature and characterization of the MRVAA is complex due to its layered nature, fine-grained cap, complicated bottom and lateral boundaries with the various formations of the Mississippi Embayment and Coastal Lowlands Aquifer Systems, and extensive interaction with surface waters where they have incised into permeable material.

The natural or pre-anthropogenic hydraulic regime has been significantly altered since the introduction and growth of agriculture to the region and, as with most depleting aquifers, the invention of the submersible centrifugal pump in the mid-1960s by Poul Due Jensen.

The Mississippi Delta has a moderate, subhumid climate that ranges in average annual temperature from 62° F (17° C) near Memphis to 66° F (19° C) near Vicksburg. Precipitation averages about 132 centimeters (52 inches) annually and generally is highest in the winter and spring seasons (Sumner, 1984).

The MRVAA and underlying ME formations in the Delta (notably the Upper and Middle Claiborne aquifer, shown in Figures 4 and 5) are in partial hydraulic connection depending on local lithology (Arthur, 2001; Renken, 1998). Where there are fine-grained sediments at the ME/MRVAA interface there is little to no hydraulic connection. Such a fine-grained barrier could be the base of the fluvial sediments or the top of an underlying silty or clayey embayment formation but in either case will impede groundwater flow. Where the base of the alluvium is coarse, it is in connection with the permeable formations of the ME (Arthur, 2001; Ackerman,

1996). While the sediments of the MRVAA have been deposited roughly horizontally, they lie unconformably on top of the ME sediments which dip at 3 - 8 meters per kilometer (15 - 40 feet per mile) to the west in Mississippi (illustrated in Figure 5).

The hydraulic properties of an aquifer include its specific storage or yield, hydraulic conductivity, and transmissivity (which is dependent on saturated thickness). Estimates of hydraulic properties from pumping tests are not very numerous but an evaluation of those performed to date by Slack and Darden (1991) give a range of storage coefficient values from 0.0003 to 0.016 depending on confinement, transmissivity from 1,000 - 5,000 meters squared per day (12,000 - 15,000 feet squared per day), and hydraulic conductivity from 40 - 122 meters per day (130 - 400 feet per day).

USGS studies of the alluvium by Ackerman (1996) indicate a hydraulic conductivity of roughly 70 meters per day (200 feet per day) and a highly variable storage coefficient of 0.0001 to 0.30 depending on confined and unconfined conditions, respectively. In constructing a groundwater flow model of the MRVAA, Arthur (2001) derived calibrated parameters of 130 meters per day (425 feet per day) for hydraulic conductivity and a storage coefficient and specific yield of 0.016 and 0.32, respectively.

Saturated thickness varies with water level in areas where the potentiometric surface has dropped below the confining cap but the average thickness of suitable aquifer material in the Delta is 34 meters (110 feet) (Arthur, 2001). Wells commonly produce over 500 gallons per minute (GPM), and can reach up to 2,500 GPM where the aquifer is thickest and most transmissive (Arthur, 2001).

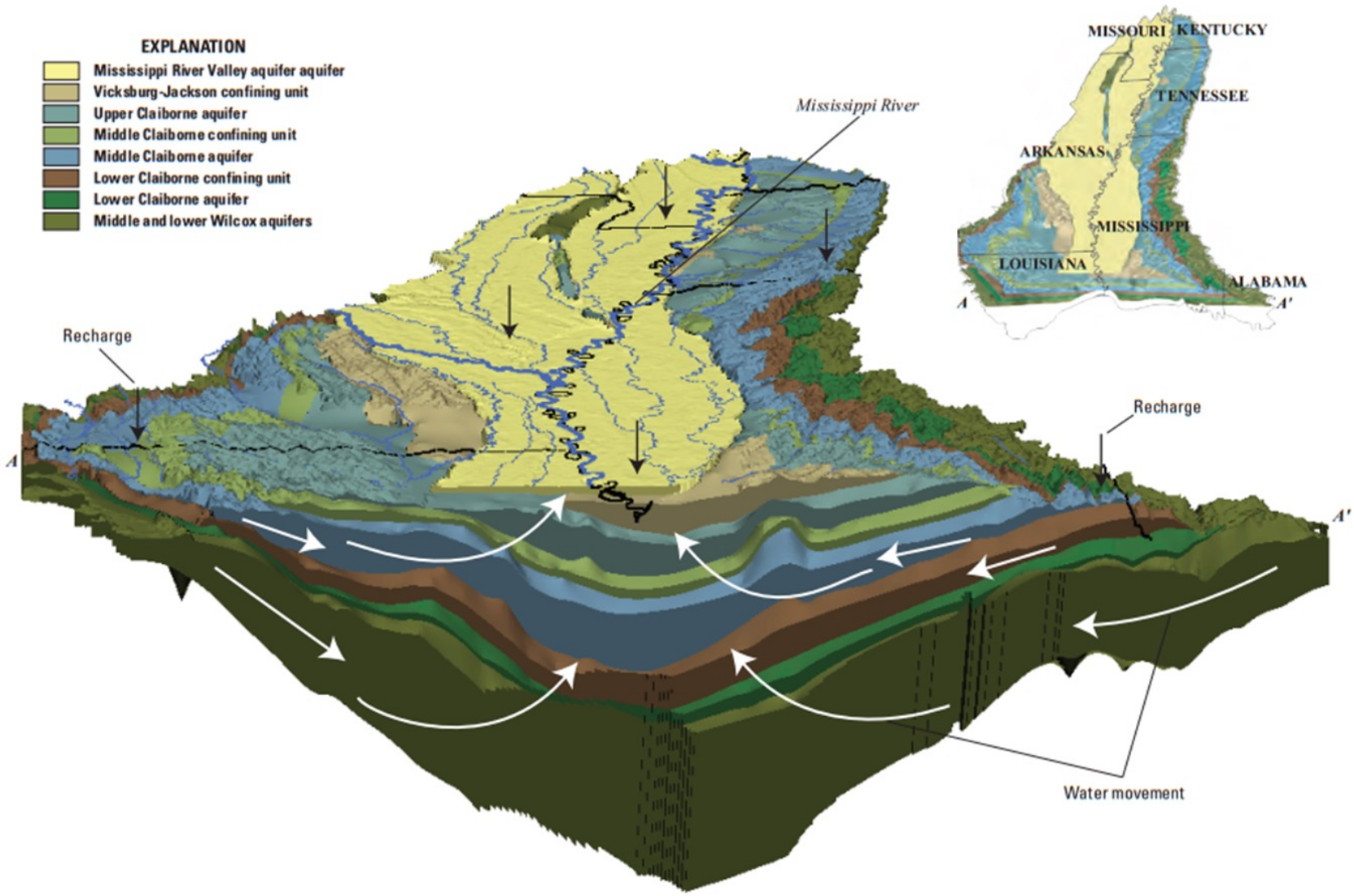

Figure 5: Hydrogeology and structure of the Mississippi Embayment. From Clark & Hart, 2009.

The predevelopment regional groundwater flow of the MRVAA in general was southwest and parallel to the river itself (Figure 6). Local groundwater flow was towards major drainage basins and followed surface topography (Sumner, 1984). In the Delta this meant that water flowed from the variable head boundary of the Mississippi river on the west and the topographically higher Bluff Hills on the east towards the center of the Delta (Figure 6). Water levels were generally less than 6 meters (20 feet) below ground level (Renken, 1998). The regional groundwater flow of the MRVAA and underlying embayment also had a southward component to it due to the dip of the embayment axis to the south. This means that water in general flowed radially towards the embayment axis while also flowing southward. However, groundwater pumping has altered regional flow patterns to some degree (Figure 7) (Renken, 1998). The average water-level decline in the Mississippi Delta area of the MRVAA as of 1996 ranged from 6 - 12 meters (20 - 40 feet) (Arthur, 2001).

The Mississippi River generally fully incises into the Quaternary sediments of the MRVAA and acts as a groundwater divide, causing the aquifer to behave independently to the east and west of the river (Arthur, 2001; Renken, 1998). The highly variable stage of the river means that it acts as a variable head boundary on the west side of the Delta, and net flux into and out of the aquifer from the river is probably small compared to other sources (Renken, 1998; Arthur, 2001). The upper boundary of the aquifer, the clay confining unit, serves as a relatively impermeable barrier to vertical flow and creates confined conditions in much of the Delta, although this is decreasing with continued groundwater decline.

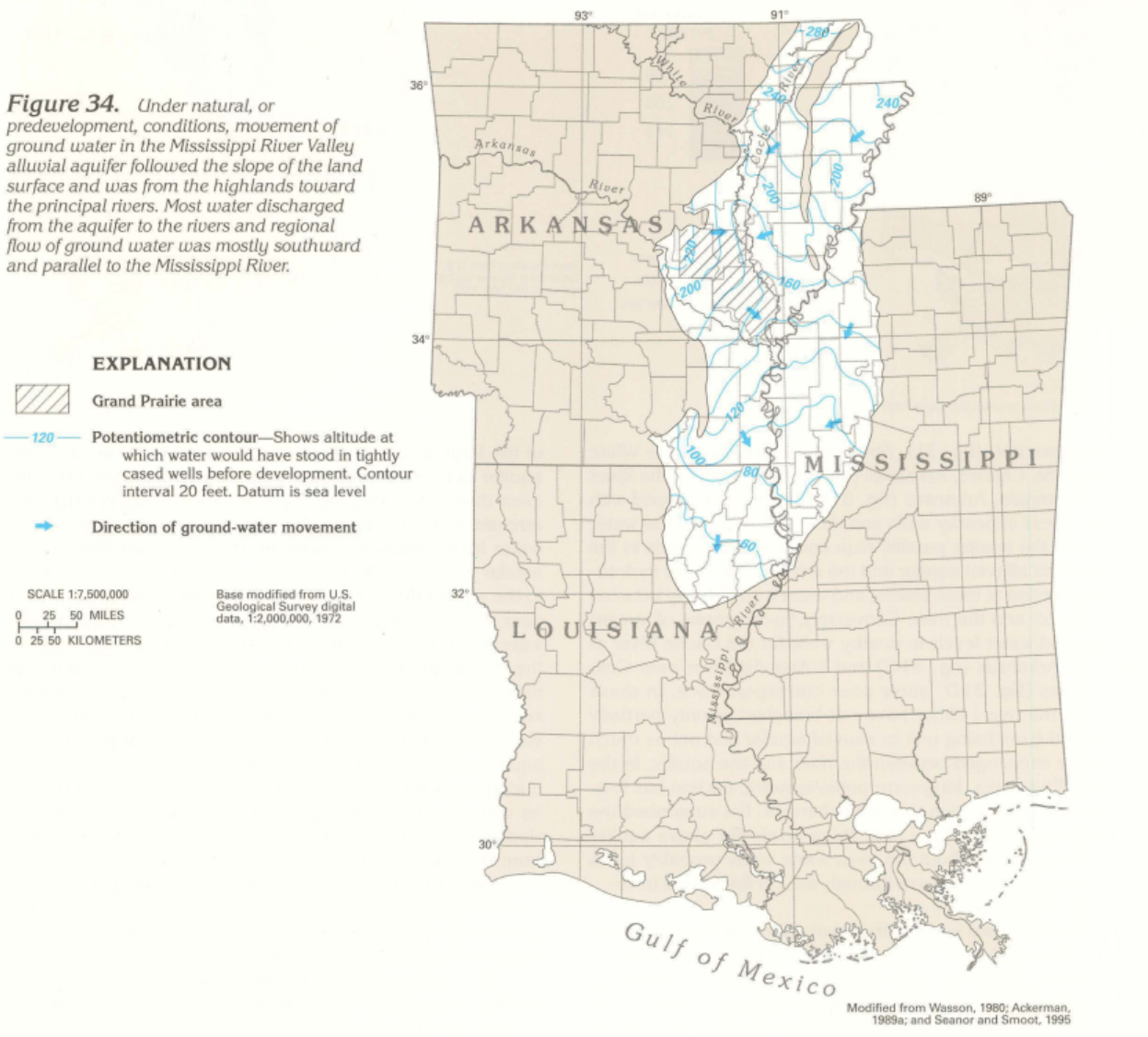

Figure 6: Regional flow patterns and heads of predevelopment MRVAA. From Renken, 1998.

Recharge to the MRVAA in the Delta region is predominately from percolation of precipitation, which ranges from 100 - 175 centimeters (40 - 68 inches) annually, but a portion also comes from the underlying aquifer units of the ME and laterally from aquifers that directly underlie the Bluff Hills, as well as an increasing amount from surface water bodies when hydraulic conditions permit (Renken, 1998, Arthur, 2001).

Estimates of recharge from percolation through the confining topstratum range from 1.25 - 2.5 centimeters per year (0.5 - 1.0 inches per year) (Ackerman, 1996; Renken, 1998). This accounts for roughly 75% of total recharge to the aquifer, with the remaining coming from underlying, lateral, and surface water inflows. With continued water level declines, some rivers such as the Big Sunflower in Mississippi have turned from sources of discharge to perennial sources of recharge as the water table remains below the streambed year round (Renken, 1998).

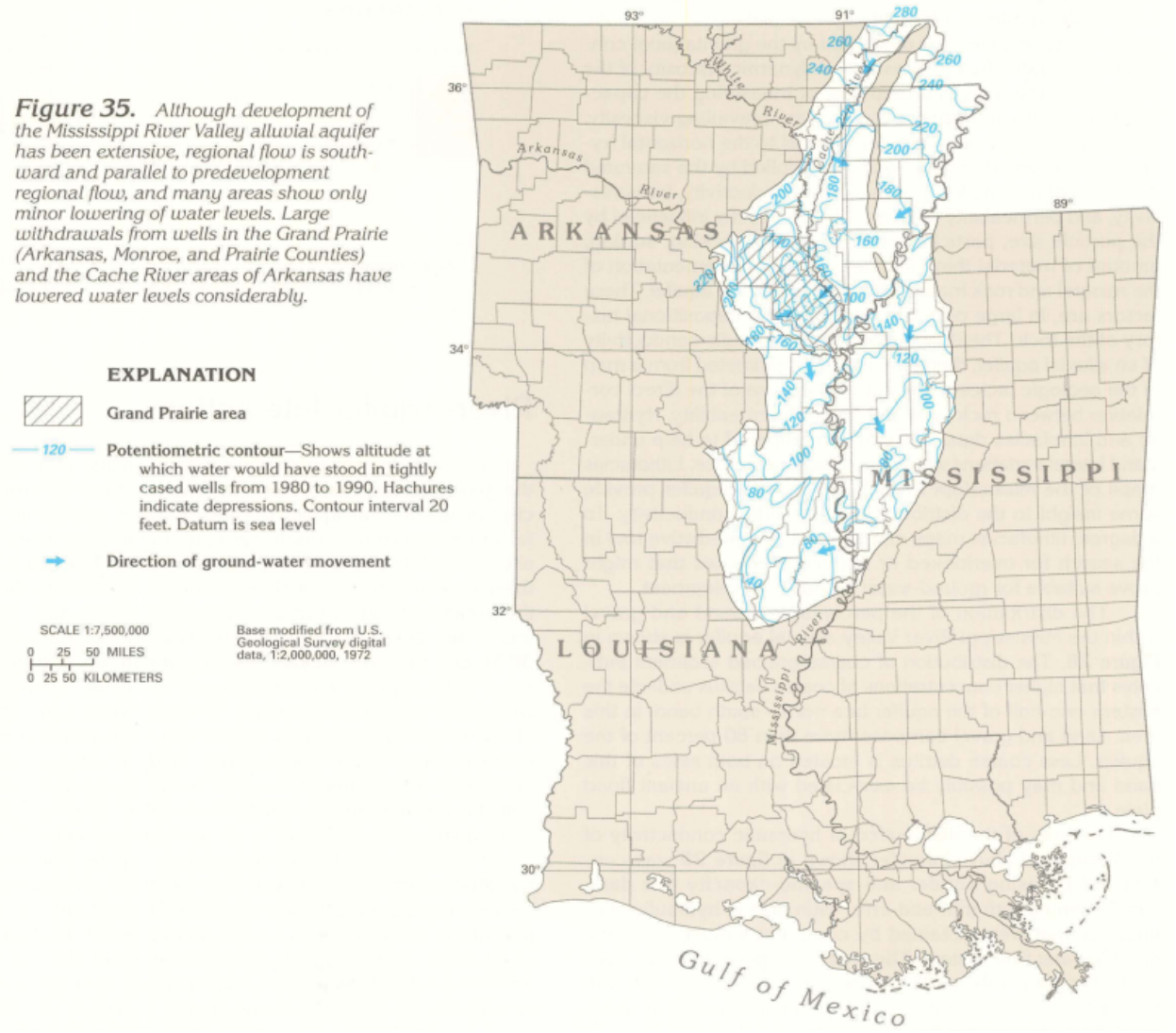

Figure 7: Regional groundwater flow from 1980-1990. From Renken 1998.

III. METHODS

1 Mathematical Representation

There exists a substantial amount of published literature regarding the construction of groundwater models (Harbaugh, 2005; Barlow, 2006; Freeze, 1971; Freeze, 1966; Freeze, 1967; Freeze, 1968; McDonald, 1984; Toth, 1970). First published in 1984, MODFLOW is a three-dimensional, finite-difference groundwater model published by the USGS that simulates steady state and transient flow in confined or unconfined aquifers. The three-dimensional movement of water through a porous medium is described using the partial-differential equation below:

$$\frac{\partial}{\partial x}\left(K_{xx}\frac{\partial h}{\partial x}\right)+\frac{\partial}{\partial y}\left(K_{yy}\frac{\partial h}{\partial y}\right)+\frac{\partial}{\partial z}\left(K_{zz}\frac{\partial h}{\partial z}\right)+W=S_s\frac{\partial h}{\partial t} \qquad (1\text{-}0)$$

Where,

Kxx, Kyy, and Kzz represent hydraulic conductivity along the x, y, and z coordinate axes, which are parallel to the major axes of hydraulic conductivity (L/T);

h is the potentiometric head (L);

W is a volumetric flux per unit volume representing sources and/or sinks of water, with W<0.0 for flow out of the ground-water system (T^{-1});

Ss is the specific storage of the porous material (L^{-1}); and

t is time (T).

This equation together with specified initial and boundary conditions compose a mathematical representation of groundwater flow (Harbaugh, 2005). Analytical solutions of the flow equation are not usually possible except in very simple systems so the heads at a given time and location are solved for using an approximation process. One such process is the finite-difference method, wherein the continuous equation 1-0 is replaced by a finite set of discrete points in space and time. This process yields simultaneous linear algebraic difference equations, which can be solved for head values at the specified time and location (Harbaugh, 2005). Due to the modularity of its design, a number of additional packages and processes have been created to simulate stresses such as wells, recharge, evapotranspiration, and gains or losses to surface waters among others.

2 Conceptual and Numerical Model

The purpose of this groundwater flow model is to evaluate potential drawdown effects from a withdrawal well adjacent to a river on the local potentiometric surface. Utilizing MODFLOW Flex Version 5.0, a three-dimensional numerical representation is constructed to simulate this situation. The model domain is centered on the withdrawal well with no flow boundaries on the North and South edges and constant head boundaries on the East and West (Figure 8). The no flow boundaries trace a groundwater flowline such that there is no flow across the boundary into or out of the model domain. The constant head boundaries follow potentiometric head contours of equal elevation as determined from interpolated USGS groundwater gage data on October 1st of 2018 (Figures 8 and 17). The bottom surface of the model is a no-flow boundary with the underlying ME. Uniform recharge is applied to the land surface across the domain.

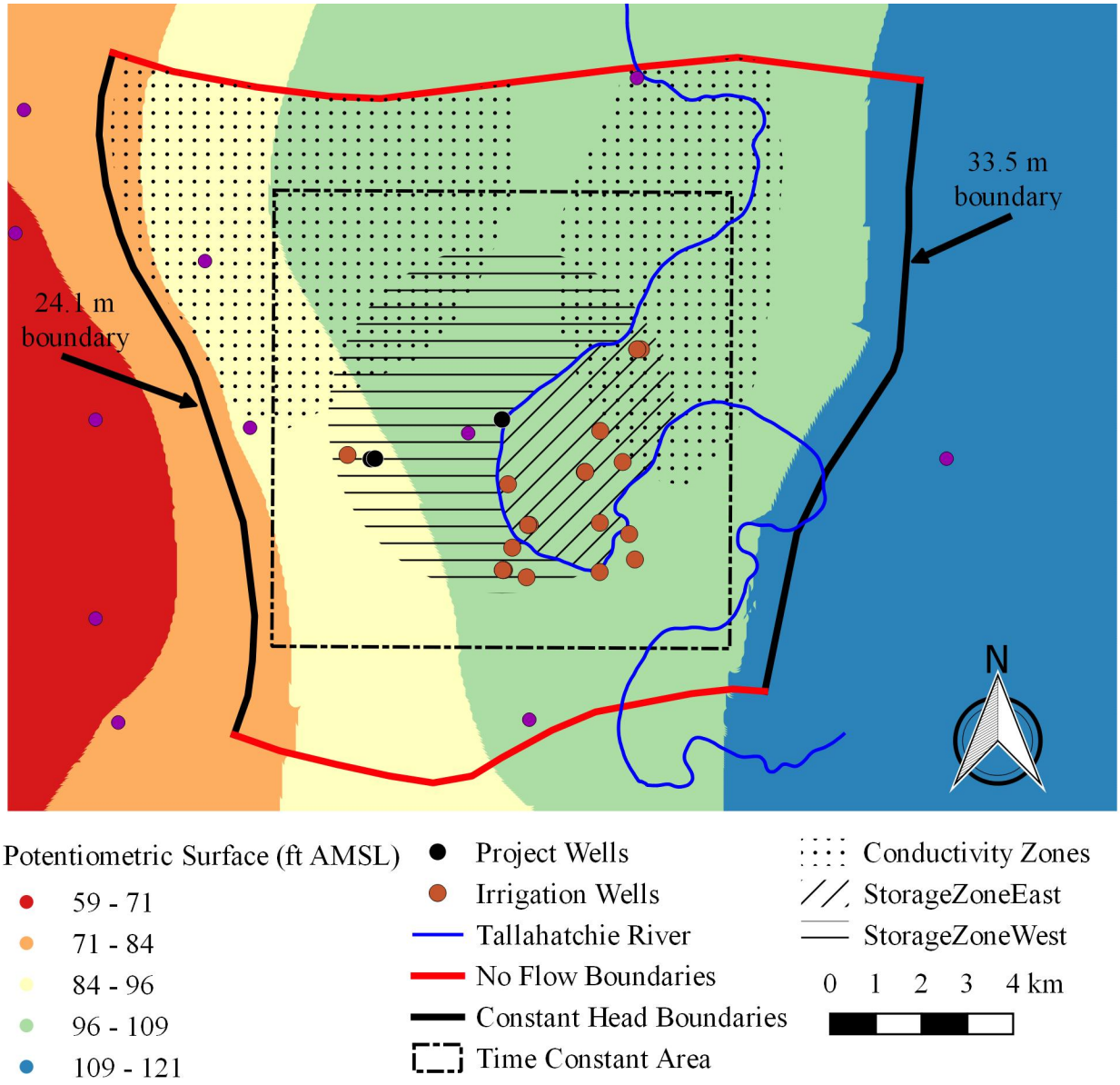

Figure 8: Model domain, boundaries, and parameters. Set against the initial interpreted potentiometric surface from USGS gage data in October of 2018.

Model domain edges are beyond the minimum distance required for the boundary conditions to substantially influence groundwater levels at the withdrawal well for the given pumping duration of 60 days. This is determined from the characteristic time-constant, τ, of the

aquifer utilizing maximum hydraulic properties for propagation of disturbances to the potentiometric surface (Gelhar, 1974).

$$\tau = \frac{SL^2}{\beta bk} \tag{2-0}$$

Where,

S is the storage coefficient (-) (0.2 from Clark & Hart, 2009)

L is the length of the aquifer (L) (value obtained from chart)

β is a geometry term (-) (3 from Gelhar, 1974)

b is the saturated thickness (L) (75 meters from Clark & Hart, 2009)

K is the hydraulic conductivity (L/T) (175 meters/day from Clark & Hart, 2009)

Conceptually, the time constant (τ) is related to the half-life of an exponentially decaying system and represents the time required for the system to reach ~63% of its steady-state value. A plot of the characteristic time constant versus length for the MRVAA in the study area is shown in Figure 9.

The duration of pumping for this project is 60 days. This value is doubled to 120 days, and equation 1 is solved for the minimum distance of the model boundaries (4,800 meters or 15,700 feet). This is the distance seen in Figure 8 from the pumping well in the center of the domain to the nearest point on model boundary.

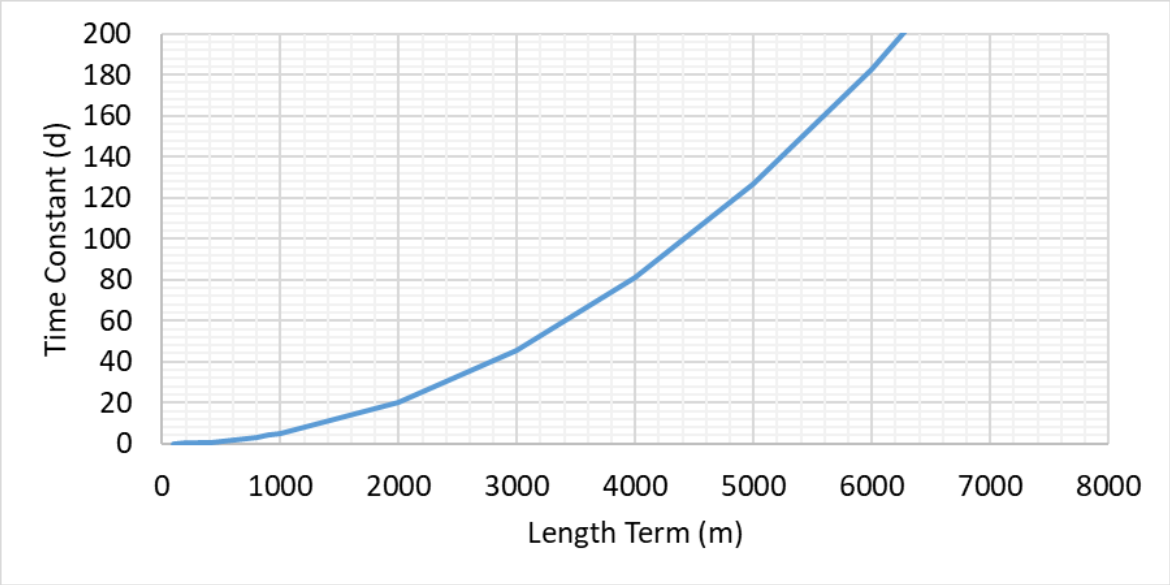

Figure 9: Time constant versus length plot for the MRVAA.

As a result of the inherent assumptions of the groundwater flow equation, namely constant density and laminar flow, there are limitations to the MODFLOW-2005 code. The numerical approximation process for solving the governing partial differential equations also introduces error to the head estimation process. This error is quantified and discussed in the results to assess model accuracy (Figure 18).

3 Sources and Interpretation of Data

The land surface for the model domain is a 10 meter (33 feet) DEM downloaded from the Mississippi Automated Resource Information System (MARIS) for Leflore County, MS (Figure 10). Geologic structure of the MRVAA, including the base of the aquifer and confining unit, is from USGS geophysical investigations of the site area in December of 2018. This data was provided in an ASCII format to be imported into Visual MODFLOW Flex. Contour maps of the geologic structure for the top and bottom aquifer surfaces are seen in Figures 11 and 12.

The polyline used to represent the river in the model domain was obtained from the USGS National Hydrography Dataset (NHD). Stage and elevation data was downloaded from USGS stream gage No. 07281600 at Money, MS (Figure 13). Groundwater levels were obtained from the USGS National Water Information System (NWIS) of both active and inactive groundwater monitoring sites. Initial heads are constructed from water levels in October of 2018 and checked for normality and detrended according to equation (3-0) (figures 14 and 15). They were subsequently fit to a variogram (Figure 16) and kriged (figure 17) in the open-source geostatistical software package SGeMS.

$$Y_2 = \beta_1 + \beta_2 * X + \beta_3 * Y + \beta_4 * X * Y \quad (3\text{-}0)$$

Where the beta values are equal to;

$$\beta = \begin{pmatrix} 78.819 \\ 1.66 \times 10^{-3} \\ -4.027 \times 10^{-4} \\ 4.671 \times 10^{-9} \end{pmatrix}$$

And,

Y_2 is the residual elevation value for the given data point;

$B_{1\text{-}4}$ are the beta weighting values;

X is x-coordinate of the data point; and

Y is the y-coordinate of the data point

Hydraulic conductivity for the MRVAA confining unit in the vertical (z-axis) direction are from D.J. Ackerman's 1996 study of the hydrology of the Mississippi River Valley Alluvial Aquifer (Table 1). The horizontal conductivity values are a factor of 10 greater, according to

published literature regarding typical anisotropy for clay formations (Freeze & Cherry, 1979). Confining unit specific storage is from D.M. Sumner and B.E. Wasson's 1990 paper on the geohydrology of the MRVAA in the Mississippi delta region. Specific yield, effective porosity, and total porosity are assumed reasonable values for the lithology according to published literature (Table 1) (Freeze & Cherry, 1979).

Hydraulic conductivity for the MRVAA is assumed to be isotropic and taken from an analysis of pumping tests on the aquifer, as is the value for specific storage (Table 1) (Slack & Darden, 1991). The specific yield is from Sumner & Wasson, 1990. Effective and total porosities are assumed reasonable values from published literature on the given lithology (Freeze & Cherry, 1979).

Property Zone	K_x (m/s)	K_y (m/s)	K_z (m/s)	Specific Storage (S_s)	Specific Yield (S_y)	Effective Porosity (n_e)	Total Porosity (n)
Confining Unit	2.39 E-8	2.39 E-8	2.39 E-9	5.0 E-4	0.35	0.39	0.40
MRVAA	9.34 E-4	9.34 E-4	9.34 E-4	3.0 E-4	0.32	0.33	0.35

Table 1: Hydraulic properties for the confining unit and underlying aquifer.

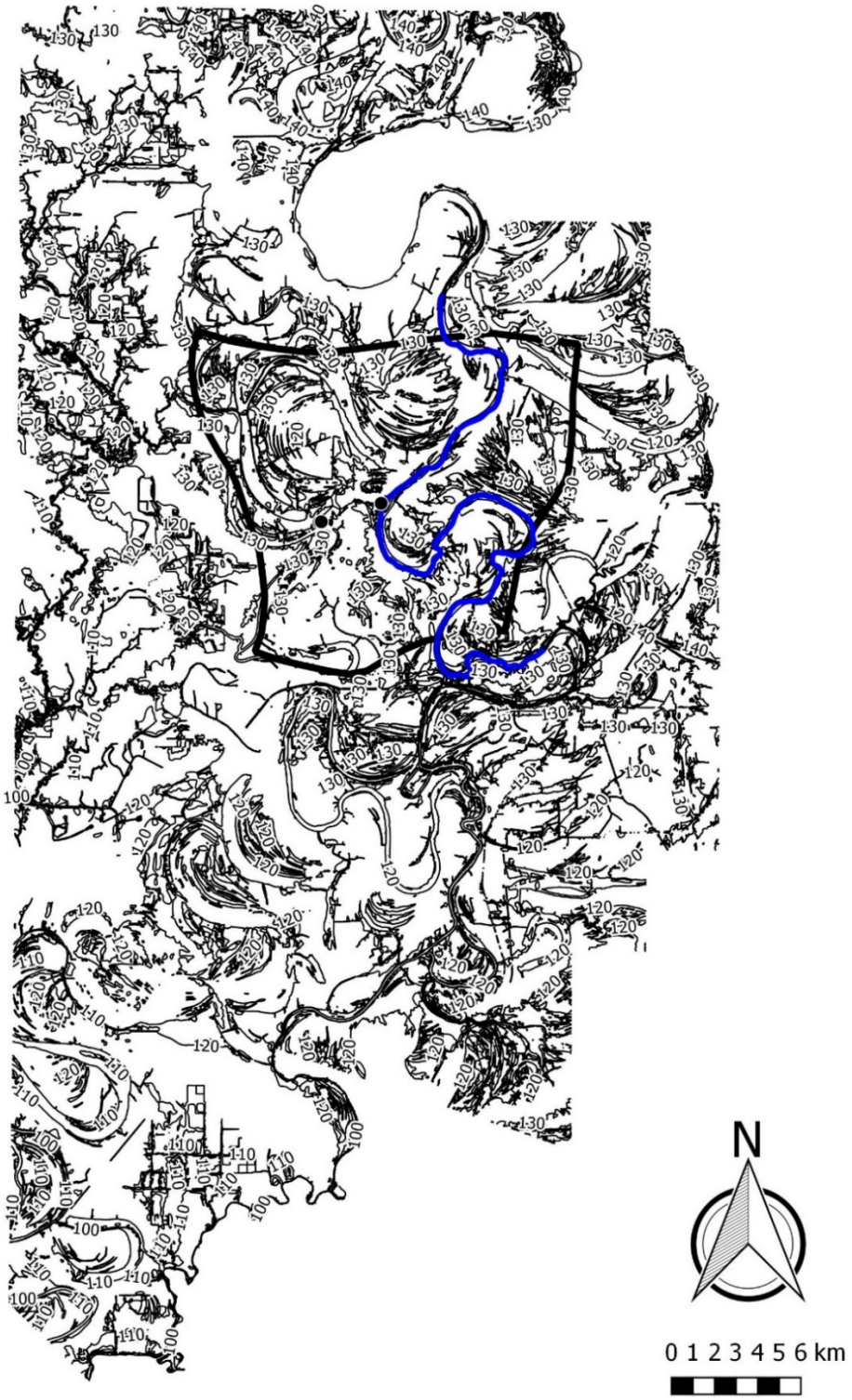

Figure 10: Contour map for Leflore county. Contour intervals are 10 meters. The model domain is defined by the thick solid line.

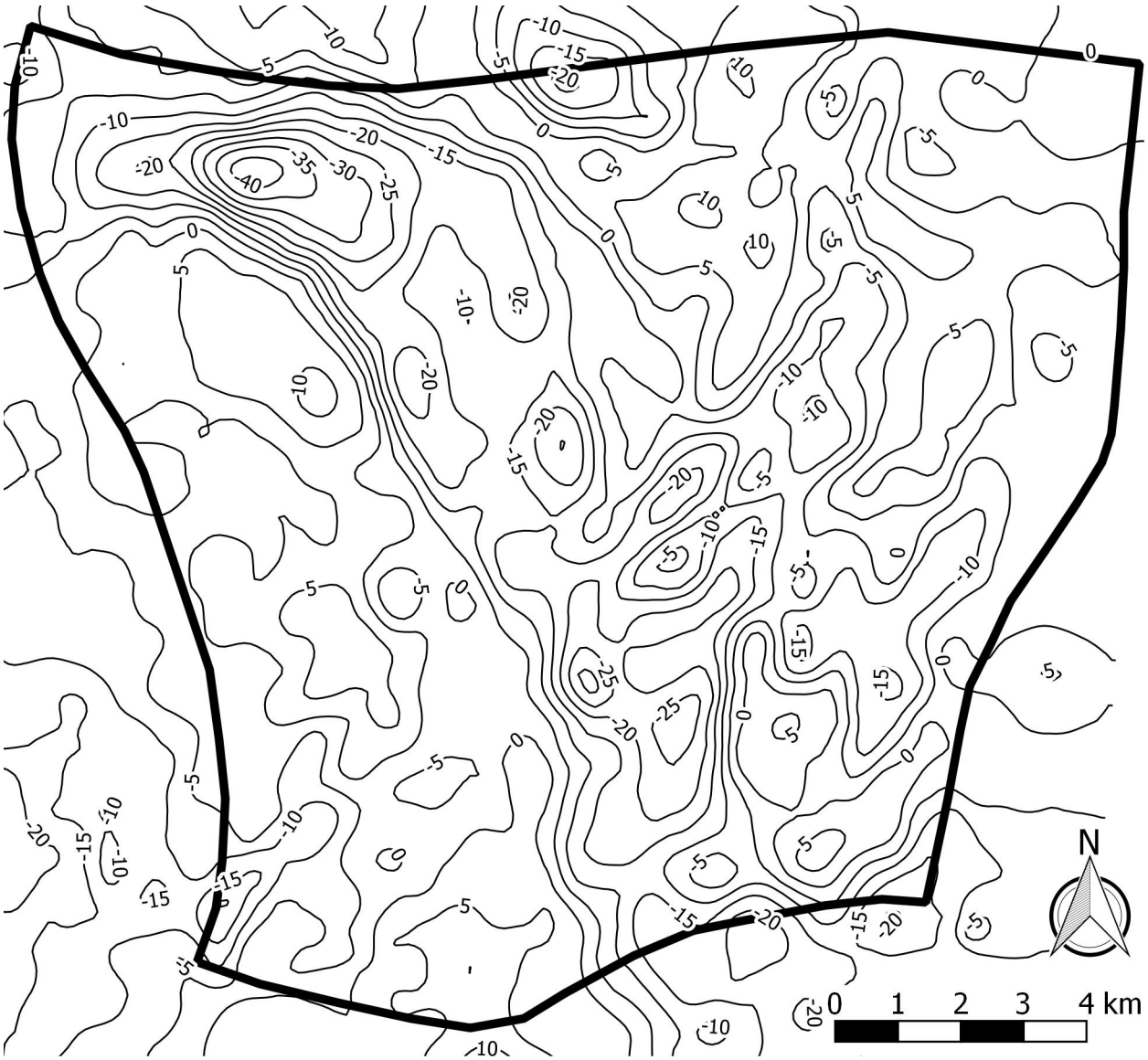

Figure 11: Contour map of the base of the MRVAA in the study area. Contour Interval is 5 meters.

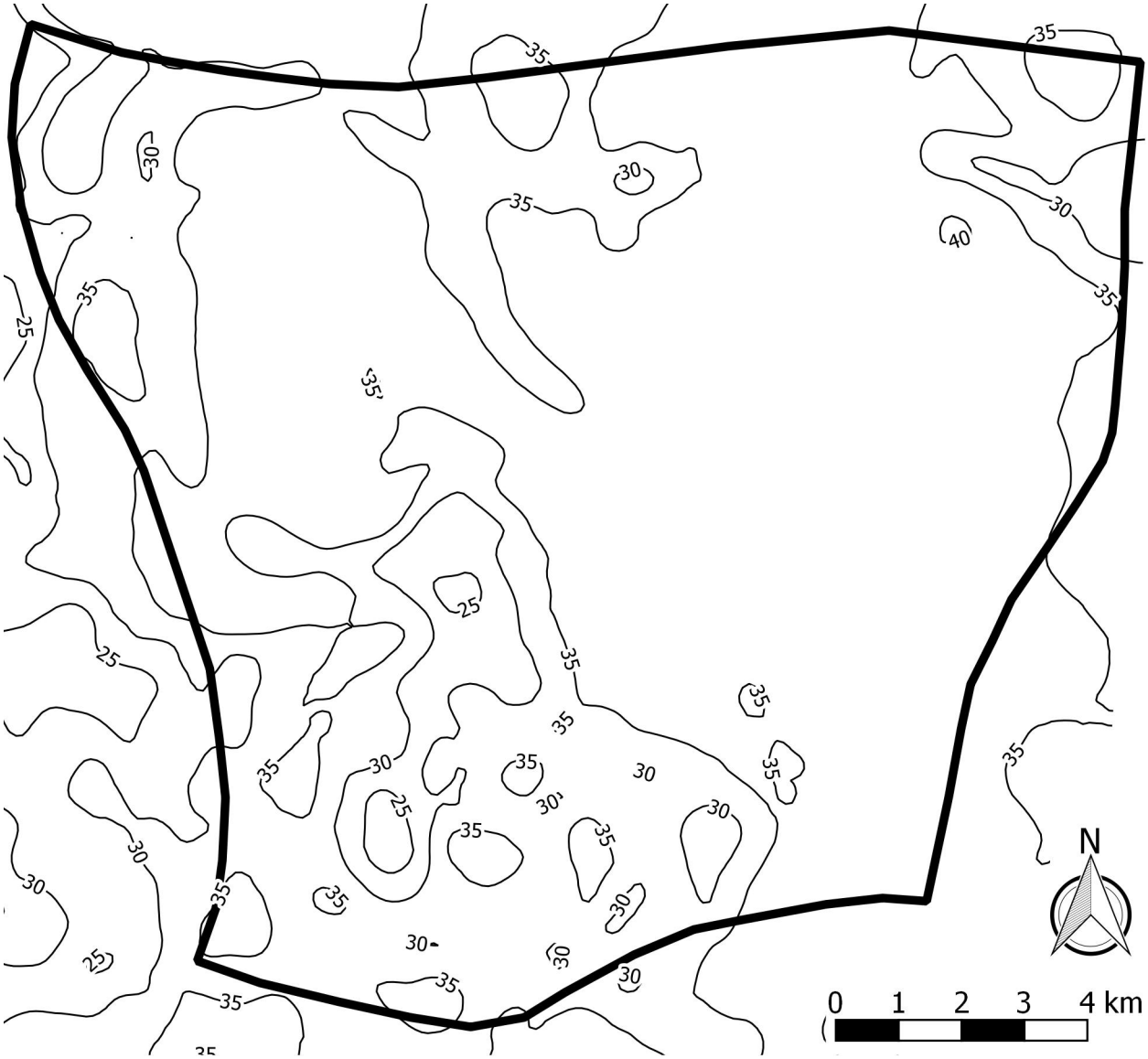

Figure 12: Contour map of the top of the MRVAA in the study area. Contour Interval is 5 meters.

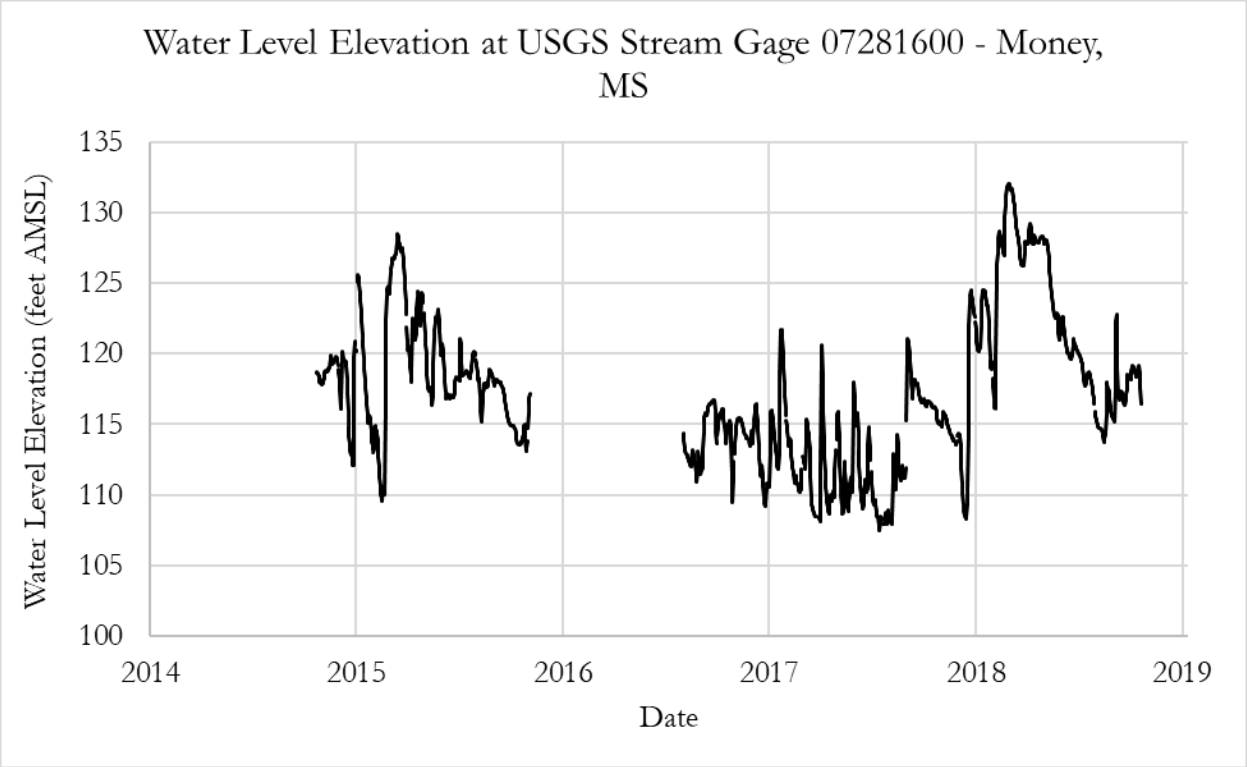

Figure 13: Stream gage stage plot for Money, MS on the Tallahatchie River.

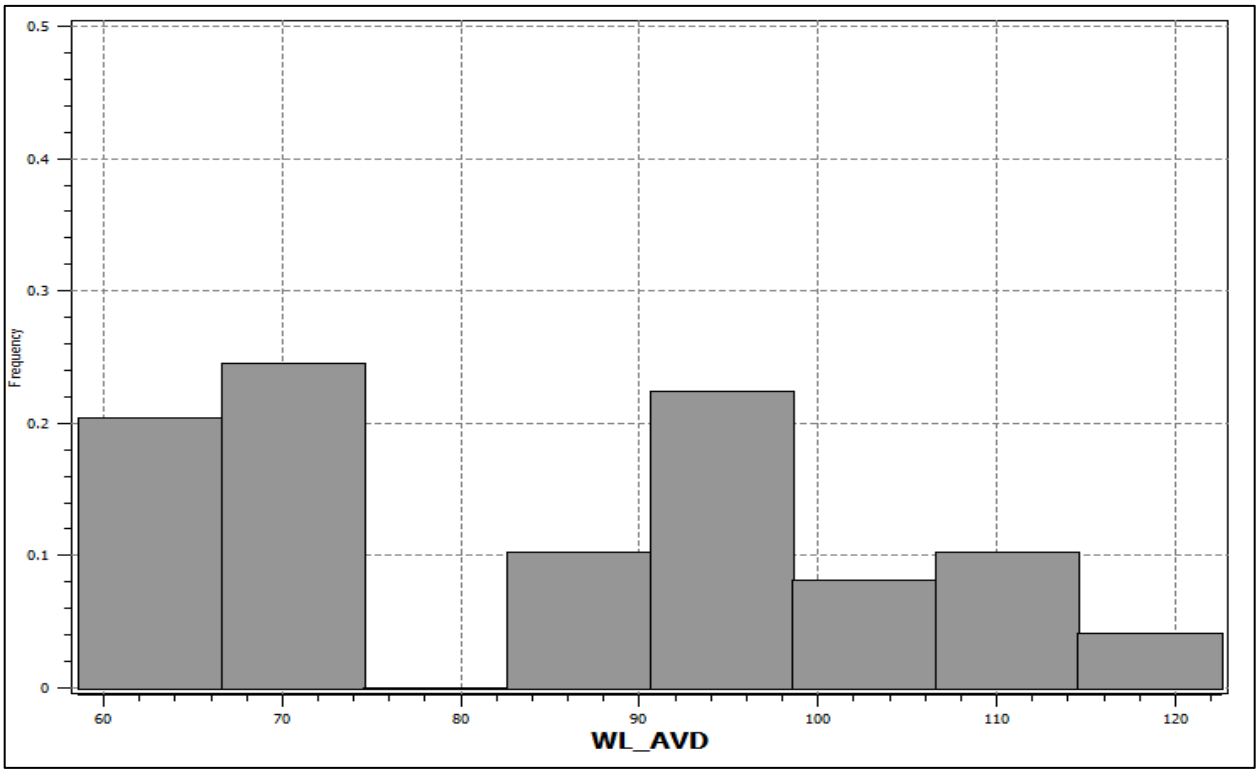

Figure 14: Initial histogram for study area USGS water levels (ft AMSL).

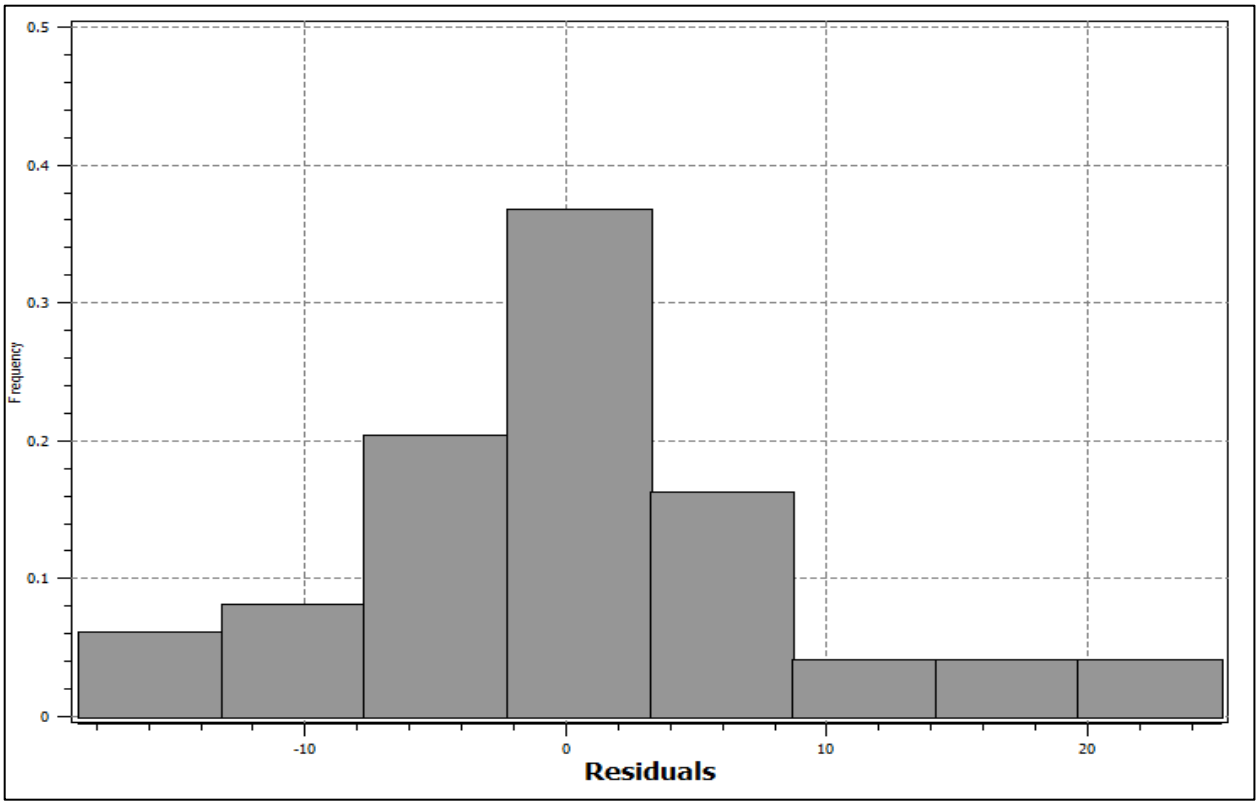

Figure 15: Histogram of residuals after detrending USGS water levels (ft AMSL).

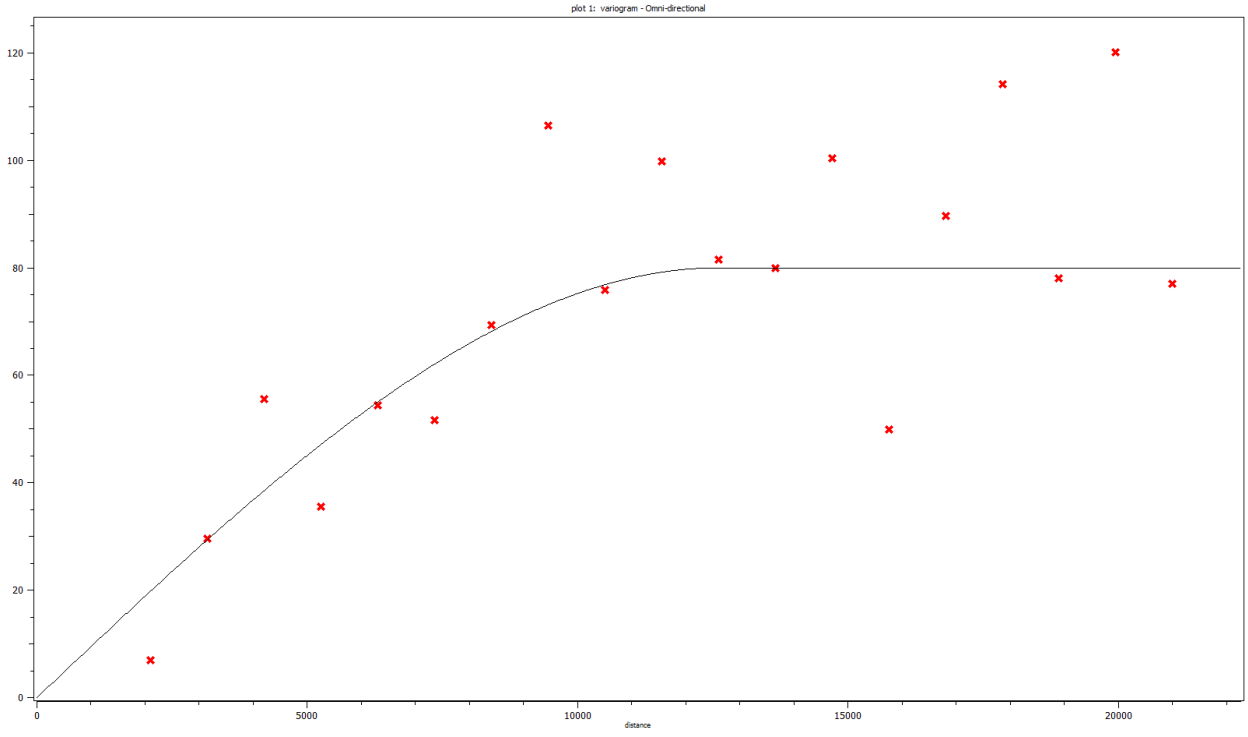

Figure 16: Variogram of water level residuals for kriging (correlation length in meters).

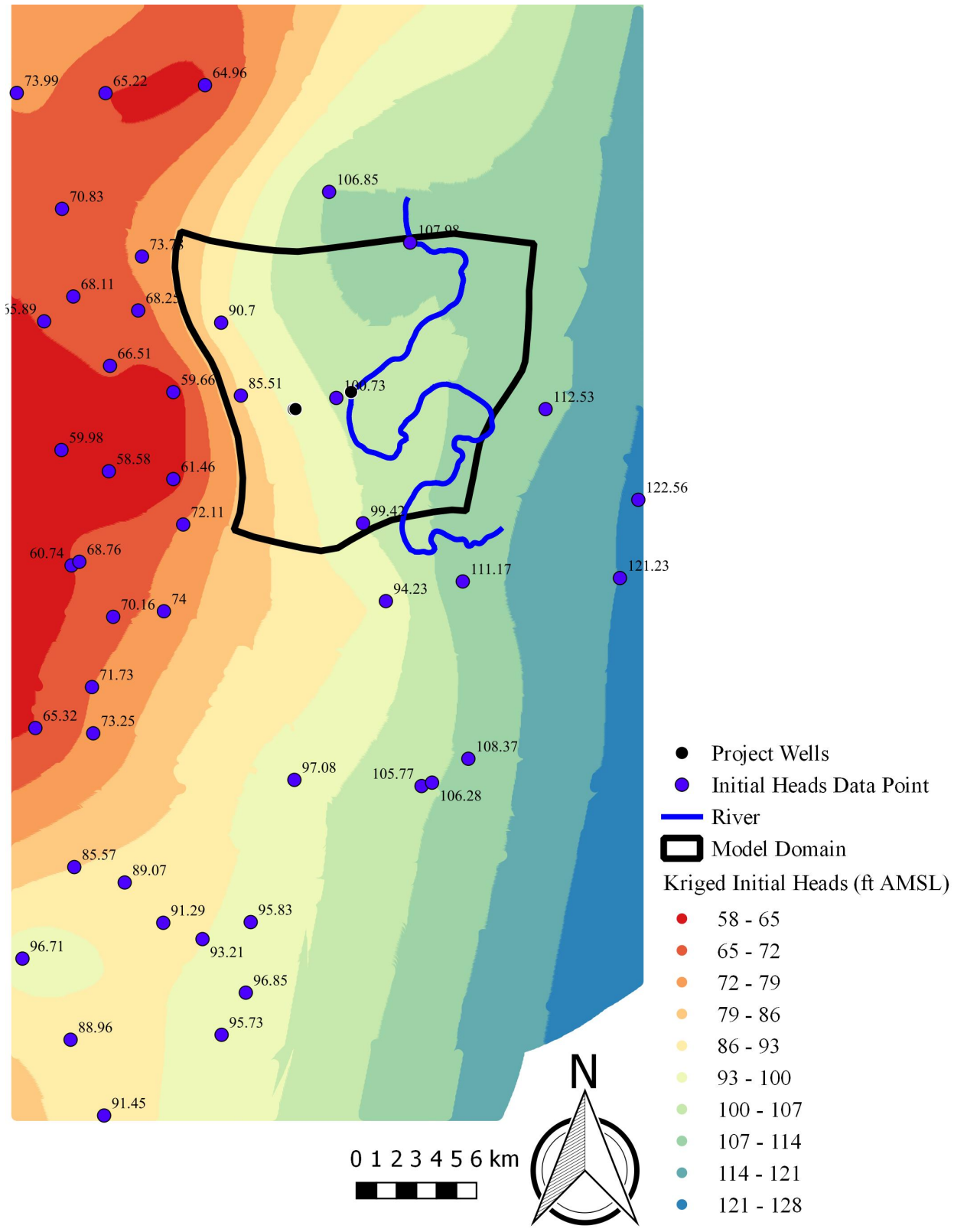

Figure 17: Interpolated heads surface from USGS gage data in October of 2018.

Aquifer Conductivity	Confining Layer K_z	River Conductance	River Stage	Pumpage (GPM)	Model Run
Medium Aquifer K 9.34×10^{-4}	Low Confining Kz 1×10^{-8}	Medium River Cond. 1×10^{-5}	Constant Stage	Steady State	1
				500	2
				1000	3
				1500	4
				2000	5
	Medium Confining Kz 1×10^{-7} m/s			Steady State	6
				500	7
				1000	8
				1500	9
				2000	10
	High Confining Kz 1×10^{-6} m/s			Steady State	11
				500	12
				1000	13
				1500	14
				2000	15
Medium Aquifer K 9.34×10^{-4}	Medium Confining Kz 1×10^{-7} m/s	Low River Cond. 1×10^{-6}	Constant Stage	Steady State	16
				500	17
				1000	18
				1500	19
				2000	20
		Medium River Cond. 1×10^{-5}		Steady State	6
				500	7
				1000	8
				1500	9
				2000	10
		High River Cond. 1×10^{-3}		Steady State	21
				500	22
				1000	23
				1500	24
				2000	25
Low Aquifer K 9.34 x 10-5	Medium Confining Kz 1×10^{-7} m/s	Medium River Cond. 1×10^{-5}	Constant Stage	Steady State	26
				500	27
				1000	28
				1500	29
				2000	30
Medium Aquifer K 9.34 x 10-4				Steady State	6
				500	7
				1000	8
				1500	9
				2000	10
High Aquifer K 9.34 x 10-3				Steady State	31
				500	32
				1000	33
				1500	34
				2000	35

Continued on following page

Medium Aquifer K 9.34×10^{-4} **1 year pumping**	Medium Confining Kz 1×10^{7} m/s	Low River Cond. 1×10^{-6}	Constant Stage	Steady State	36
				500	37
				1000	38
				1500	39
				2000	40
		Medium River Cond. 1×10^{-5}		Steady State	41
				500	42
				1000	43
				1500	44
				2000	45
		High River Cond. 1×10^{-3}		Steady State	46
				500	47
				1000	48
				1500	49
				2000	50
Medium Aquifer K 9.34×10^{-4}	Medium Confining Kz 1×10^{-7} m/s	Medium River Cond. 1×10^{-5}	Low River Stage 34 meters	Steady State	51
				500	52
				1000	53
				1500	54
				2000	55
			Medium River Stage 36 meters	Steady State	6
				500	7
				1000	8
				1500	9
				2000	10
			High River Stage 39 meters	Steady State	56
				500	57
				1000	58
				1500	59
				2000	60

Table 2: List of individual model runs and parameter variation scenarios.

4 Model Construction and Calibration

The construction of the groundwater flow model was performed in MODFLOW Visual Flex 5.0. The conceptual model consists of two structural zones that represent the upper confining unit and the underlying aquifer material (zones one and two, respectively). Zone one extends from land surface down to the top of the aquifer and represents the MRVAA confining layer. It has uniform hydraulic and lithologic properties throughout. The initial heads for steady-state simulation correspond to land surface. Zone two extends from the top to the bottom of the aquifer and has three property zones that represent areas of different hydraulic conductivity

laterally, while conductivity for the given zone is constant vertically. These zones of higher and lower conductivity were created to match the observed water levels during the calibration process. Lithologic properties representing storage and porosity are uniform throughout (Table 1). Initial heads are interpreted from USGS gage data in October of 2018, model start date thus is October 1st, 2018.

The western constant head boundary follows the potentiometric surface contour corresponding to 24 meters (79 feet) and the eastern constant head boundary follows the 33.5 meter (110 feet) contour. The upper surface of the model represents the land surface and receives a uniform 19.05 millimeters per year (0.75 inches) of recharge (Clark & Hart, 2009). Boundary conditions corresponding to pumping wells are screened throughout the length of the aquifer and pumping rates and schedules are varied.

The river boundary condition is assigned to the top of the model domain where the river polyline intersects the grid cells and steady state simulation utilizes a constant stage value of 36 meters AMSL (118 feet), except where it is different as specified, with a river bottom elevation of 33.5 meters AMSL (110 feet) and riverbed thickness of 1.22 meters (4.00 feet). River width is a uniform 70 meters (230 feet) and riverbed conductivity for steady state simulation is 10^{-5} with the corresponding conductance in units of volume per time calculated once the conceptual model is converted to a numerical model according to the following calculation:

$$Q_{river} = \frac{[K*L*W*(H_{river} - H_{aquifer})]}{M} \quad (4\text{-}0)$$

Where,

Q_{river} is the leakage through the given reach of the riverbed (L^3/T)

K is the hydraulic conductivity of the riverbed (L/T)

L is the length of the reach (L)

W is the width of the reach (L)

M is the thickness of the riverbed (L)

H_{river} is the head of the river (L)

$H_{aquifer}$ is the head of the aquifer on the side of the river bed (L)

Model calibration was performed to match the interpolated heads from October of 2018.

The conceptual model was discretized into a numerical model consisting of 220 rows by 200 columns and 4 layers. Layer 1 represents the confining unit and layers 2 through 4 the aquifer. Grid sizes are 80 by 90 meters (262 by 295 feet) at the edge of the domain and refine down to a size of 30 by 35 meters (98 by 115 feet) near the withdrawal well.

5 Pumping Scenarios and Assessment Criteria

The numerical model was used to first produce a steady state result of groundwater heads with no pumping and no hydraulic or temporal parameters varied, this is referred to as the base case, which are runs 6 through 10 in Table 2. From this baseline, parameters such as the confining layer vertical hydraulic conductivity (runs 1 through 15), aquifer hydraulic conductivity (26 through 35), river conductivity (runs 16 through 25), river stage (51 through 60), and length of pumping were varied (36 through 50). A total of 60 unique scenarios were modeled.

All simulations involving pumping were modeled as transient and run with pumping rates of 500, 1000, 1500, and 2000 GPM (2725, 5451, 8176, and 10,902 m^3/d). For each scenario the

pumping period was 60 days long except for those of extended pumping duration, which were 365 days of constant withdrawal. Maximum change in head and total change in storage to the east and the west of the river were calculated within the zones depicted in Figure 8 to assess effects of the different conditions. In addition, mass balance totals were tabulated along with the volume of river leakage into and out of the model domain (Tables 4, 6, and 8).

IV RESULTS & DISCUSSION

1 Model Calibration

The model was calibrated by running to steady state with the base case conditions and comparing the resulting heads to those interpreted from the observed USGS gage data in October of 2018. Figure 18 displays the difference between the interpolated heads and steady state output in meters.

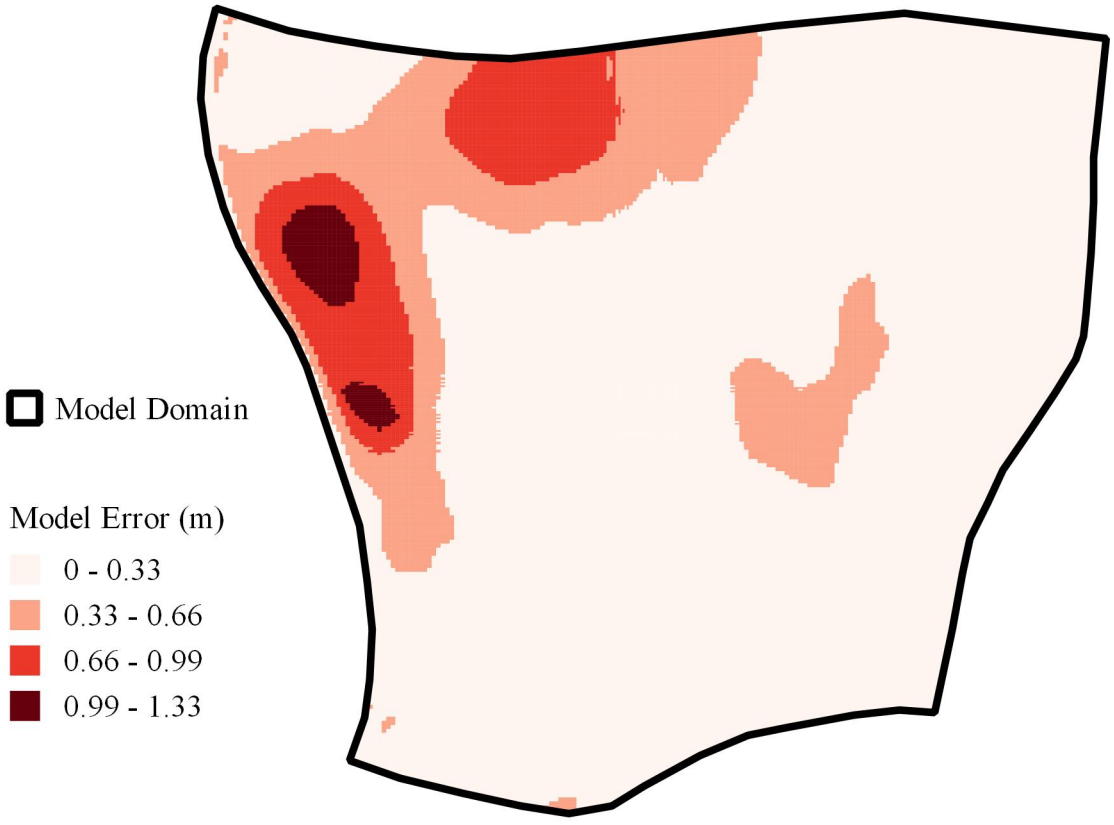

Figure 18: Model domain error in meters.

While the entire model domain exhibits less than 1.33 meters of error, which is an acceptable value, spatial analysis shows that all error above 1 meter is limited to the western edge of the lower conductivity zone in the western area of the model domain. This region is outside the minimum distance defined by the time constant and in a region not impacted by the various pumping scenarios.

2 Varied Confining Layer Vertical Conductivity

Varying the confining layer vertical hydraulic conductivity has very little effect on the resulting heads (Figures 19 through 21). In all situations, drawdown varies from 0.58 meters to 2.36 meters from steady state. The change in storage is also nearly identical for increased and decreased confining layer conductivity compared to the base case (Table 3). There is no measurable difference in the amount of river leakage into the domain with varying confining layer conductivity across all pumping rates (it is nearly constant) (Table 4). Likewise there is no detectable difference in the water level profiles (Figures 46 through 48). Total change in storage plotted versus the pumping rates is the same for increased and decreased confining conductivity in both the eastern and western zone (Figures 31 and 36). The normalized change in leakage for variable confining conductivity (Figure 41), is not measurably different than a 1:1 ratio with the base case.

3 Varied River Conductance

The effect of changing the river conductance on the resulting heads is substantial. Figure 23 shows the heads with increased river conductance and it is higher at both steady state and with pumping than most all other situations except for decreased aquifer conductivity and increased river conductance with extended pumping duration. While the drawdown profiles for the low and high river conductance are similar (Figures 49 and 51), a noticeable mounding of the

potentiometric surface is visible in the higher river conductance scenario (Figure 50). In both the eastern and western zone, the total change in storage is roughly identical for the medium and low river conductance scenarios, but it is measurably lower when river conductance is higher (Figures 32 and 37). The normalized change in leakage shows an increase of 75 times over the base case for higher river conductance, and no difference for the lowered conductance (Figure 42). Lowering the river conductivity compared to the base case does not affect the river leakage (Table 4). Increasing the pumping rate does not affect the amount of river leakage into the model domain when it is lowered or at the moderate value. However, increasing the pumping rates causes increasing gains in river leakage when conductance is high (Table 9).

4 Varied Aquifer Conductivity

Varying the aquifer conductivity has a substantial effect on the resulting change in heads. Low aquifer conductivity causes the highest heads observed in all scenarios at steady state and the maximum amount of drawdown observed in all scenarios (Figure 24 and Table 5). Drawdown increases from a range of 0.58 to 2.35 feet in the base case to 4.20 to 15.41 feet when aquifer conductivity is lowered. When it is raised, drawdown is drastically decreased to 0.07 to 0.29 feet. These changes are reflected in the water level profiles (Figures 51 and 52). The change in storage in both the western and eastern zones (Figures 38 and 33, respectively) is reduced for the higher aquifer conductivity and increased for the lower aquifer conductivity, although the effect curtails at the highest pumping rate in both zones for the lowered conductivity. Leakage from the river in the medium and high aquifer conductivity scenarios is not affected, but it is substantially lowered when aquifer conductivity is low and the low conductivity scenario is the only one in which river leakage out of the model domain is measured (Table 6). However, the total change in leakage into the model domain when there is pumping versus steady state ranges

from 3,441 to 10,355 cubic meters for the entire simulation period in the low aquifer conductivity scenario. That is to say, higher pumping induces greater leakage from the river when aquifer conductivity is low, although the total amount is less than when aquifer conductivity is at a moderate or higher level (Table 6).

5 Varied Pumping Duration

Extending the duration of pumping from 60 to 365 days does not have a substantial effect on the resulting heads (Table 7 and Figures 26 through 28). While the high river conductance scenarios with short and extended pumping shows a higher overall groundwater level compared to when river conductance is moderate or low, the reduction in it is not substantially different between the two situations. Figures 49 and 50 show the water level profile for the low and high river conductance scenarios, and they are nearly identical to Figures 53 and 55 which show the same situations with extended pumping. The total amount of change in storage in the western and eastern zones is greater for extended pumping, although the pattern of a smaller reduction with the higher river conductivity holds the same (Table 7 and Figures 32, 35, 37, and 40). The normalized change in leakage to the base case (Figure 42) for regular pumping durations and varied river conductance shows a substantial increase in leakage (on the order of 75 times) when river conductance is high, and the proportion is the same for the same case with extended pumping time (Figure 45). Table 9 shows the volumetric increase in leakage relative to steady state is greater when pumping time is longer.

6 Varied River Stage

Varying the river stage had little to no effect on the resulting heads (Table 5, Figures 20, 29, and 30), however a small decease in the total head reduction is observed with increased stage. Neither water level profile is substantially different from the base case (Figures 47, 56, and

57). The change in storage in the western and eastern zones with changing river stage is nearly identical (Figure 34 and 39). The normalized change in leakage for change in river stage is roughly 250% higher when stage is elevated, and roughly 90% lower when stage is lowered (Figure 44, Table 6). The change in pumping rate across different river stage scenarios does not induce any more or less flow into the model domain from the river (Table 9).

Scenario	Run No.	Rate (GPM)	Max Δ Head (m)	Δ Storage East (m^3)	Δ Storage West (m^3)	Total Δ Storage (m^3)	Total Volume Pumped (m^3)	Δ Storage / Amount Pumped
Low Confining Kz 1×10^{-8} m/s	1	0	-	-	-	-	-	-
	2	500	0.58	67858	166303	234161	652787	0.36
	3	1000	1.16	136048	333358	469405	1305575	0.36
	4	1500	1.76	204276	500528	704804	1958242	0.36
	5	2000	2.36	272590	667906	940496	2611150	0.36
Medium Confining Kz 1×10^{-7} m/s	6	0	-	-	-	-	-	-
	7	500	0.58	66372	161187	227558	652787	0.35
	8	1000	1.16	133921	324549	458469	1305575	0.35
	9	1500	1.76	201160	487483	688642	1958242	0.35
	10	2000	2.35	268460	650575	919035	2611150	0.35
High Confining Kz 1×10^{-6} m/s	11	0	-	-	-	-	-	-
	12	500	0.58	66280	161159	227439	652787	0.35
	13	1000	1.17	133697	323906	457603	1305575	0.35
	14	1500	1.76	200825	486479	687304	1958242	0.35
	15	2000	2.35	268004	649225	917229	2611150	0.35
Low River Conductivity 1×10^{-6} m/s	16	0	-	-	-	-	-	
	17	500	0.58	67302	162945	230247	652787	0.35
	18	1000	1.16	134506	325768	460274	1305575	0.35
	19	1500	1.76	201755	488711	690466	1958242	0.35
	20	2000	2.36	269089	651837	920925	2611150	0.35
Medium River Conductivity 1×10^{-5} m/s	6	0	-	-	-	-	-	-
	7	500	0.58	66372	161187	227558	652787	0.35
	8	1000	1.16	133921	324549	458469	1305575	0.35
	9	1500	1.76	201160	487483	688642	1958242	0.35
	10	2000	2.35	268460	650575	919035	2611150	0.35
High River Conductivity 1×10^{-3} m/s	21	0	-	-	-	-	-	-
	22	500	0.55	59239	149690	208928	652787	0.32
	23	1000	1.10	119103	300808	419911	1305575	0.32
	24	1500	1.67	179249	452595	631845	1958242	0.32
	25	2000	2.23	239638	604920	844558	2611150	0.32

Table 3: Head change, storage, and pumping information for runs 1 through 25.

Scenario	Storage In (m^3)	Constant Head in (m^3)	River In (m^3)	Recharge in (m^3)	Storage Out (m^3)	Constant Head Out (m^3)	River Out (m^3)	Mass Balance (Total In-Out) (m^3)	Percent Difference
Low Confining Kz 1×10^{-8} m/s	-	20619060	723030	12621840	-	33963930	0	1.0	0
	1037461	20637522	723521	12622311	413155	33955064	0	-76.0	0
	2076077	20656756	723521	12622311	826511	33946660	0	-84.0	0
	3114570	20675990	723521	12622311	1239978	33938248	0	-76.0	0
	4153715	20695238	723521	12622311	1653877	33929836	0	-76.0	0
Medium Confining Kz 1×10^{-7} m/s	-	20619060	723030	12621840	-	33963930	0	1.2	0
	1083148	20635912	723521	12622312	455848	33956328	0	-72.0	0
	2079365	20654918	723521	12622311	826052	33948840	0	-84.0	0
	3119855	20673526	723520	12622311	1239387	33941544	0	-80.0	0
	4160352	20692134	723521	12622311	1653008	33934244	0	-84.0	0
High Confining Kz 1×10^{-6} m/s	0	20616750	723030	12621840	0	33961620	0	0.6	0
	1082442	20634072	723521	12622312	454269	33955364	0	-76.0	0
	2077827	20652858	723521	12622311	823057	33948356	0	-472.0	0
	3117781	20671154	723521	12622311	1234871	33941612	0	-80.0	0
	4157609	20689450	723521	12622311	1646970	33934852	0	-80.0	0
Low River Conductivity 1×10^{-6} m/s	-	21150360	72765	12621840	-	33846120	0	-0.7	0
	1040004	21169144	72352	12622311	412945	33838164	0	-84.0	0
	2079997	21187732	72352	12622311	826029	33830872	0	-84.0	0
	3120068	21206324	72352	12622311	1239312	33823576	0	-76.0	0
	4160802	21224922	72352	12622311	1653038	33816280	0	-76.0	0
Medium River Conductivity 1×10^{-5} m/s	-	20619060	723030	12621840	-	33963930	0	1.2	0
	1083148	20635912	723521	12622312	455848	33956328	0	-72.0	0
	2079365	20654918	723521	12622311	826052	33948840	0	-84.0	0
	3119855	20673526	723520	12622311	1239387	33941544	0	-80.0	0
	4160352	20692134	723521	12622311	1653008	33934244	0	-84.0	0
High River Conductivity 1×10^{-3} m/s	-	3641715	53570055	12621840	-	69833610	0	0.5	0
	978997	3642334	53636956	12622311	416207	69811656	0	-48.0	0
	1965013	3642632	53699368	12622311	834731	69789088	0	-72.0	0
	2953852	3642932	53759364	12622311	1253867	69766416	0	-64.0	0
	3944956	3643233	53817712	12622311	1673461	69743688	0	-96.0	0

Table 4: Mass balance information for runs 1 through 25, top to bottom, in the scenarios varying the confining conductivity and river conductance.

Scenario	Run No.	Rate (GPM)	Max Δ Head (m)	Δ Storage East (m^3)	Δ Storage West (m^3)	Total Δ Storage (m^3)	Total Volume Pumped (m^3)	Δ Storage / Amount Pumped
Low Aquifer Conductivity 1×10^{-6} m/s	26	0	-	-	-	-	-	-
	27	500	4.20	101128	204996	306124	652787	0.47
	28	1000	8.67	201921	410349	612270	1305575	0.47
	29	1500	13.50	303111	617043	920154	1958242	0.47
	30	2000	15.41	364086	739149	1103235	2611150	0.42
Medium Aquifer Conductivity 1×10^{-5} m/s	6	0	-	-	-	-	-	-
	7	500	0.58	66372	161187	227558	652787	0.35
	8	1000	1.16	133921	324549	458469	1305575	0.35
	9	1500	1.76	201160	487483	688642	1958242	0.35
	10	2000	2.35	268460	650575	919035	2611150	0.35
High Aquifer Conductivity 1×10^{-3} m/s	31	0	-	-	-	-	-	-
	32	500	0.07	27516	68434	95950	652787	0.15
	33	1000	0.14	54750	136308	191058	1305575	0.15
	34	1500	0.22	81995	204196	286191	1958242	0.15
	35	2000	0.29	109260	272135	381395	2611150	0.15
Low River Stage	36	0	-	-	-	-	-	-
	37	500	0.58	66669	161767	228436	652787	0.35
	38	1000	1.17	133485	323955	457440	1305575	0.35
	39	1500	1.76	200335	486234	686569	1958242	0.35
	40	2000	2.36	267257	648665	915922	2611150	0.35
Medium River Stage	6	0	-	-	-	-	-	-
	7	500	0.58	66372	161187	227558	652787	0.35
	8	1000	1.17	133921	324549	458469	1305575	0.35
	9	1500	1.76	201160	487483	688642	1958242	0.35
	10	2000	2.36	268460	650575	919035	2611150	0.35
High River Stage	41	0	-	-	-	-	-	-
	42	500	0.58	66444	161337	227781	652787	0.35
	43	1000	1.17	133180	323322	456502	1305575	0.35
	44	1500	1.76	199952	485429	685381	1958242	0.35
	45	2000	2.36	266799	647737	914536	2611150	0.35

Table 5: Head change, storage, and pumping information for runs 26 through 45.

Scenario	Storage In (m^3)	Constant Head in (m^3)	River In (m^3)	Recharge in (m^3)	Storage Out (m^3)	Constant Head Out (m^3)	River Out (m^3)	Mass Balance (Total In-Out) (m^3)	Percent Difference
Low Aquifer Conductivity 1×10^{-6} m/s	-	297584	203280	12621840	-	13108095	15015	0.1	0
	1111034	297626	206690	12622312	461634	13108347	15035	-22.0	0
	2223664	297626	209555	12622312	924233	13108347	15014	-12.0	0
	3336836	297626	212150	12622312	1387655	13108346	14994	-13.0	0
	3980782	297626	213635	12622312	1647990	13108346	14982	-18.0	0
Medium Aquifer Conductivity 1×10^{-5} m/s	-	20619060	723030	12621840	-	33963930	0	1.2	0
	1083148	20635912	723521	12622312	455848	33956328	0	-72.0	0
	2079365	20654918	723521	12622311	826052	33948840	0	-84.0	0
	3119855	20673526	723520	12622311	1239387	33941544	0	-80.0	0
	4160352	20692134	723521	12622311	1653008	33934244	0	-84.0	0
High Aquifer Conductivity 1×10^{-3} m/s	-	279678630	723030	12621840	-	293035050	0	-9.2	0
	767437	279930720	723521	12622312	459261	292929696	0	2208.0	0
	1533406	280175008	723521	12622312	921107	292825216	0	2336.0	0
	2299265	280418880	723521	12622312	1382729	292720864	0	2144.0	0
	3065337	280663360	723521	12622312	1844310	292616352	0	2720.0	0
Low River Stage	-	21146895	78540	12621840	-	33846325	0	1.2	0
	1082173	21164466	78987	12622312	455986	33839248	0	-84.0	0
	2165350	21182646	78987	12622312	911652	33832148	0	-80.0	0
	3248546	21200822	78987	12622312	1367445	33825048	0	-72.0	0
	4332367	21218996	78987	12622312	1823635	33817952	0	-72.0	0
Medium River Stage	-	20619060	723030	12621840	-	33963389	0	1.2	0
	1083148	20635912	723521	12622312	455848	33956328	0	-72.0	0
	2079365	20654918	723521	12622311	826052	33948840	0	-84.0	0
	3119855	20673526	723520	12622311	1239387	33941544	0	-80.0	0
	4160352	20692134	723521	12622311	1653008	33934244	0	-84.0	0
High River Stage	-	19698525	1848000	12621840	-	34167000	0	1.5	0.01
	1082506	19715590	1848294	12622312	455920	34160060	0	-64.0	0
	2165628	19733798	1848294	12622312	911573	34152964	0	-80.0	0
	3248752	19752008	1848294	12622312	1367337	34145856	0	-68.0	0
	4332454	19770226	1848294	12622312	1823458	34138752	0	-72.0	0

Table 6: Mass balance information for runs 26 through 45, top to bottom, in the scenarios varying the aquifer conductivity and river stage.

Scenario	Run No.	Rate (GPM)	Max Δ Head (m)	Δ Storage East (m^3)	Δ Storage West (m^3)	Total Δ Storage (m^3)	Total Volume Pumped (m^3)	Δ Storage / Amount Pumped
Low River Conductivity 1×10^{-6} m/s 1 year pumping	46	0	-	-	-	-	-	-
	47	500	0.67	144464	323186	467650	992599	0.47
	48	1000	1.36	289014	646438	935452	1985562	0.47
	49	1500	2.05	433605	969590	1403195	2978160	0.47
	50	2000	2.75	578407	1293200	1871607	3971124	0.47
Medium River Conductivity 1×10^{-5} m/s 1 year pumping	51	0	-	-	-	-	-	-
	52	500	0.67	144233	322781	467014	992599	0.47
	53	1000	1.36	288761	646104	934865	1985562	0.47
	54	1500	2.05	433328	969199	1402527	2978160	0.47
	55	2000	2.75	578062	1292682	1870744	3971124	0.47
High River Conductivity 1×10^{-3} m/s 1 year pumping	56	0	-	-	-	-	-	-
	57	500	0.64	135477	310118	445595	992599	0.45
	58	1000	1.28	272661	623590	896251	1985562	0.45
	59	1500	1.94	410572	938144	1348716	2978160	0.45
	60	2000	2.6	549037	1253419	1802456	3971124	0.45

Table 7: Head change, storage, and pumping information for runs 46 through 60.

Scenario	Storage In (m^3)	Constant Head in (m^3)	River In (m^3)	Recharge in (m^3)	Storage Out (m^3)	Constant Head Out (m^3)	River Out (m^3)	Mass Balance (Total In-Out) (m^3)	Percent Difference
Low River Conductivity 1×10^{-6} m/s 1 year pumping	-	6702111	22927	3999797	-	10725085	0	-0.7	0
	992262	6702865	22927	3999799	164	10724916	0	-9.0	0
	1984016	6703656	22927	3999799	116	10724736	0	-16.0	0
	2975732	6704404	22927	3999799	149	10724570	0	-17.0	0
	3967687	6705193	22927	3999799	108	10724391	0	-17.0	0
Medium River Conductivity 1×10^{-5} m/s 1 year pumping	-	6533727	229272	3999797	-	10762362	0	1.2	0
	991367	6534488	229272	3999799	146	10762187	0	-7.0	0
	1983362	6535258	229272	3999799	131	10762012	0	-17.0	0
	2975009	6536028	229272	3999799	124	10761839	0	-17.0	0
	3967027	6536798	229272	3999799	119	10761664	0	-13.0	0
High River Conductivity 1×10^{-3} m/s 1 year pumping	-	1154100	16975432	3999797	-	22129159	0	0.5	0
	955296	1154110	17011912	3999799	155	22128194	0	-14.0	0
	1920406	1154119	17038578	3999799	141	22127216	0	-16.0	0
	2889416	1154128	17061172	3999799	134	22126236	0	-16.0	0
	3861625	1154138	17080940	3999799	129	22125260	0	-12.0	0

Table 8: Mass balance information for runs 46 through 60, top to bottom, in the scenarios varying the pumping time to 365 days.

	Rate	Confining K_z	River Conductance	Aquifer Conductivity	River Stage	Extended Pumping
Low	500	491	-413	3410	447	0
	1000	491	-413	6275	447	0
	1500	491	-413	8870	447	0
	2000	491	-413	10355	447	0
Med	500	491	491	491	491	761
	1000	491	491	491	491	1531
	1500	490	490	490	490	2301
	2000	491	491	491	491	3071
High	500	491	66901	491	294	36480
	1000	491	129313	491	294	63146
	1500	491	189309	491	294	85740
	2000	491	247657	491	294	105508

Table 9: Volumetric (m^3) change in river leakage into the model domain compared to its steady state value for each scenario.

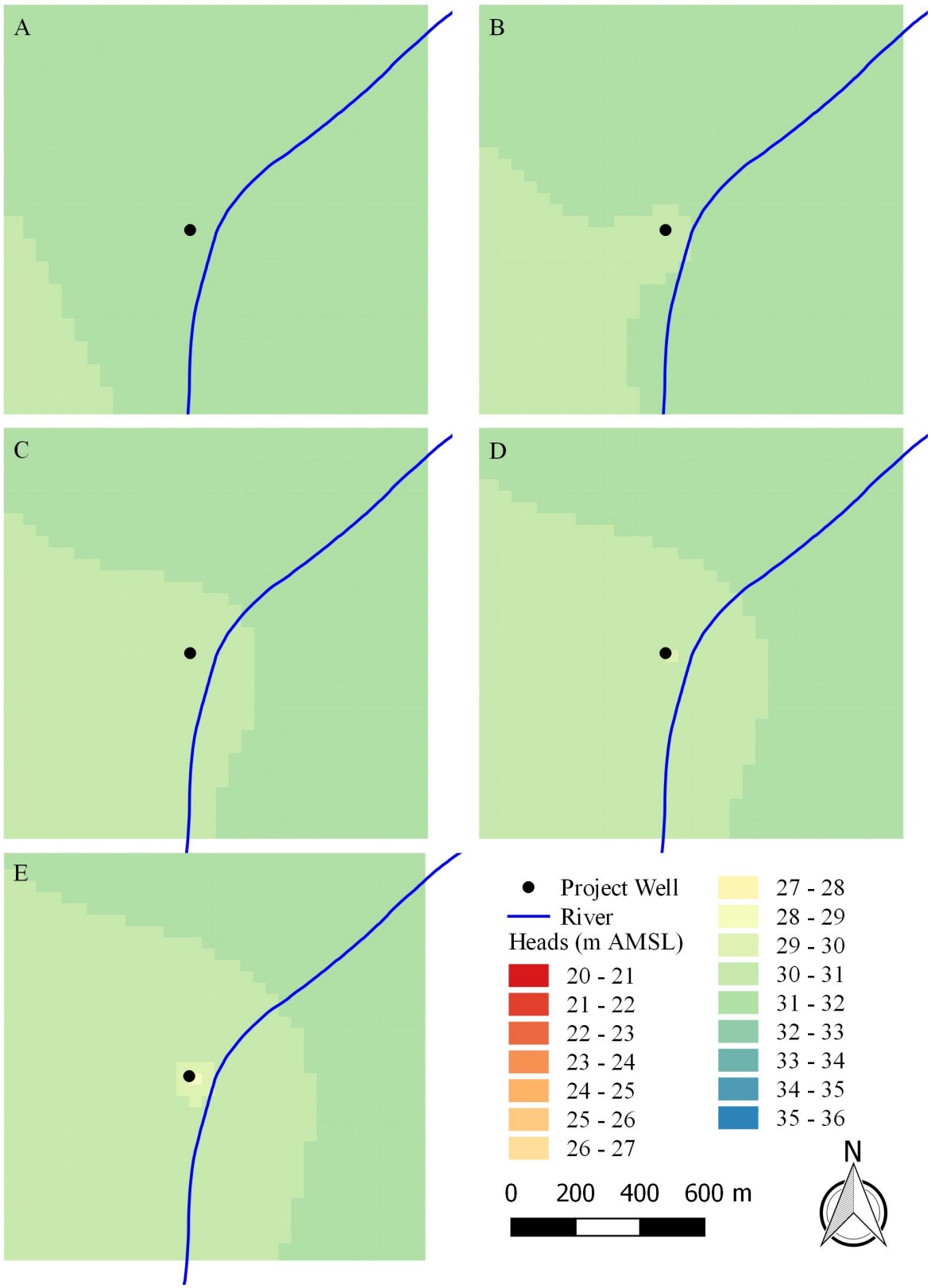

Figure 19: Heads for run 1-5 (A - E, respectively). Low confining layer conductivity scenario.

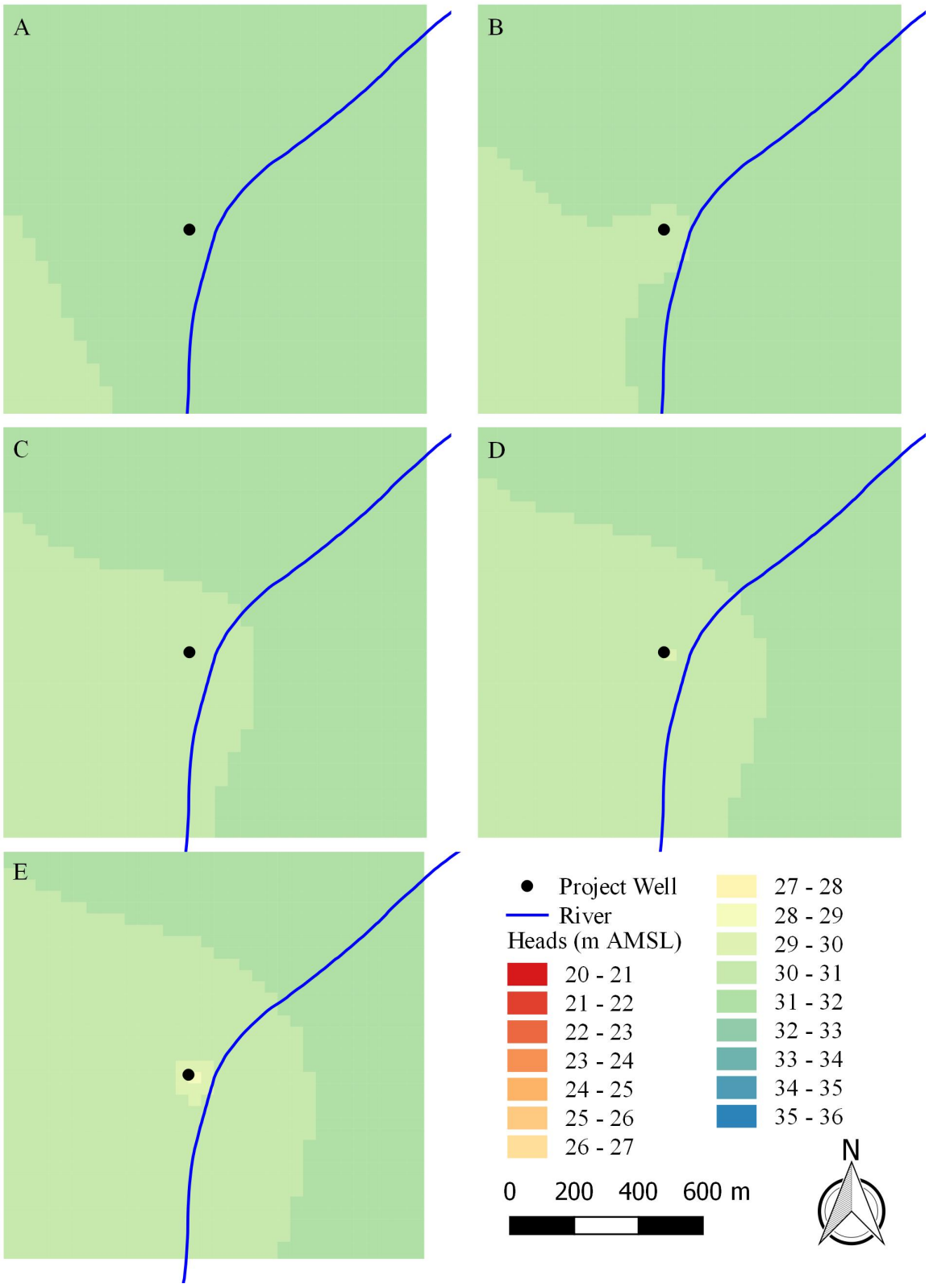

Figure 20: Heads for runs 6 – 10 and 21 – 25 (A – E, respectively to each). Medium confining layer conductivity, the base case.

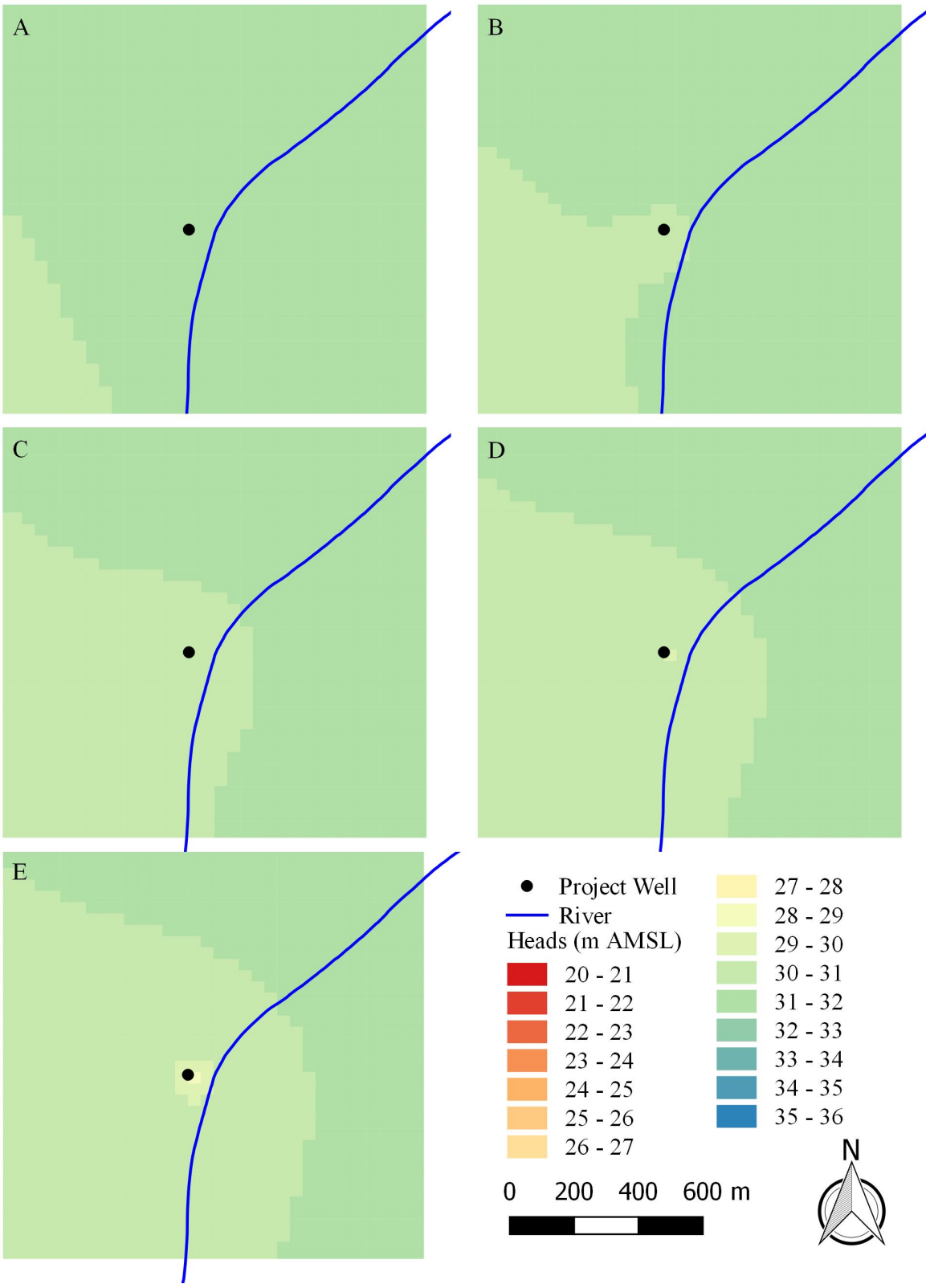

Figure 21:Heads for runs 11 – 15 (A – E, respectively). High confining layer conductivity scenario.

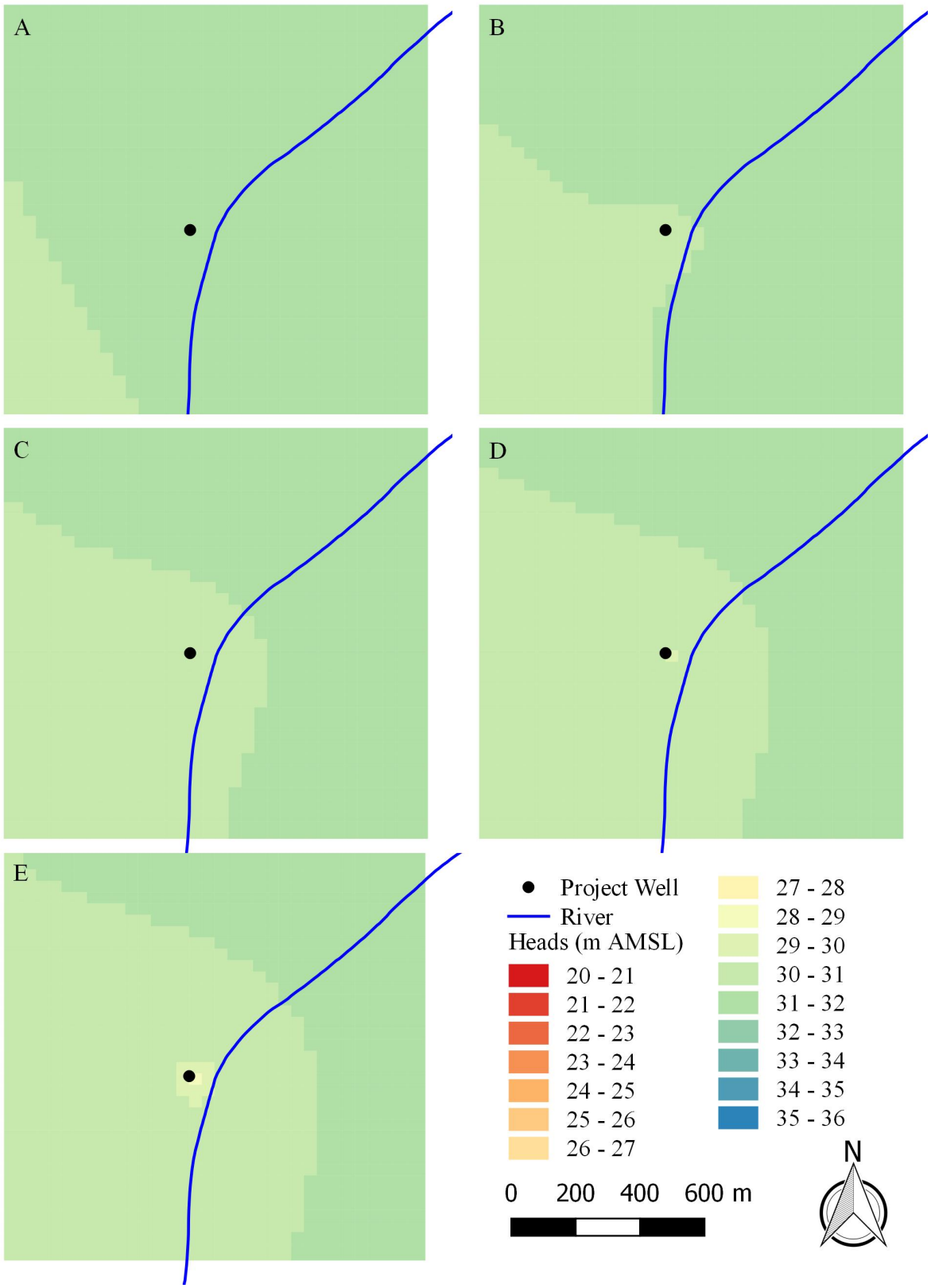

Figure 22: Heads for runs 16 – 20 (A – E, respectively). Low river conductance scenario.

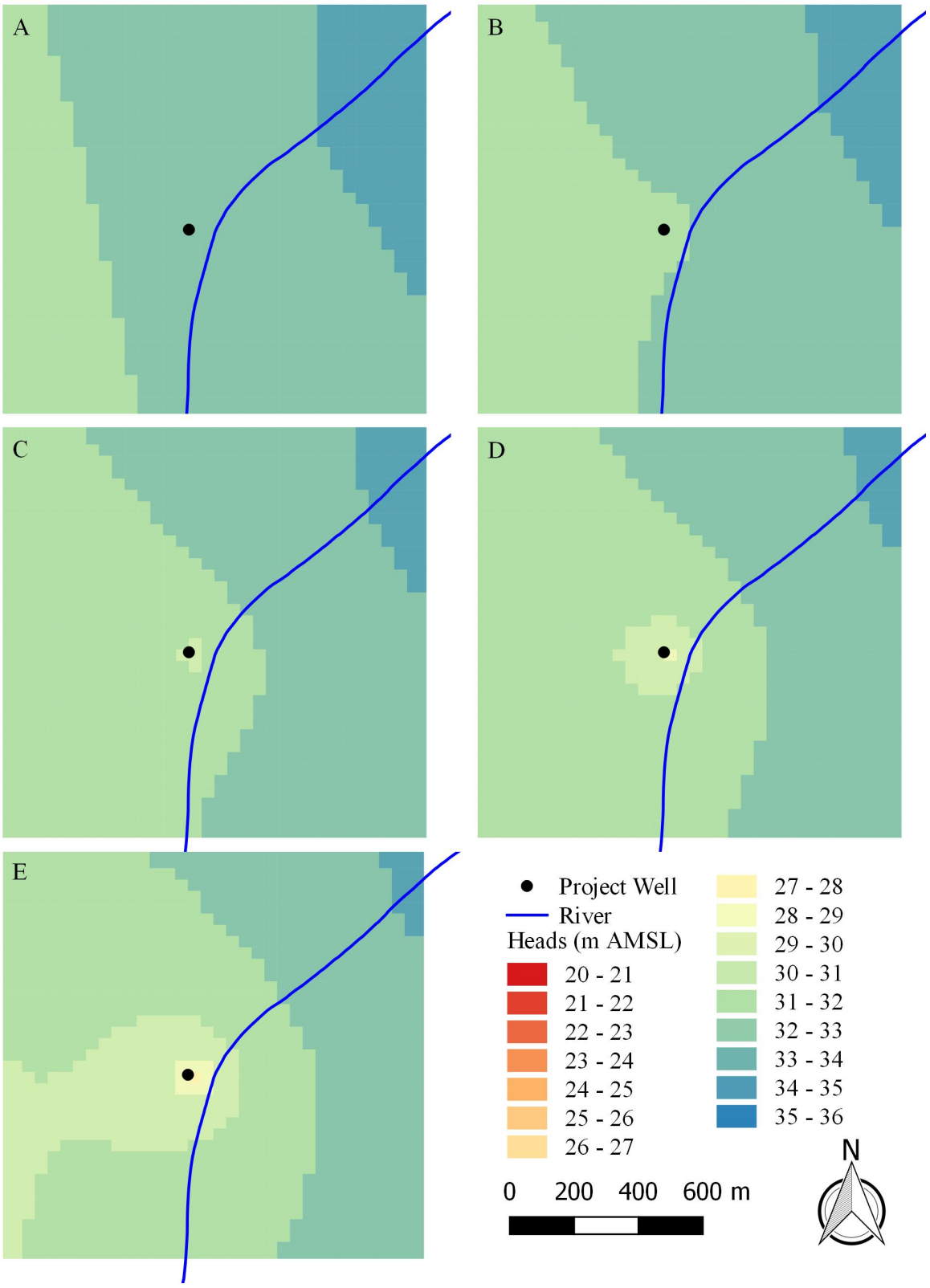

Figure 23: Heads for runs 25 – 30 (A – E, respectively). Medium confining layer conductivity and high river conductance scenario.

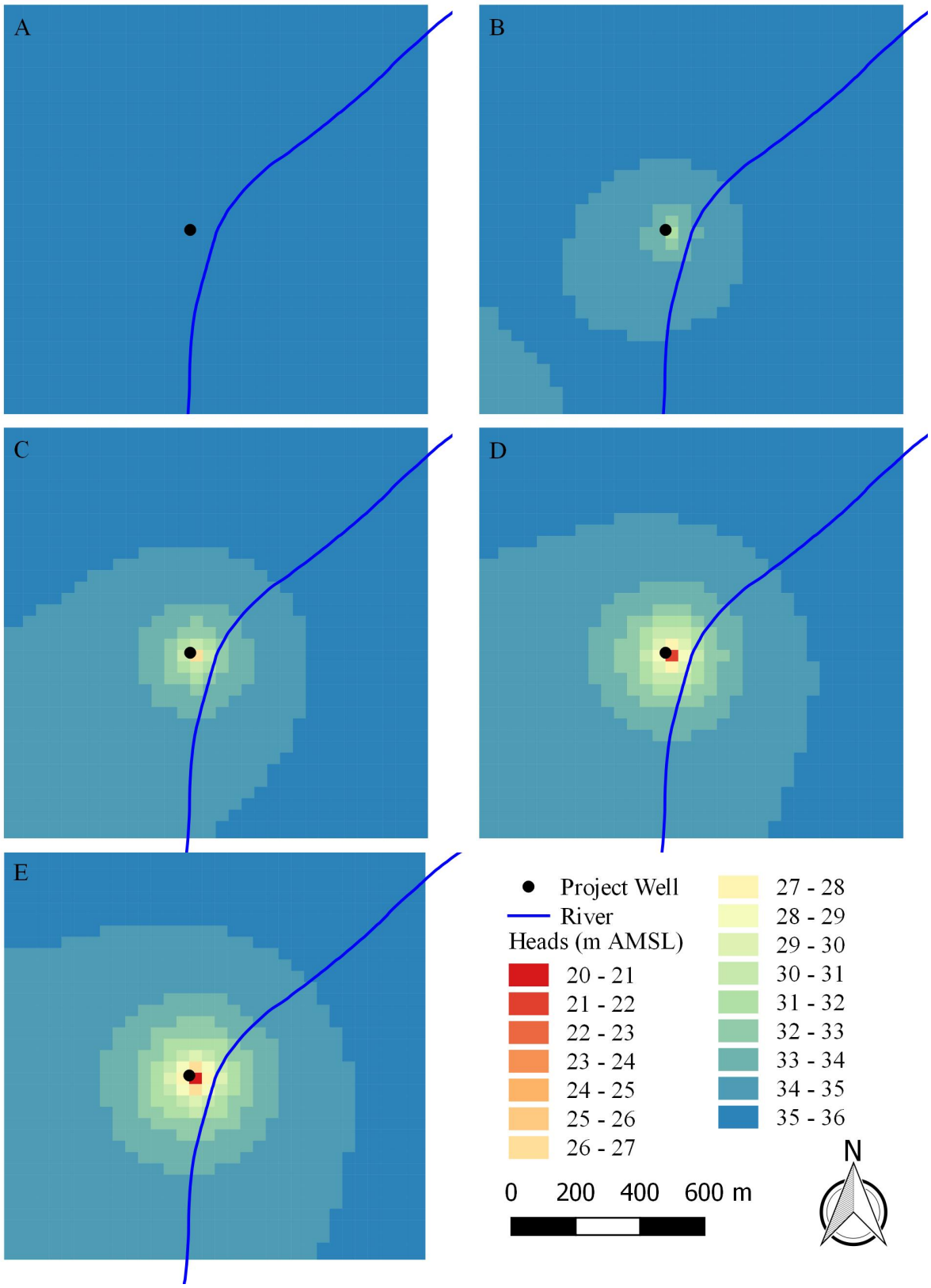

Figure 24: Heads for runs 26 - 30 (A - E, respectively). Low aquifer conductivity scenario.

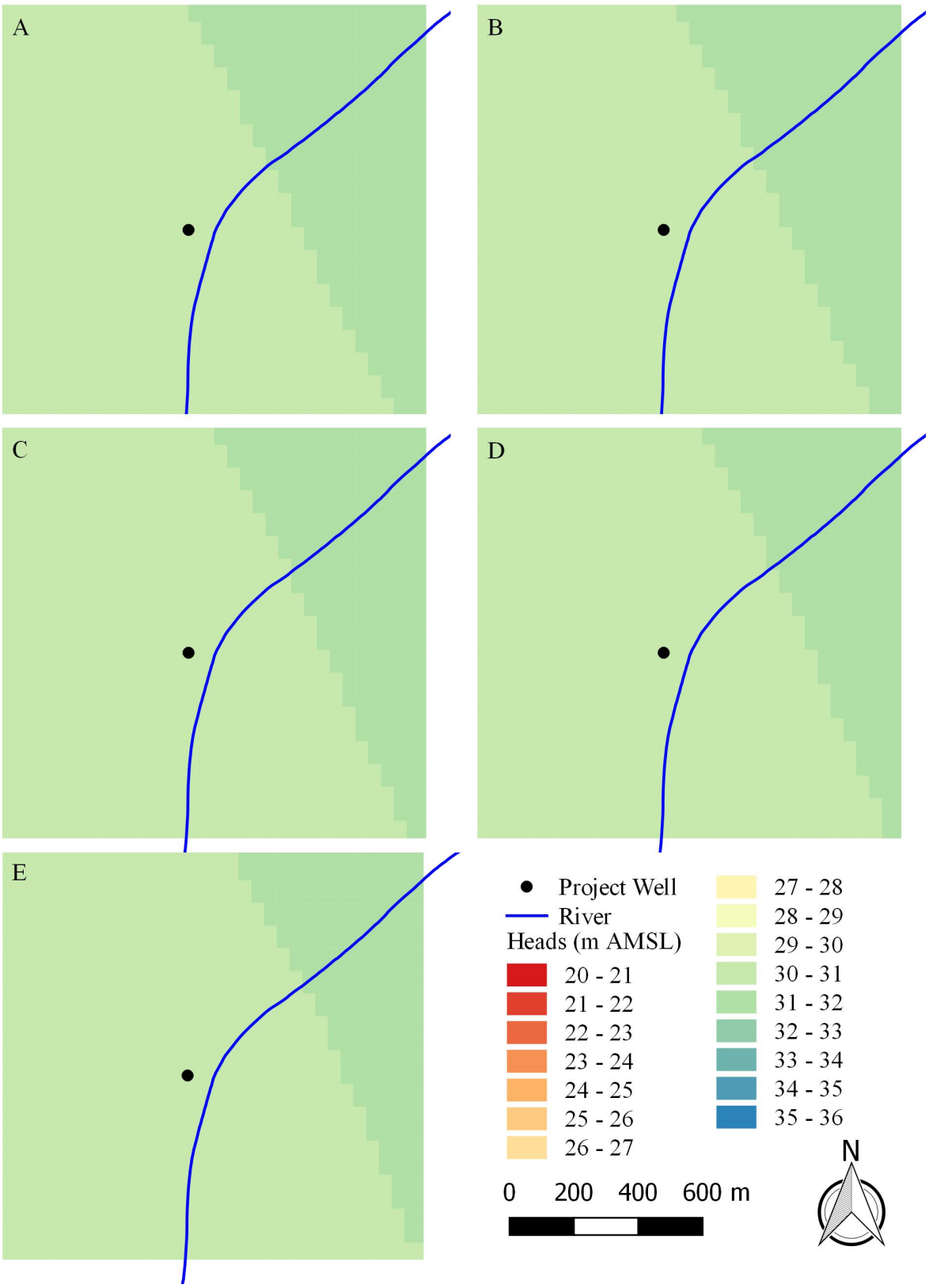

Figure 25: Heads for runs 31 - 35 (A - E, respectively). High aquifer conductivity scenario.

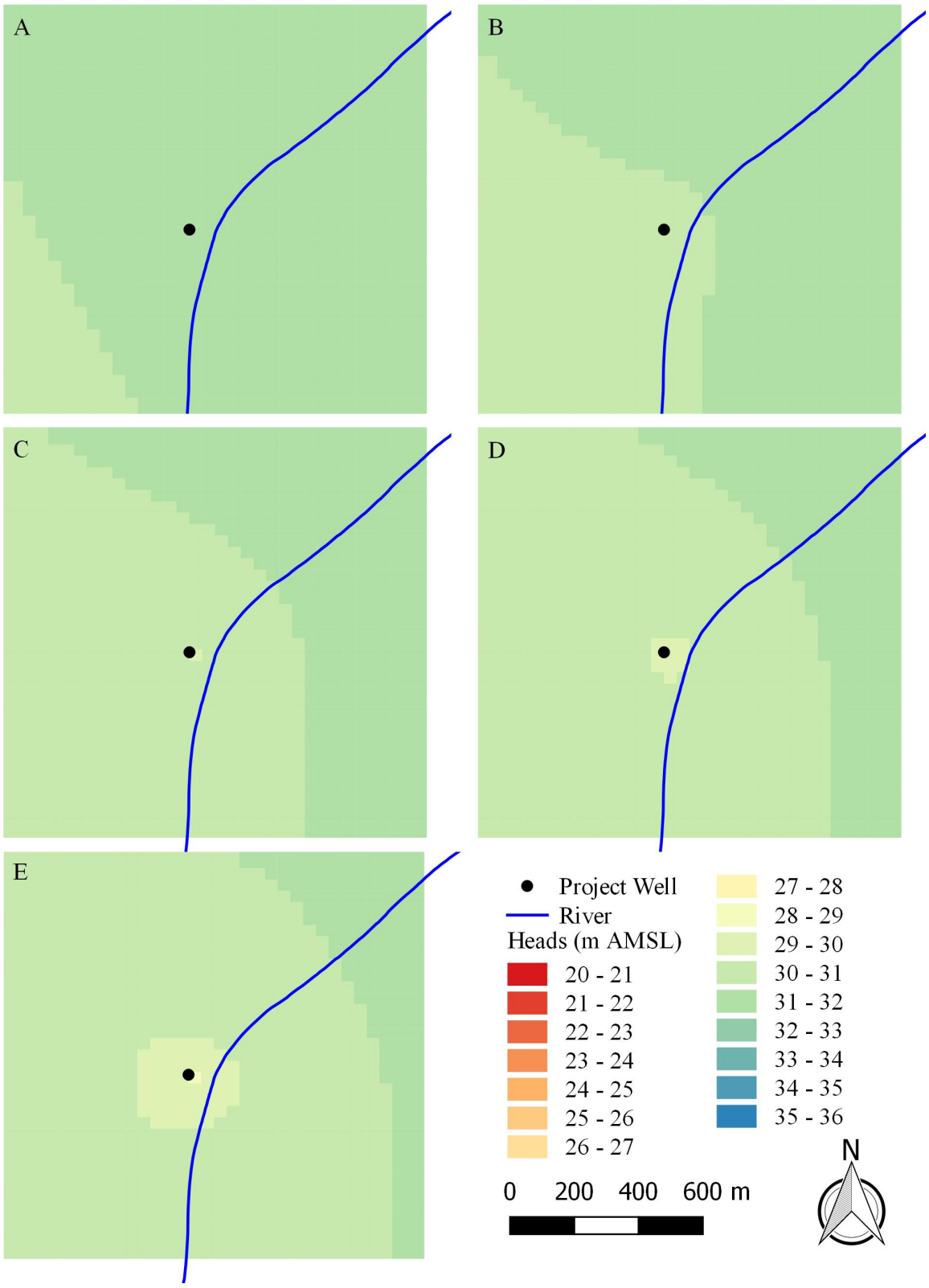

Figure 26: Heads for runs 36 - 40 (A - E, respectively). Low river conductance and extended pumping duration scenario.

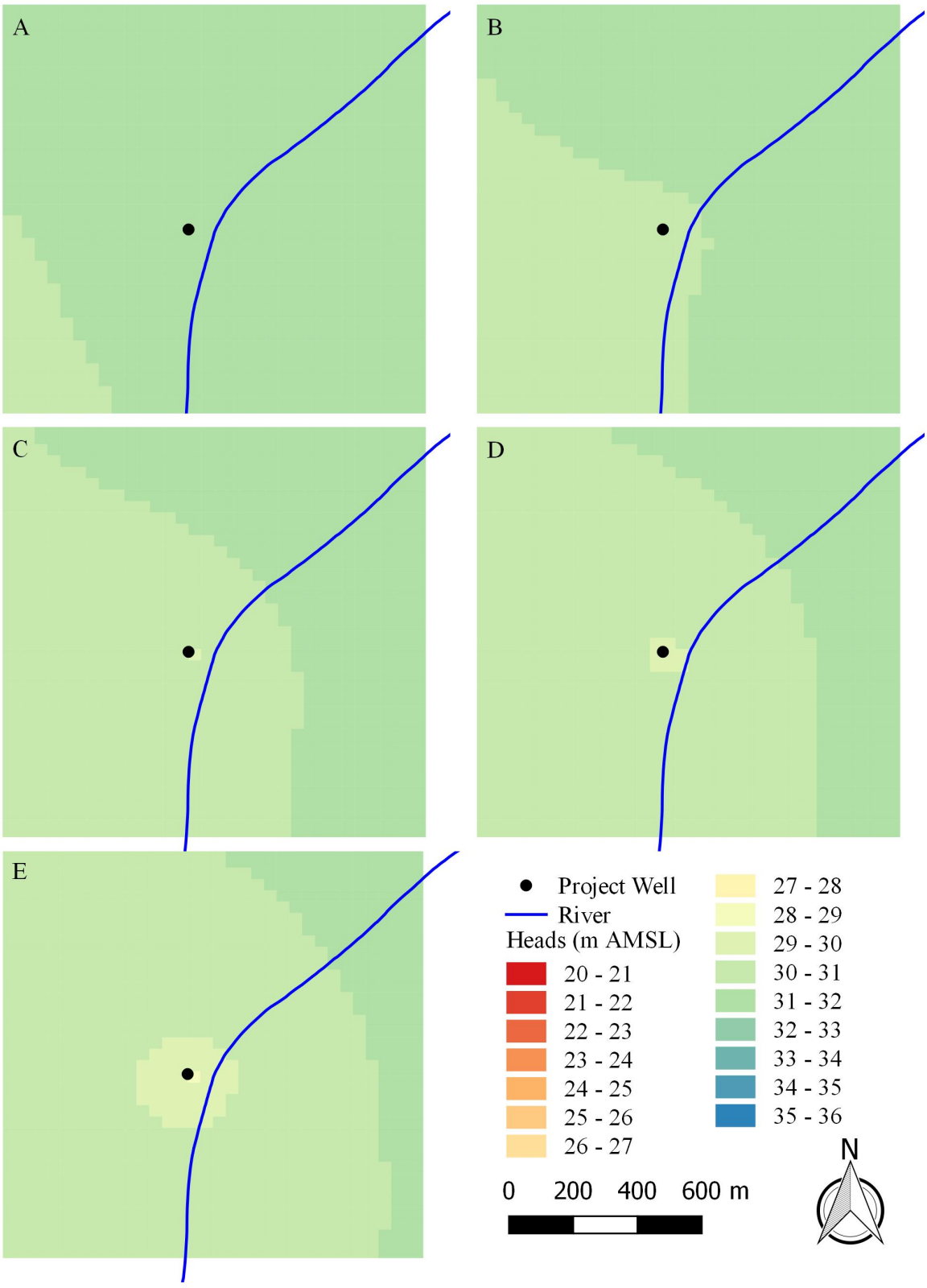

Figure 27: Heads for runs 41 - 45 (A - E, respectively). Medium river conductance and extended pumping duration scenario.

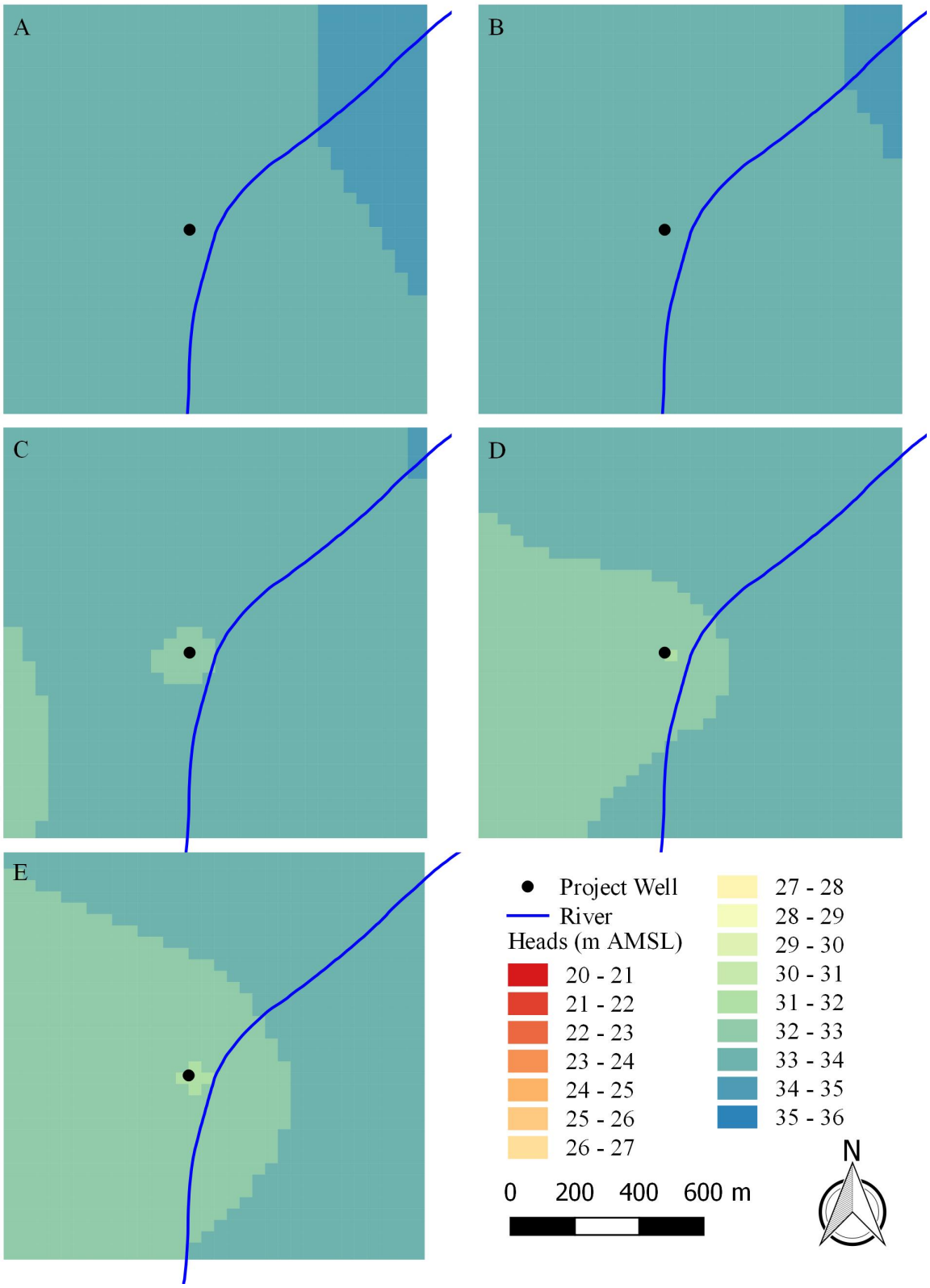

Figure 28: Heads for runs 45 - 50 (A - E, respectively). High river conductance and extended pumping duration scenario.

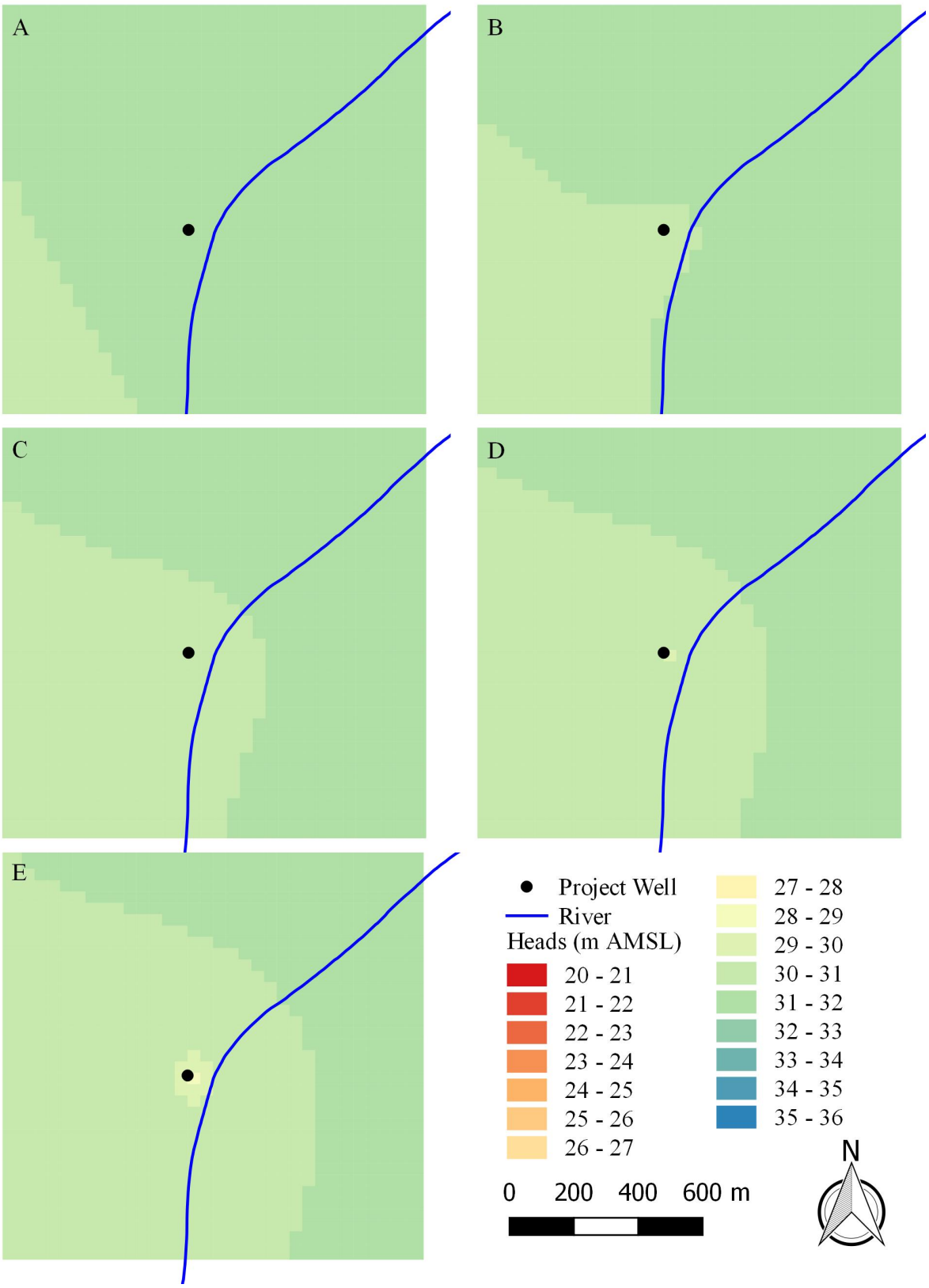

Figure 29: Heads for runs 51 - 55 (A - E, respectively). Low river stage scenario.

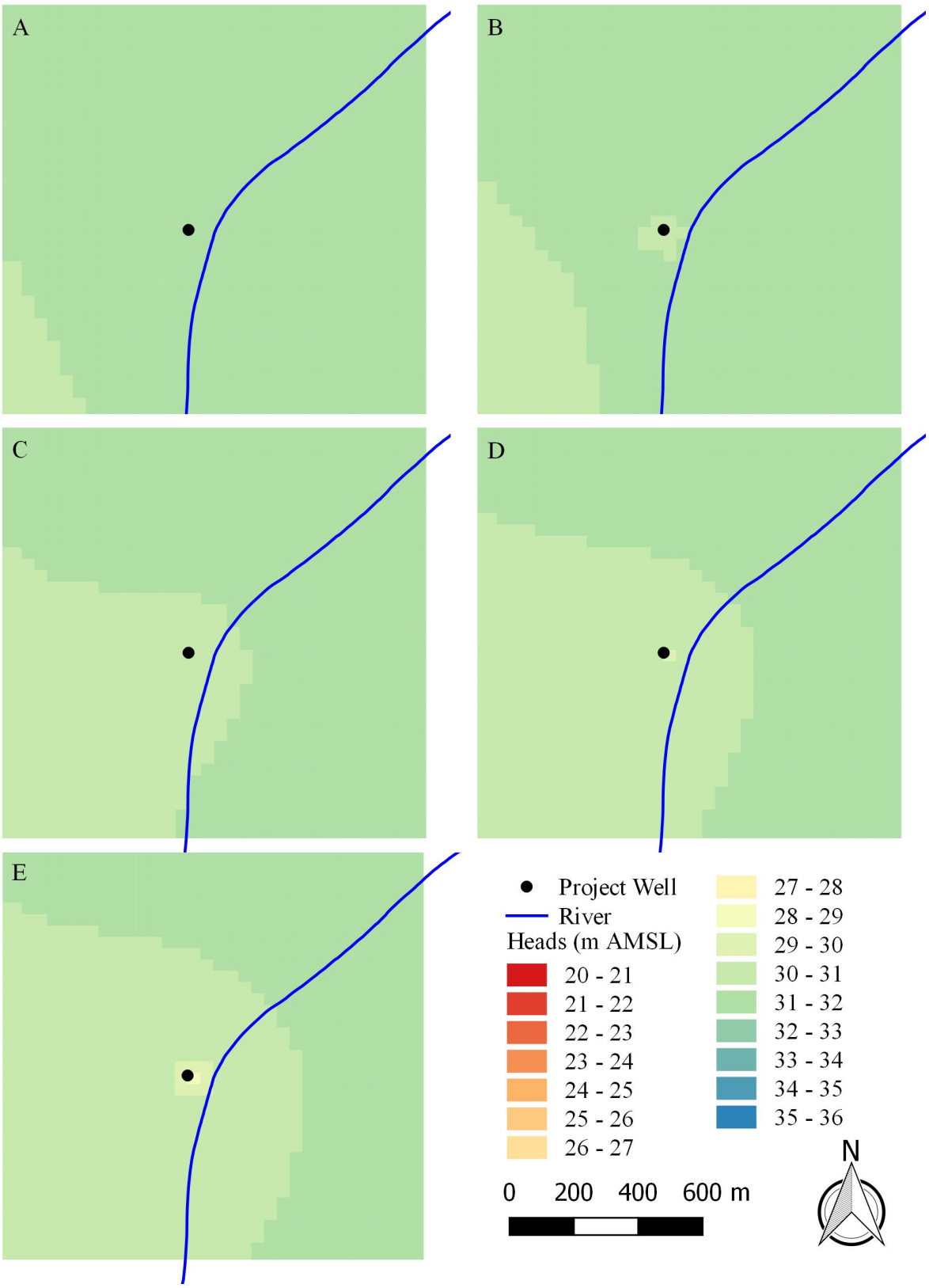

Figure 30: Heads for runs 55 - 60 (A - E, respectively). High river stage scenario.

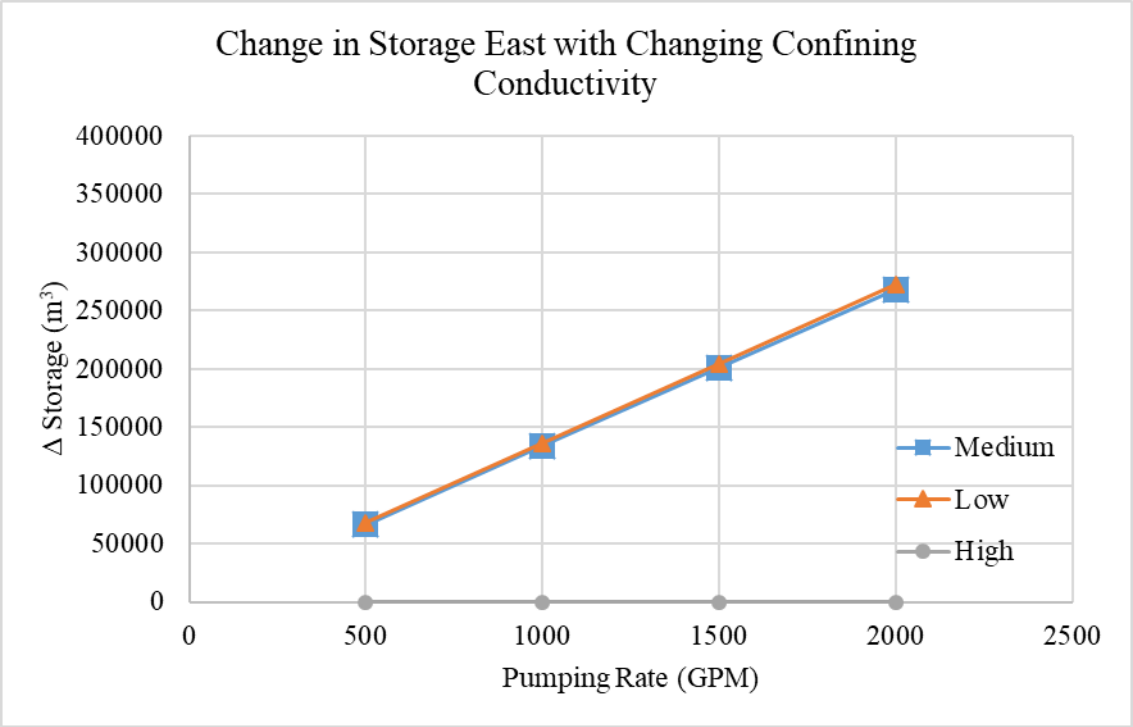

Figure 31: Change in storage in the eastern zone versus pumping rate for low, medium, and high vertical confining layer conductivity.

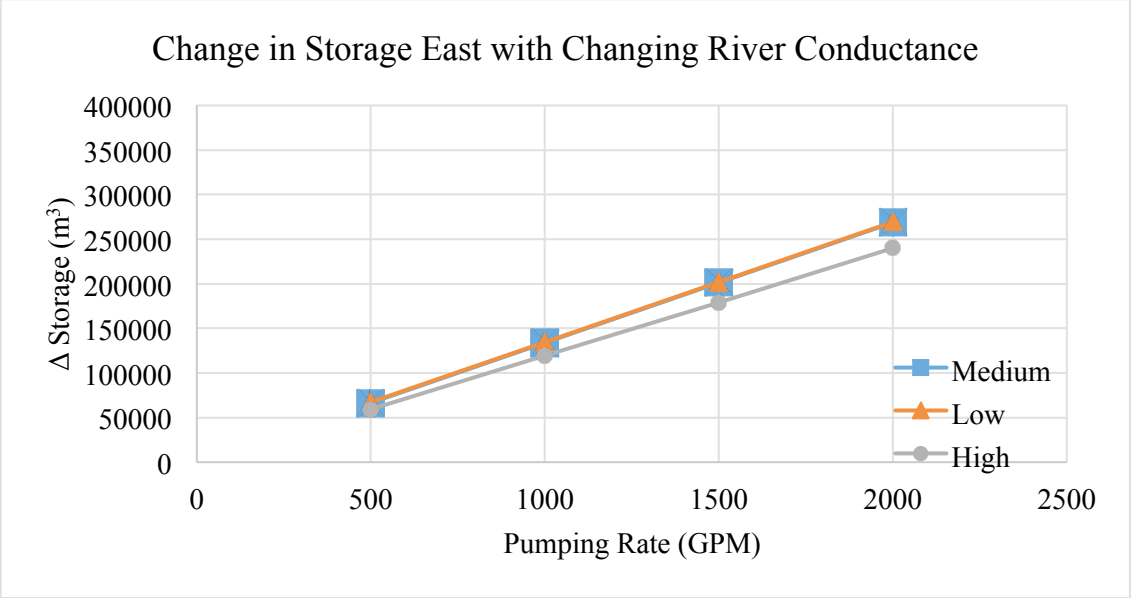

Figure 32: Change in storage in the eastern zone versus pumping rate for low, medium, and high river conductance scenarios.

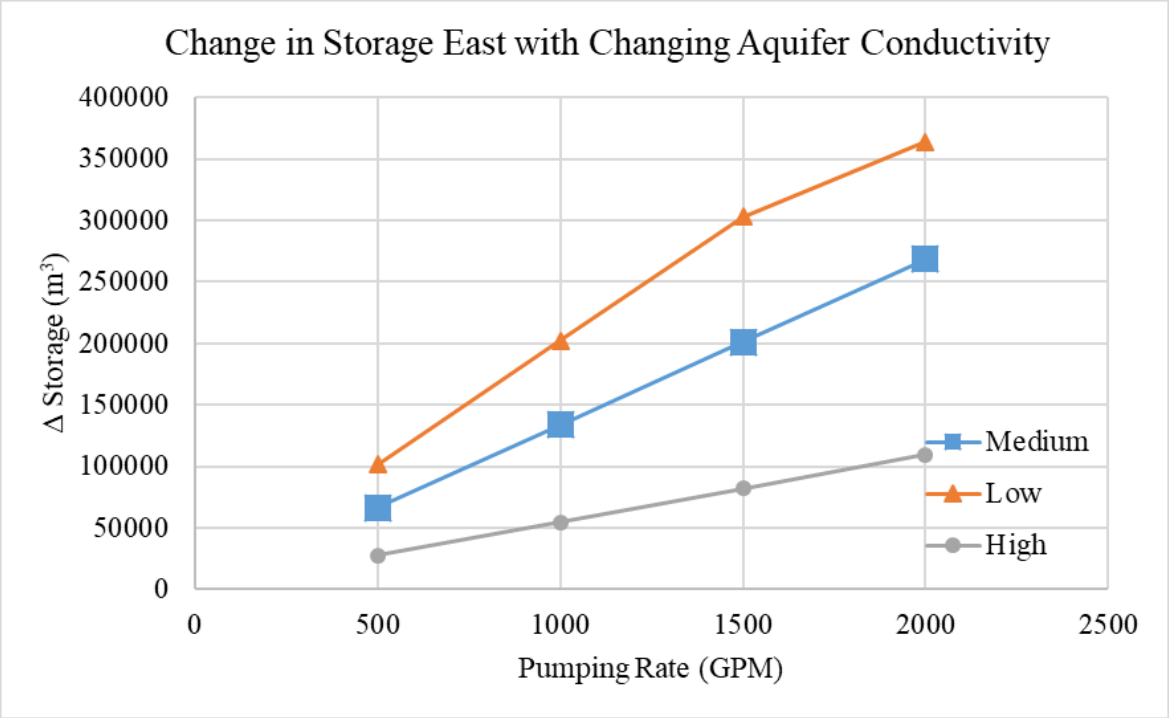

Figure 33: Change in storage in the eastern zone versus pumping rate for low, medium, and high aquifer conductivity scenarios.

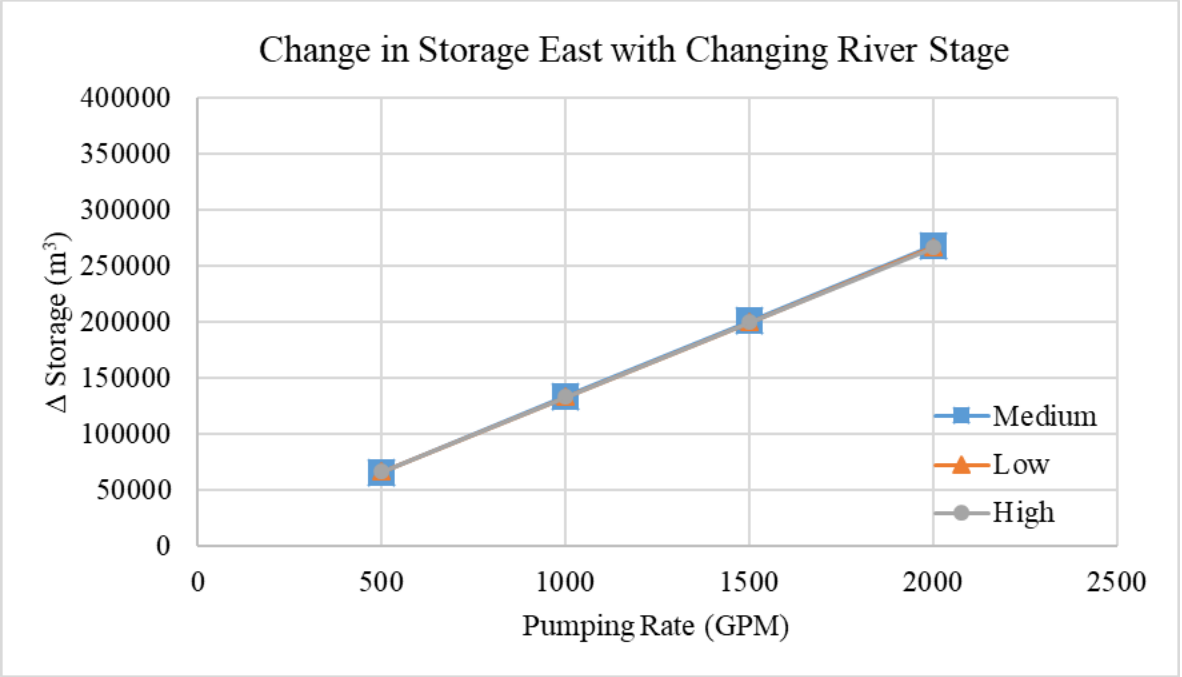

Figure 34: Change in storage in the eastern zone versus pumping rate for low, medium, and river stage scenarios.

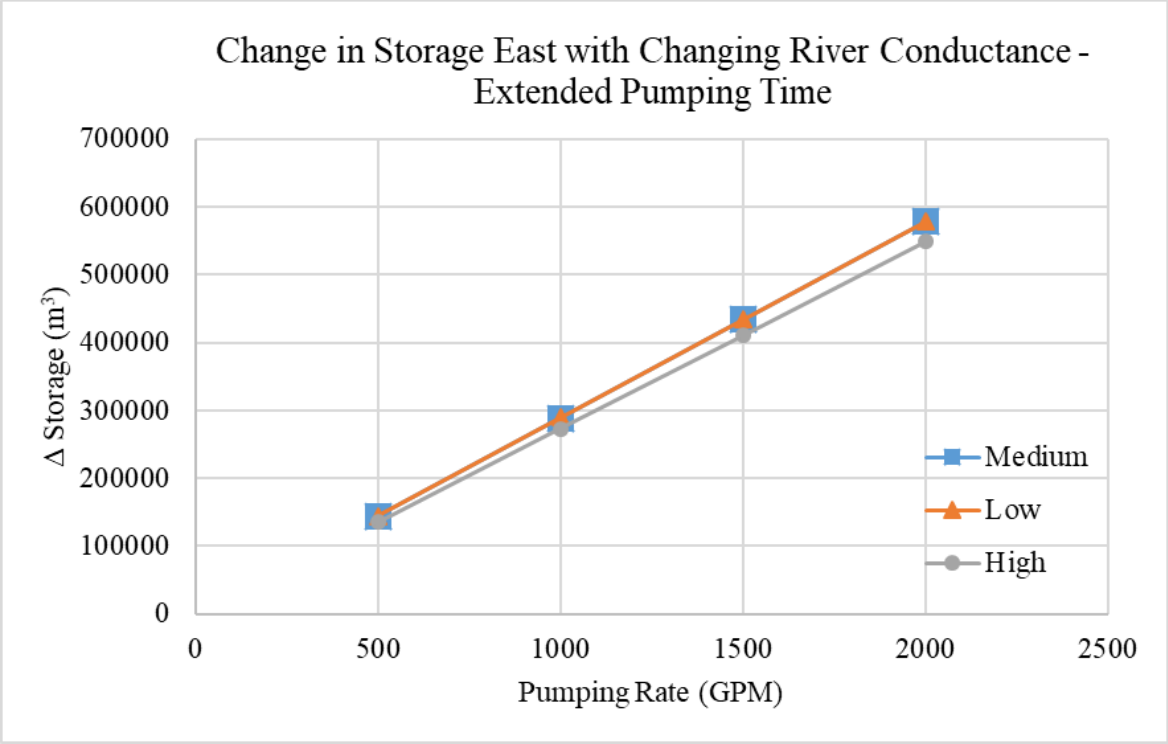

Figure 35: Change in storage in the eastern zone versus pumping rate for the extended pumping scenarios.

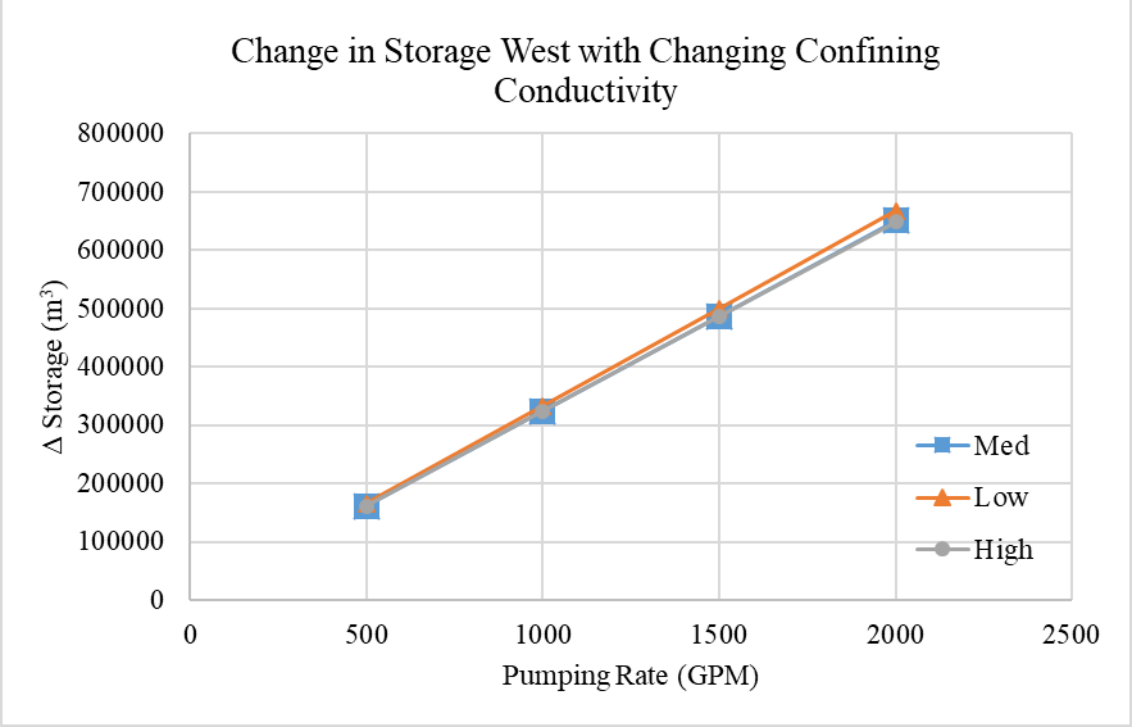

Figure 36: Change in storage in the western zone versus pumping rate for low, medium, and high vertical confining layer conductivity.

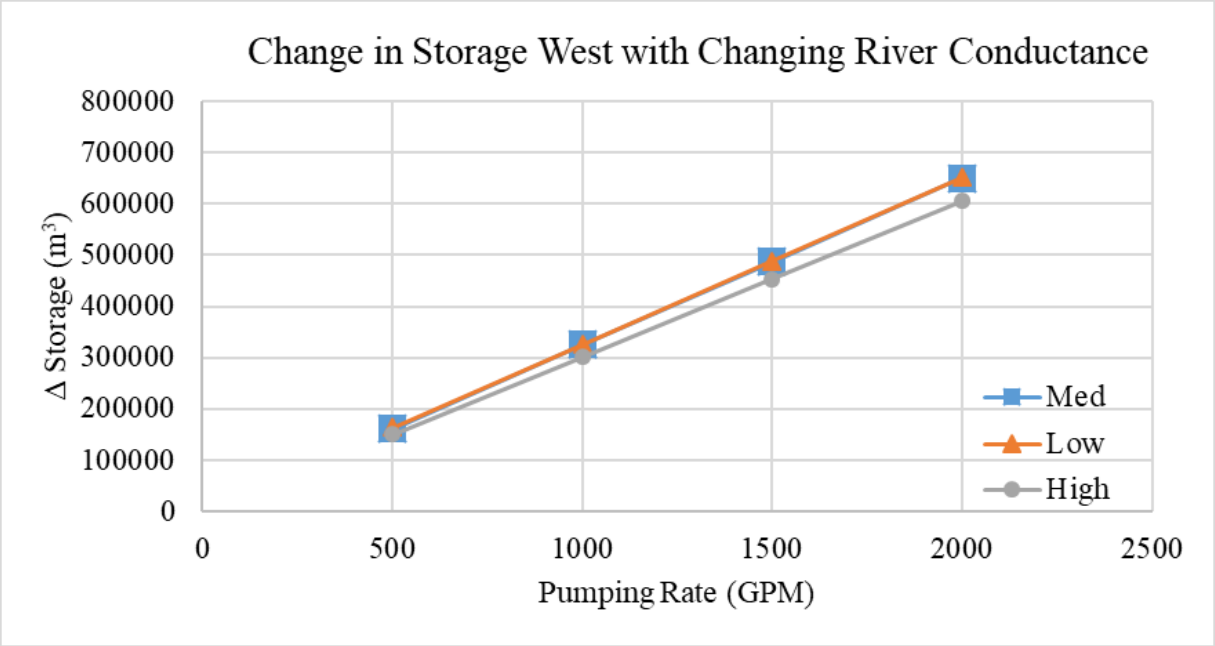

Figure 37: Change in storage in the western zone versus pumping rate for low, medium, and high river conductance scenarios.

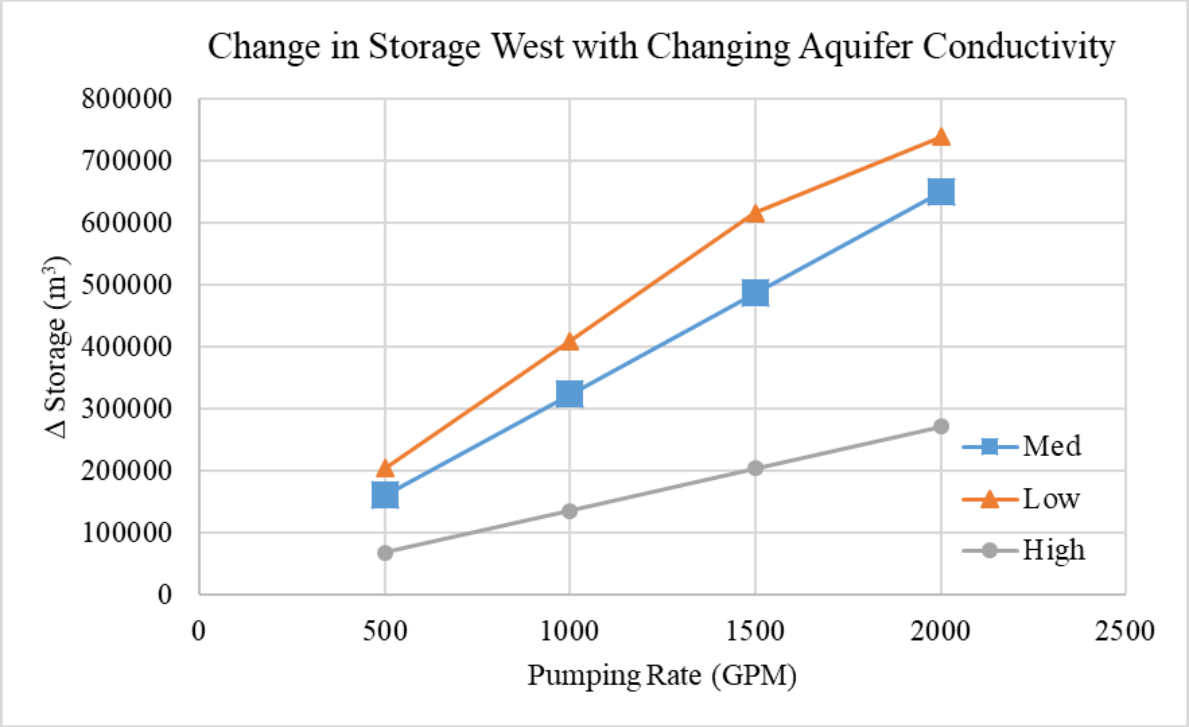

Figure 38: Change in storage in the western zone versus pumping rate for low, medium, and high aquifer conductivity scenarios.

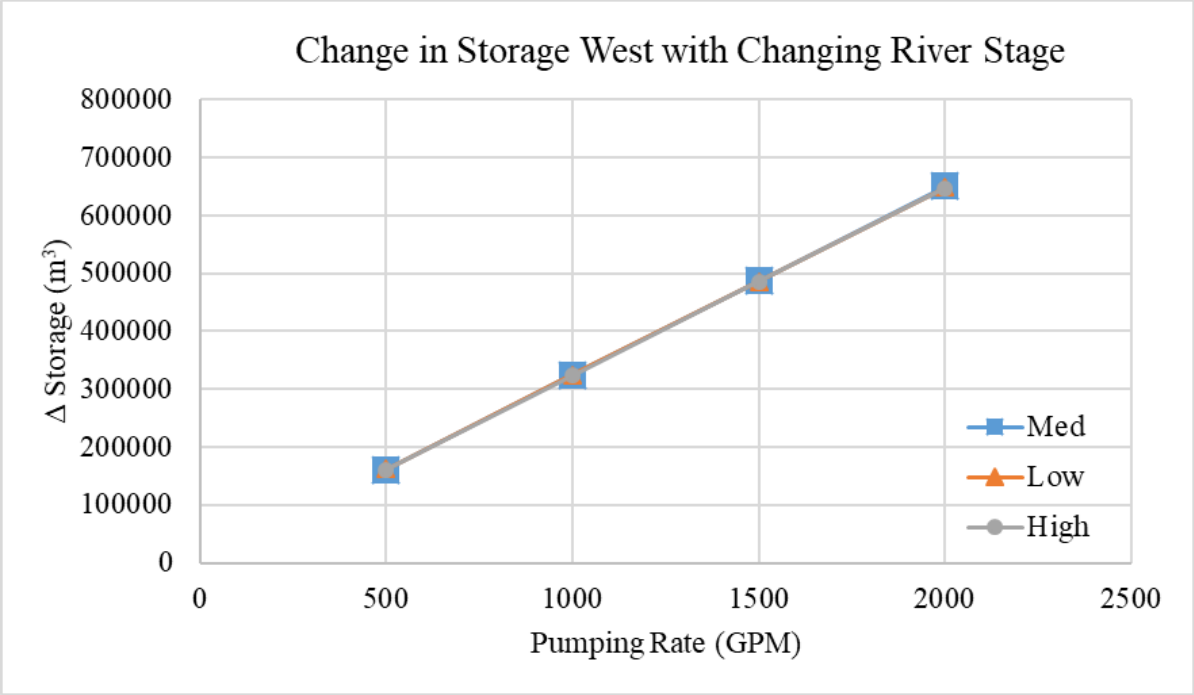

Figure 39: Change in storage in the western zone versus pumping rate for low, medium, and river stage scenarios.

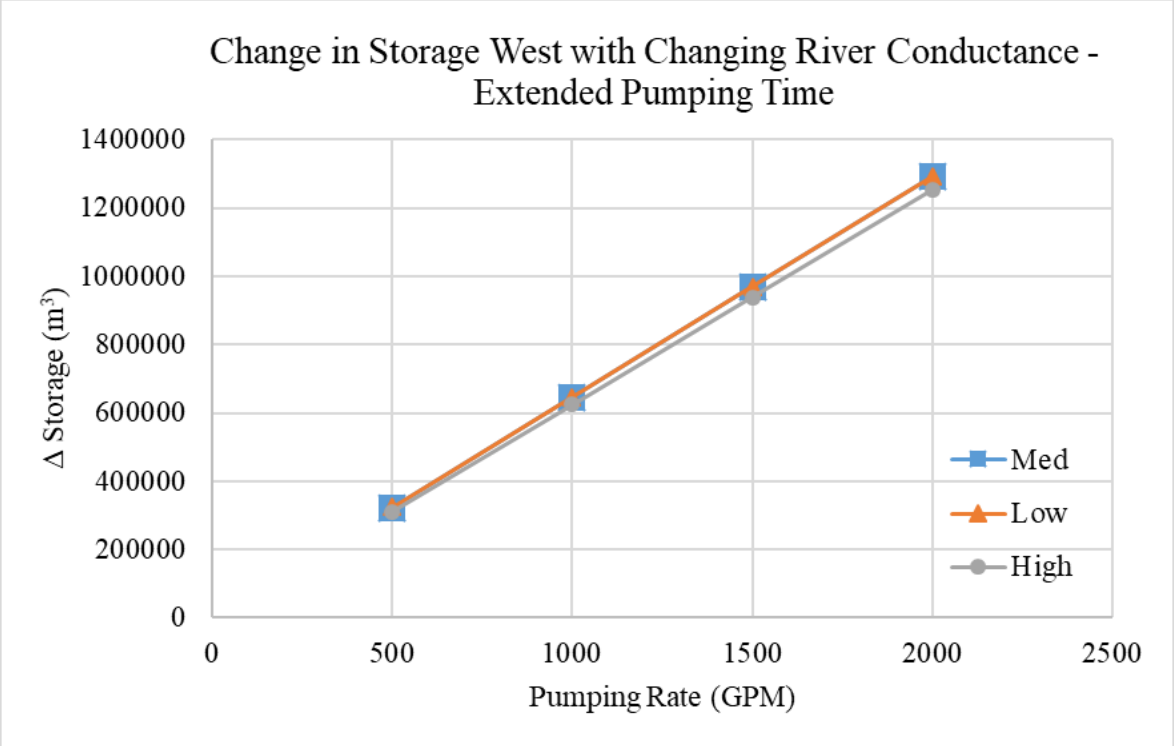

Figure 40: Change in storage in the western zone versus pumping rate for the extended pumping scenarios.

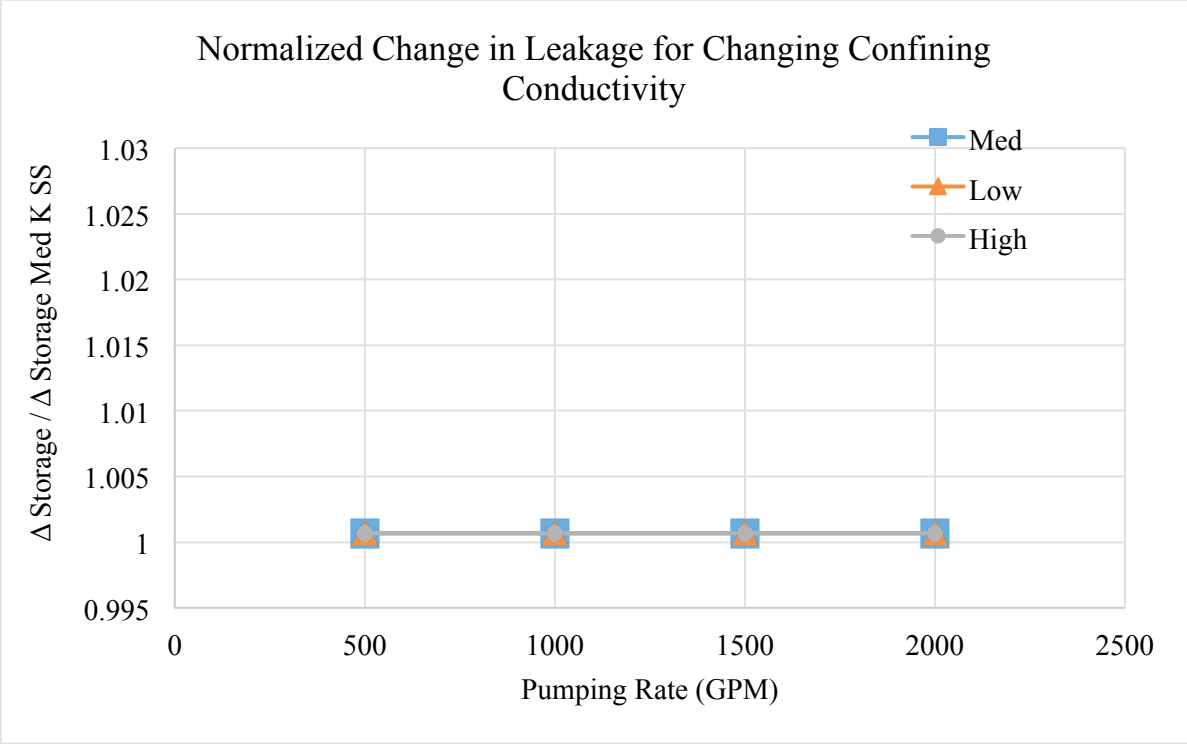

Figure 41: Chart for the change in leakage normalized to the steady state scenario for changing confining conductivity.

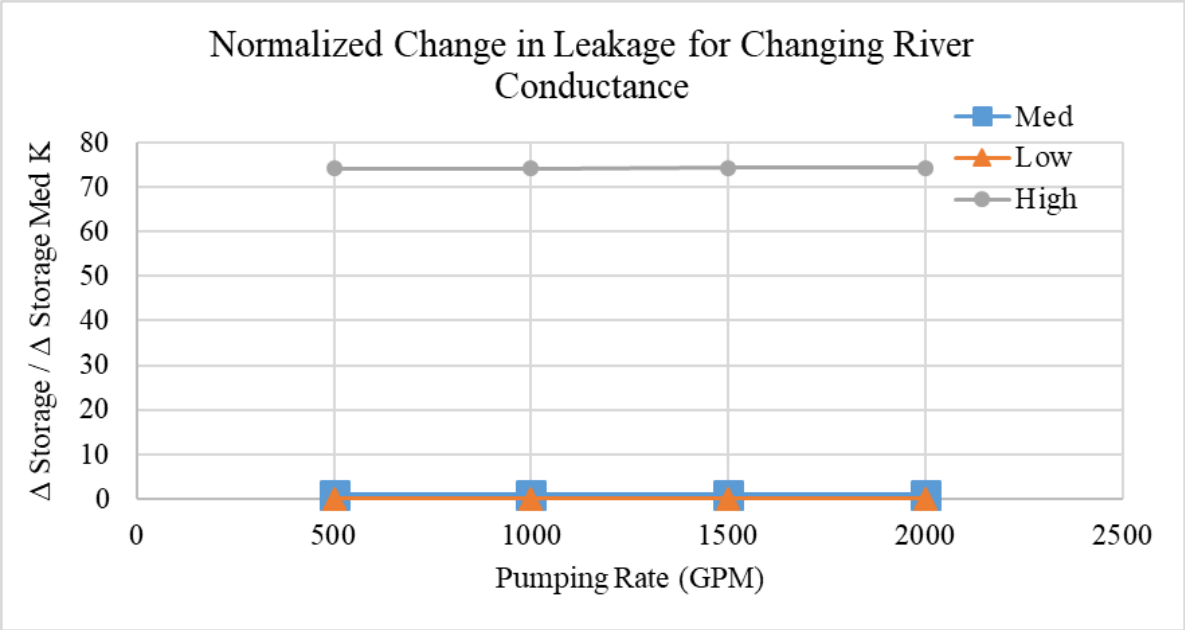

Figure 42: Chart for the change in leakage normalized to the steady state scenario for changing river conductance.

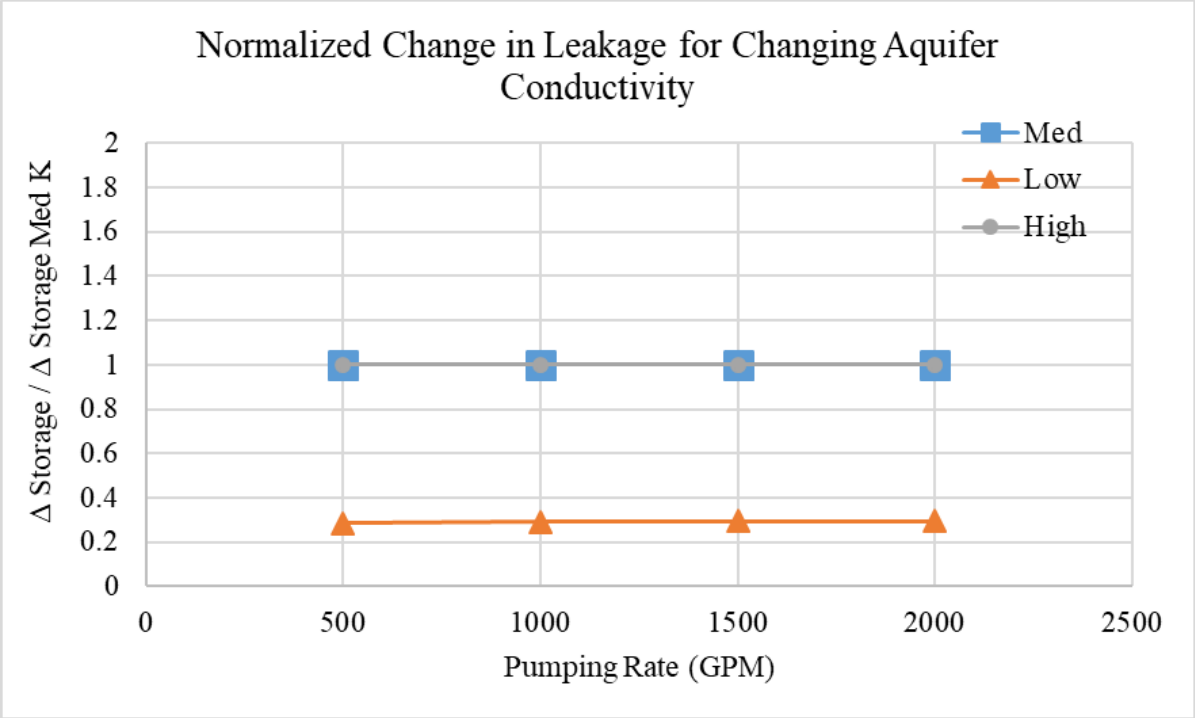

Figure 43: Chart for the change in leakage normalized to the steady state scenario for changing aquifer conductivity.

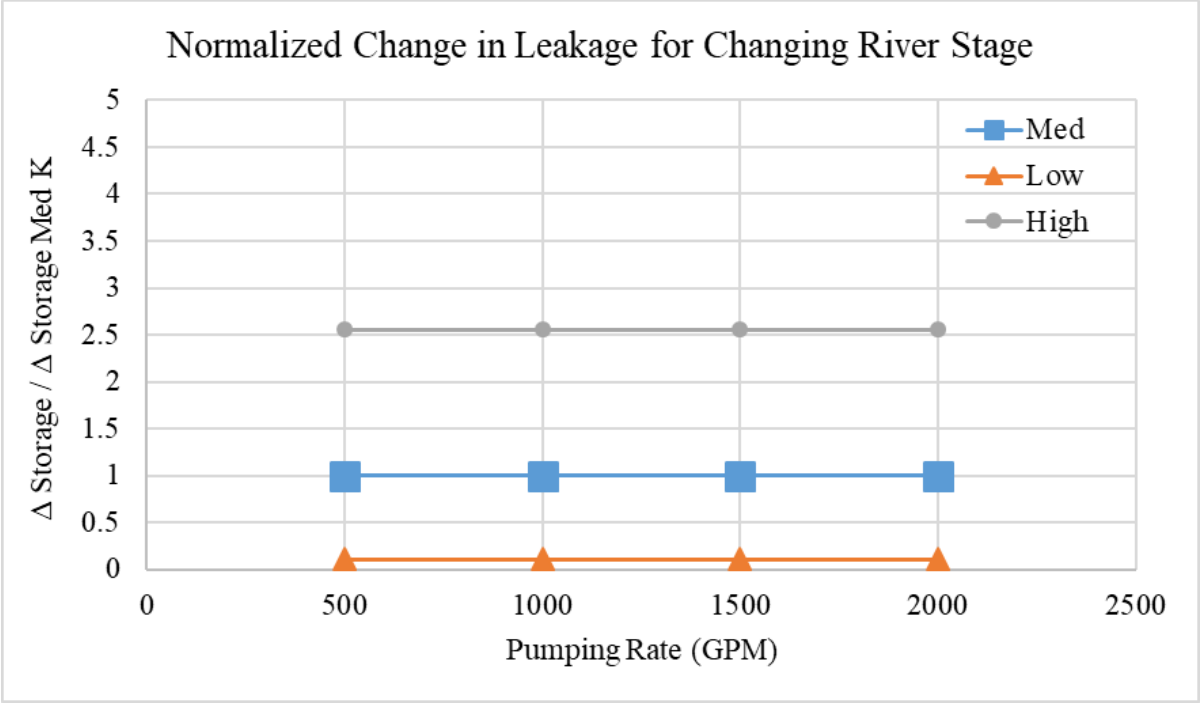

Figure 44: Chart for the change in leakage normalized to the steady state scenario for changing river stage.

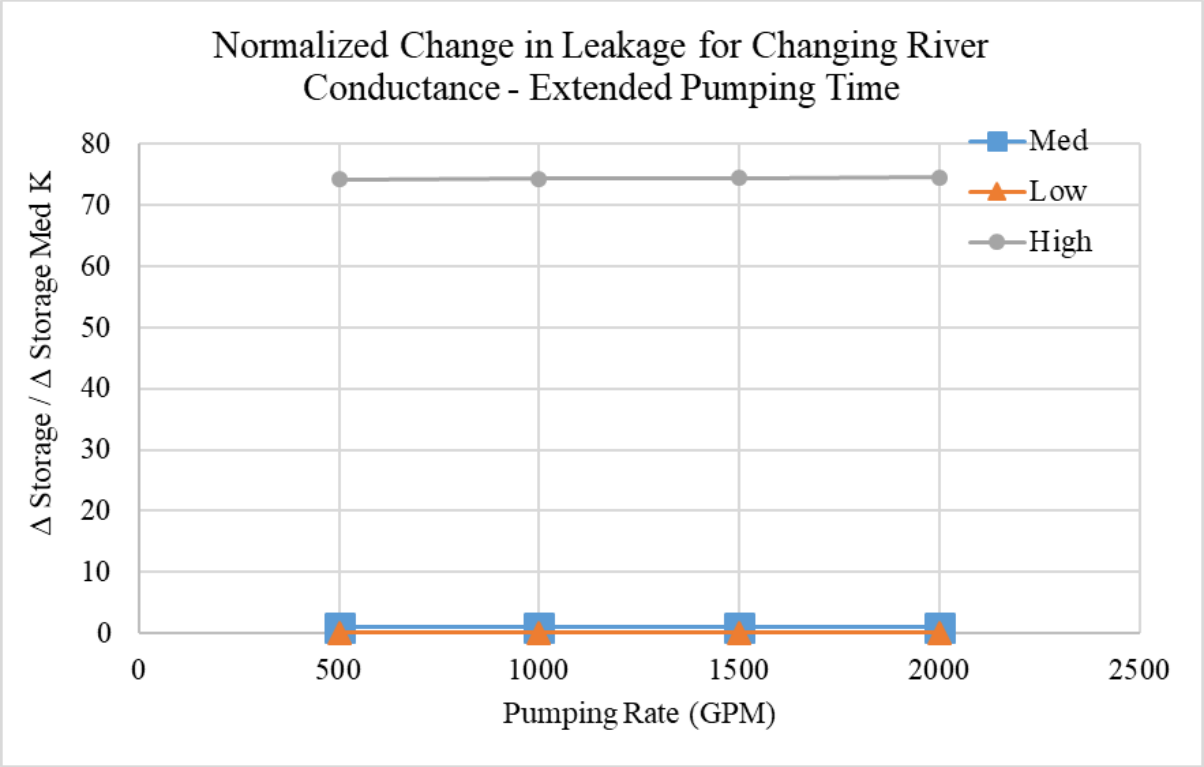

Figure 45: Chart for the change in leakage normalized to the steady state scenario for the extended pumping duration scenarios.

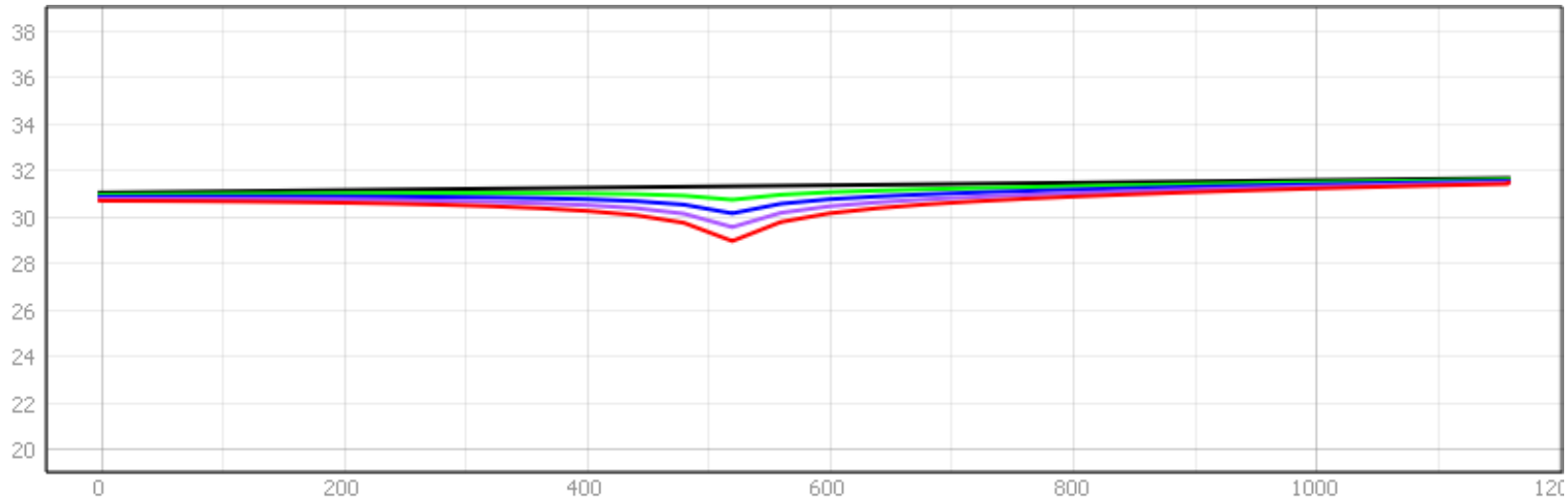

Figure 46: Water table profiles from West (0 m) to East (1150 m) through the pumping well for steady state and 500, 1000, 1500, and 2000 GPM. Measured in meters AMSL on y-axis. Low confining layer conductivity scenario.

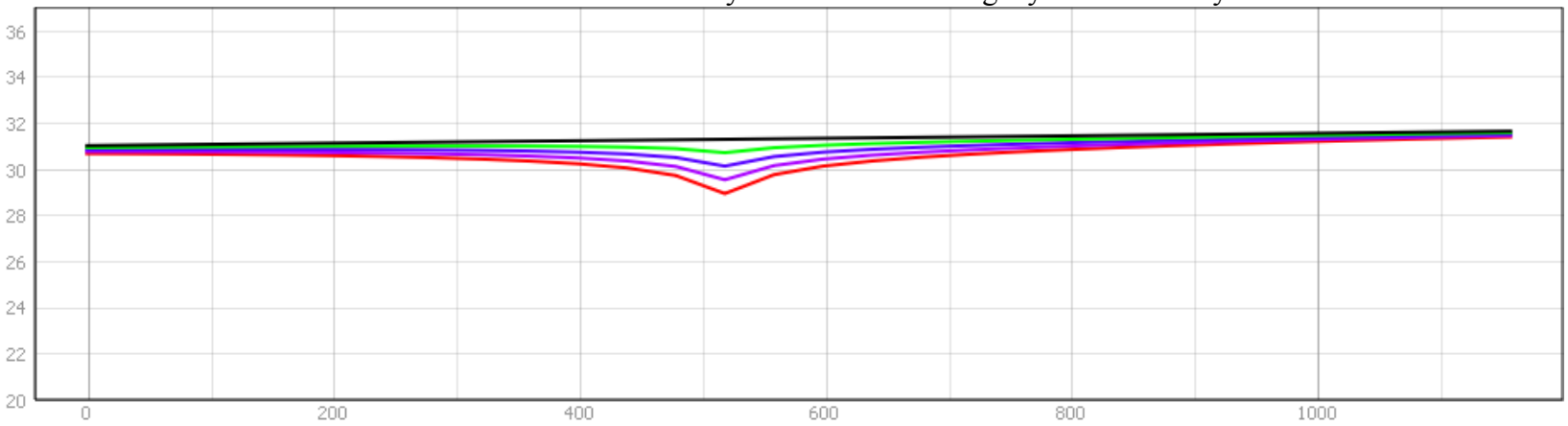

Figure 47: Water table profiles from West (0 m) to East (1150 m) through the pumping well for steady state and 500, 1000, 1500, and 2000 GPM. Measured in meters AMSL on y-axis. Base case scenario.

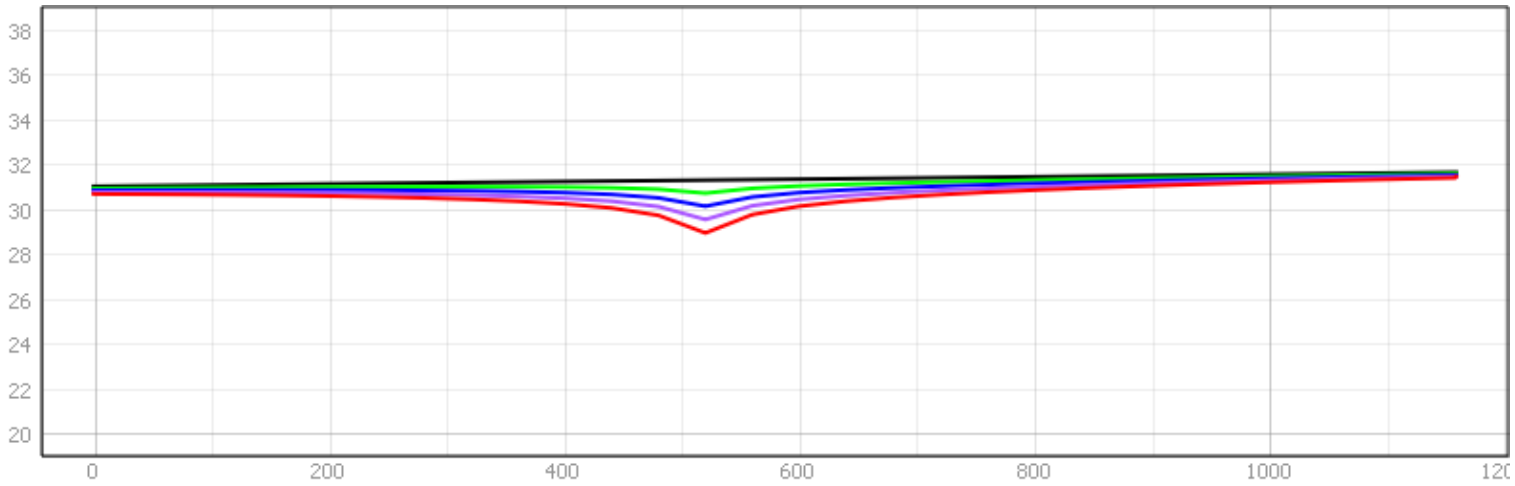

Figure 48: Water table profiles from West (0 m) to East (1150 m) through the pumping well for steady state and 500, 1000, 1500, and 2000 GPM. Measured in meters AMSL on y-axis. High confining layer conductivity scenario.

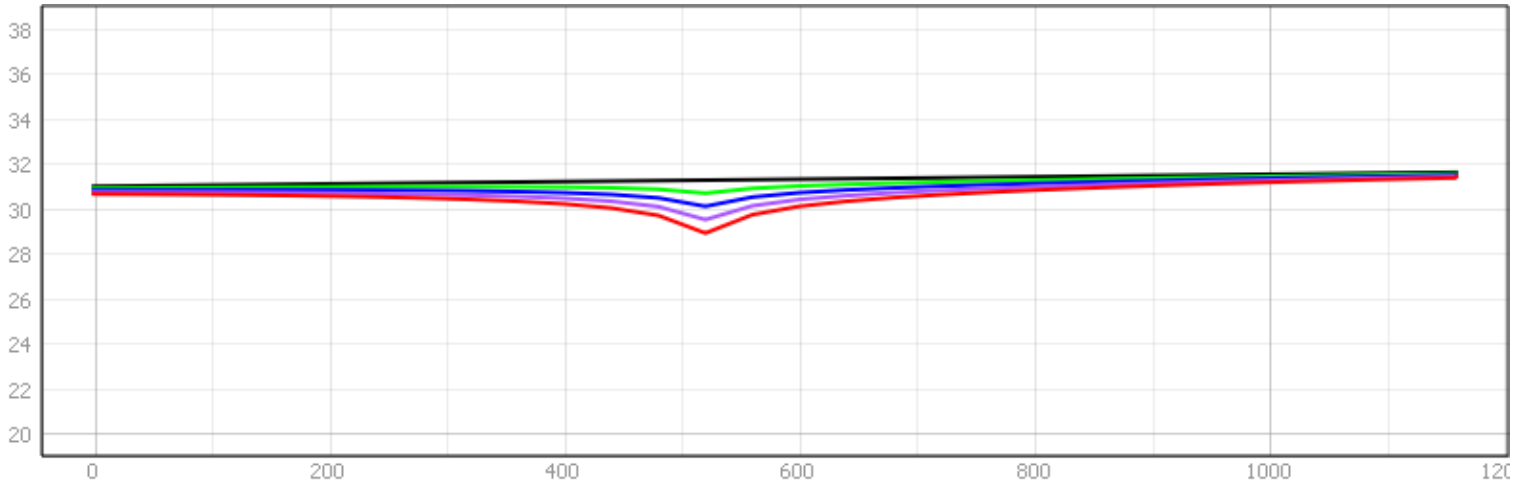

Figure 49: Water table profiles from West (0 m) to East (1150 m) through the pumping well for steady state and 500, 1000, 1500, and 2000 GPM. Measured in meters AMSL on y-axis. Low river conductance scenario.

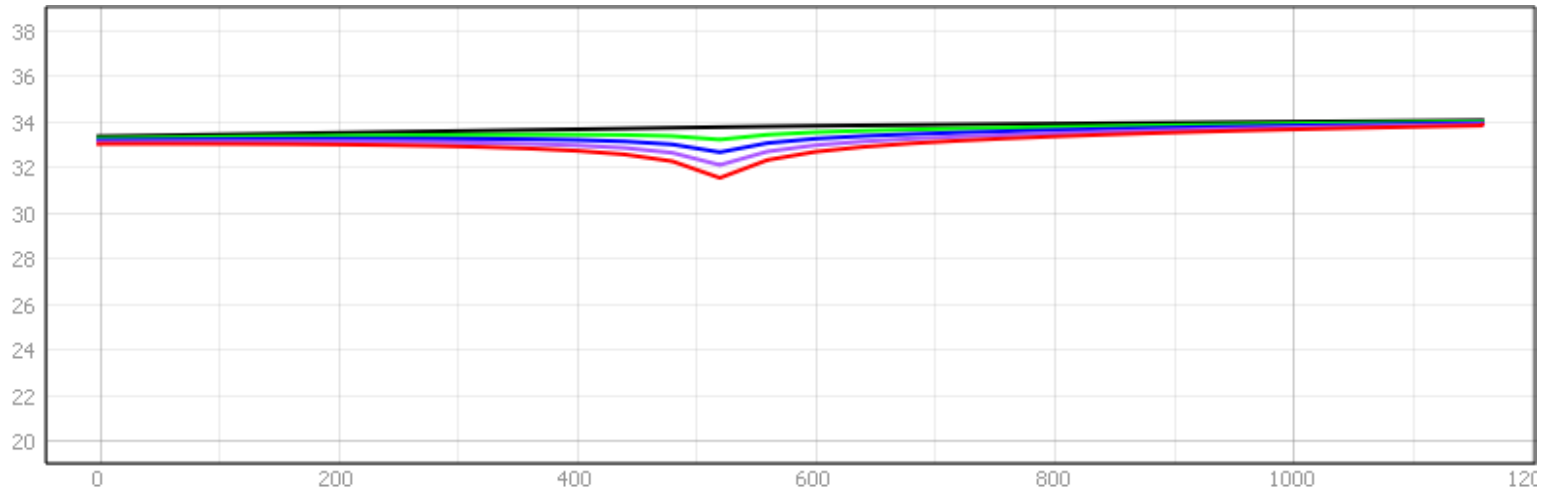

Figure 50: Water table profiles from West (0 m) to East (1150 m) through the pumping well for steady state and 500, 1000, 1500, and 2000 GPM. Measured in meters AMSL on y-axis. High river conductance scenario.

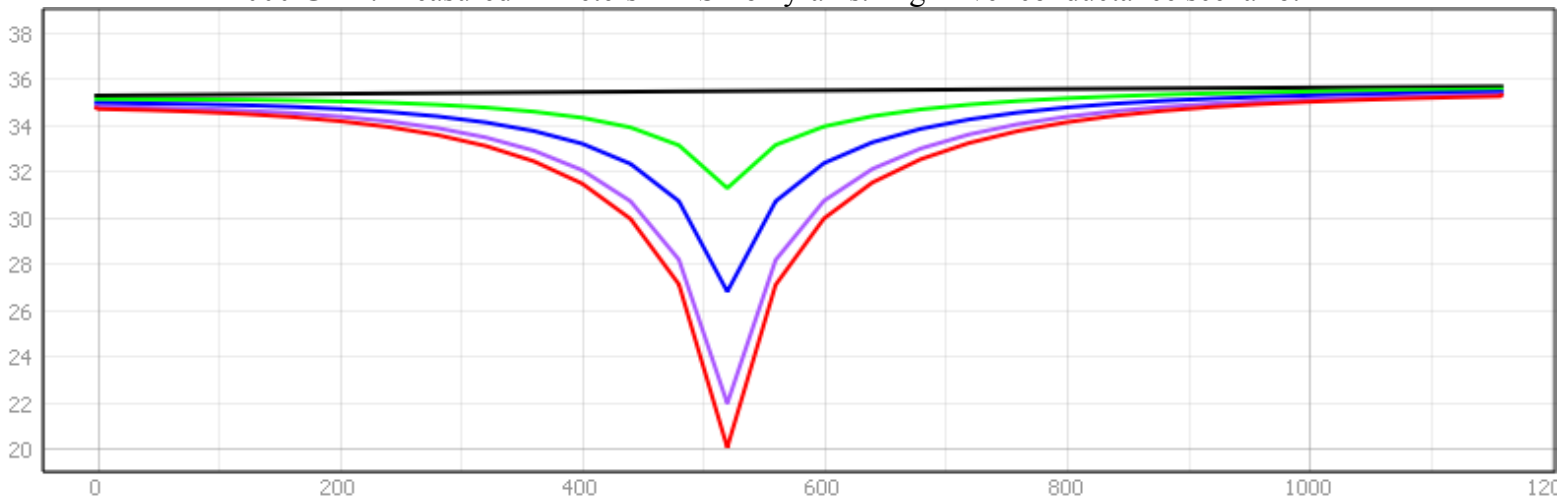

Figure 51: Water table profiles from West (0 m) to East (1150 m) through the pumping well for steady state and 500, 1000, 1500, and 2000 GPM. Measured in meters AMSL on y-axis. Low aquifer conductivity scenario.

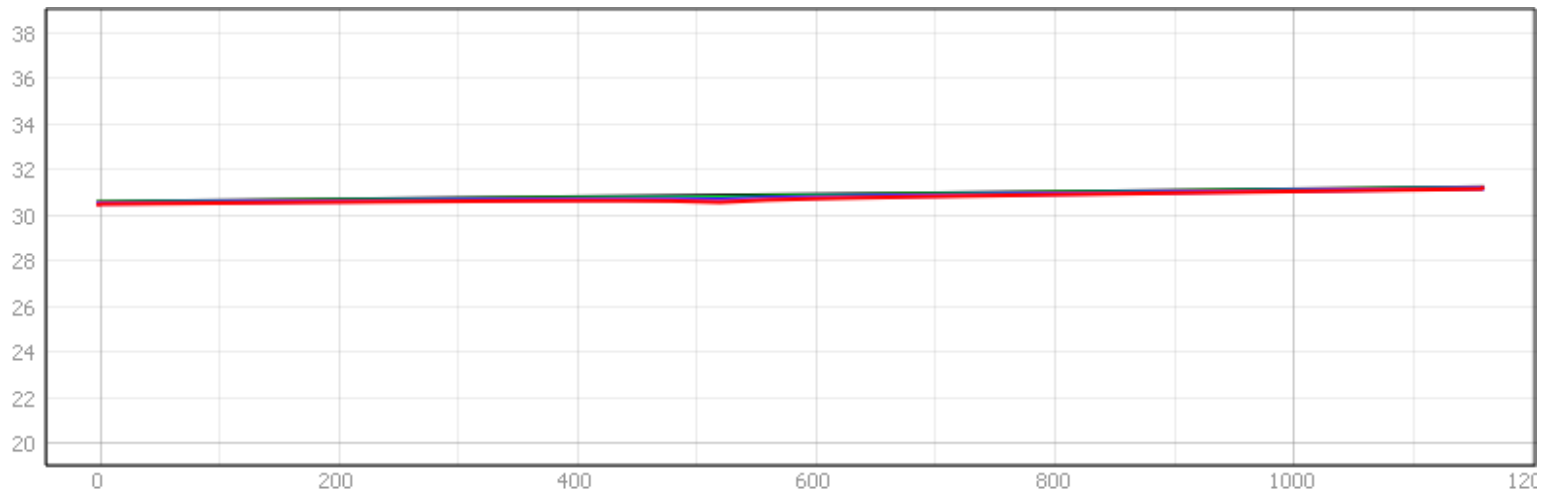

Figure 52: Water table profiles from West (0 m) to East (1150 m) through the pumping well for steady state and 500, 1000, 1500, and 2000 GPM. Measured in meters AMSL on y-axis. High aquifer conductivity scenario.

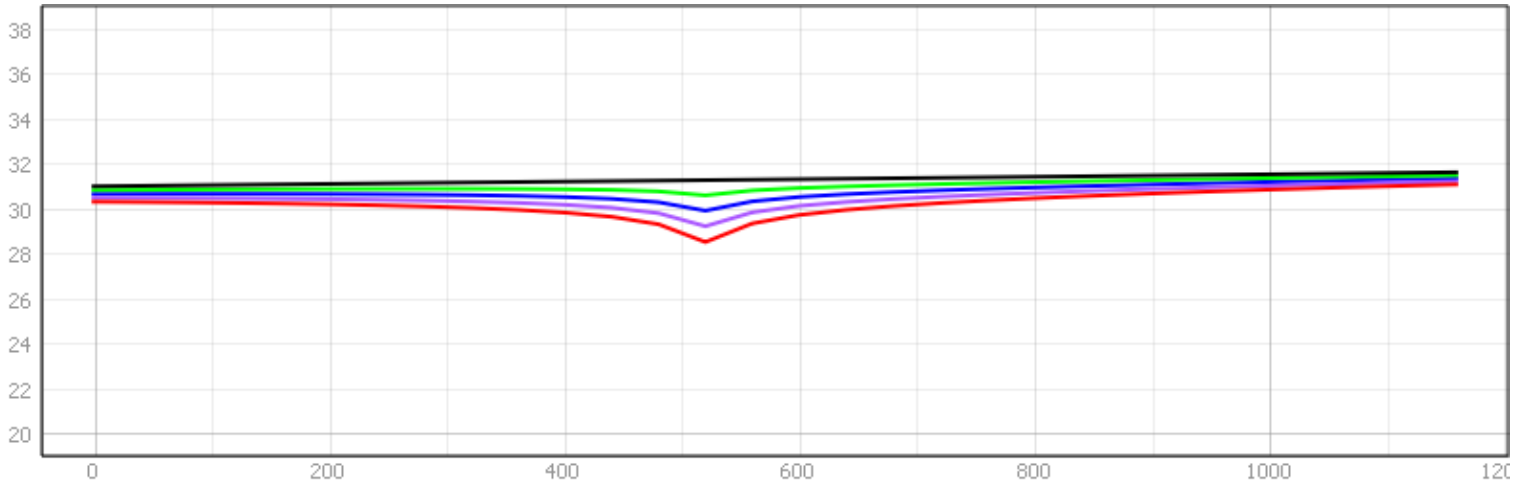

Figure 53: Water table profiles from West (0 m) to East (1150 m) through the pumping well for steady state and 500, 1000, 1500, and 2000 GPM. Measured in meters AMSL on y-axis. Low river conductance and extended pumping duration scenario.

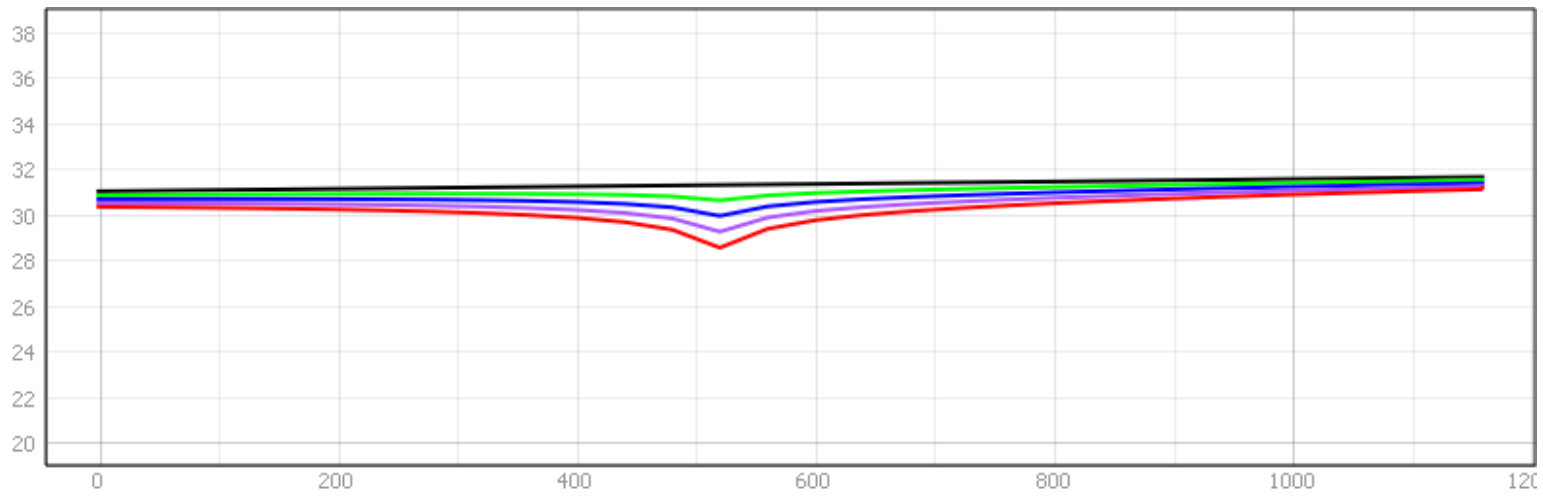

Figure 54: Water table profiles from West (0 m) to East (1150 m) through the pumping well for steady state and 500, 1000, 1500, and 2000 GPM. Measured in meters AMSL on y-axis. Medium river conductance and extended pumping duration scenario.

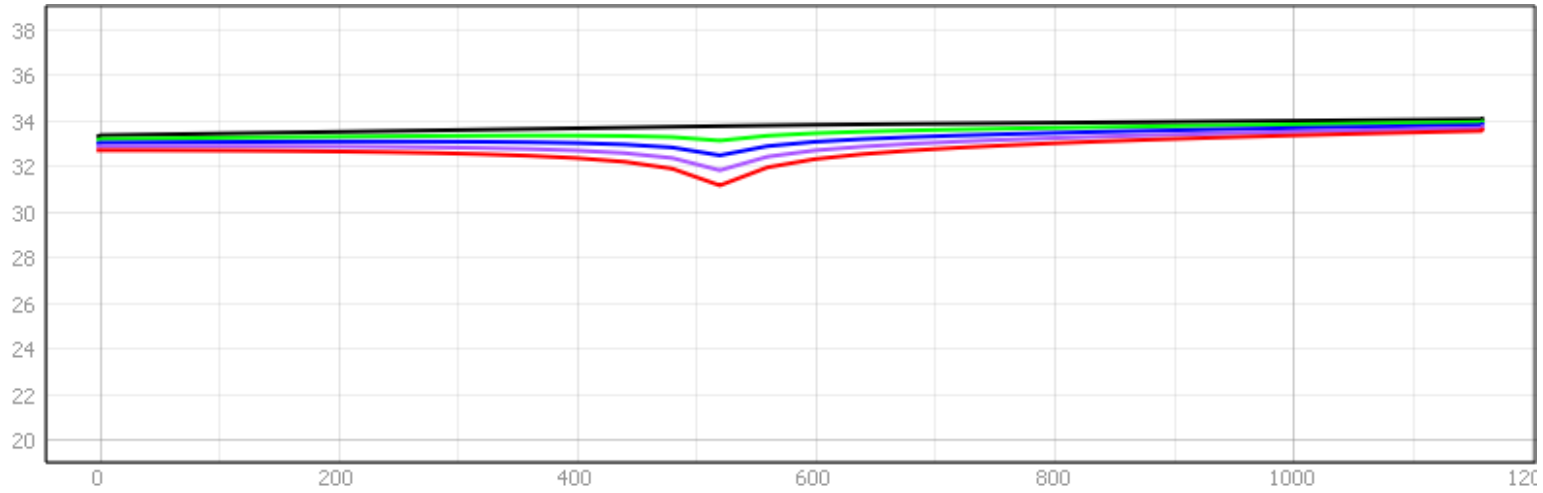

Figure 55: Water table profiles from West (0 m) to East (1150 m) through the pumping well for steady state and 500, 1000, 1500, and 2000 GPM. Measured in meters AMSL on y-axis. High river conductance and extended pumping duration scenario.

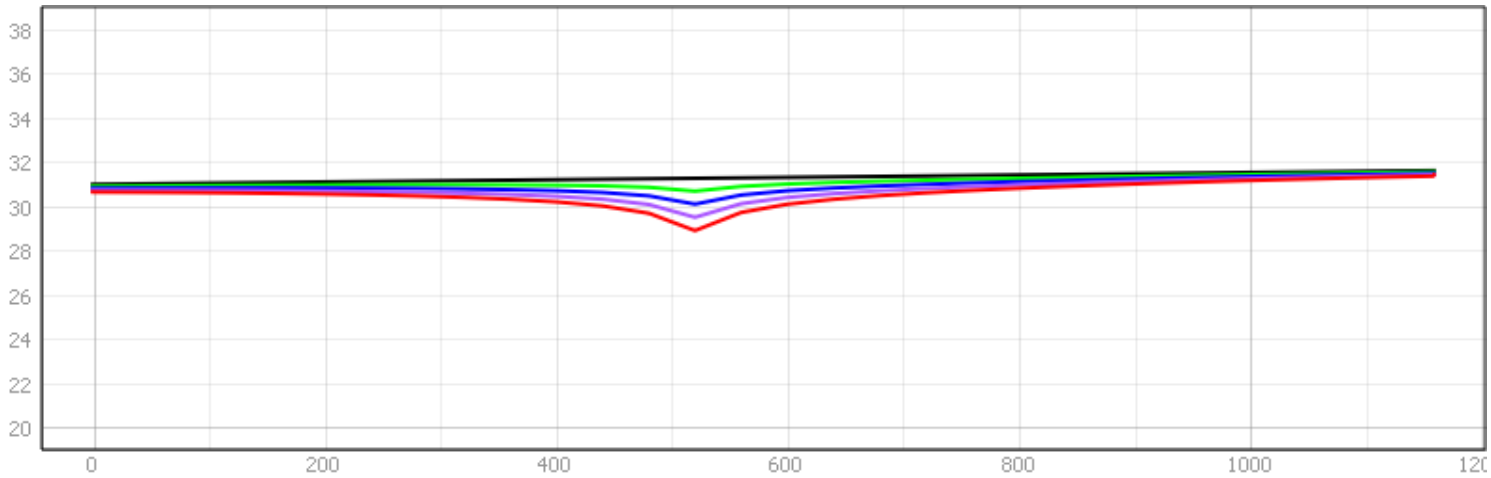

Figure 56: Water table profiles from West (0 m) to East (1150 m) through the pumping well for steady state and 500, 1000, 1500, and 2000 GPM. Measured in meters AMSL on y-axis. Low river stage scenario.

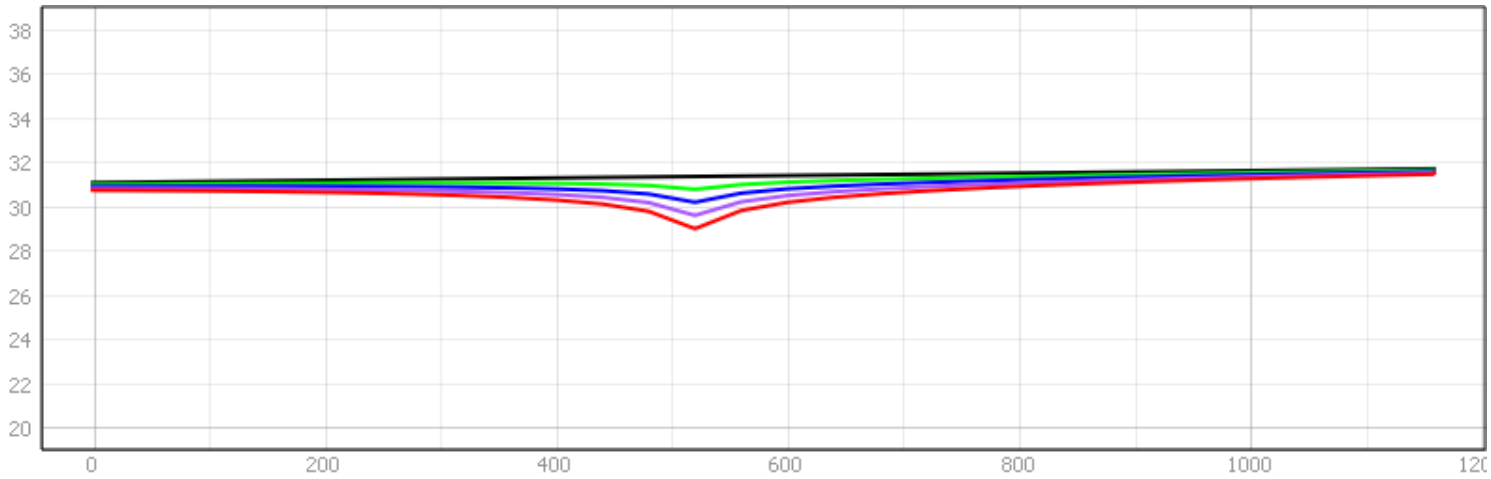

Figure 57: Water table profiles from West (0 m) to East (1150 m) through the pumping well for steady state and 500, 1000, 1500, and 2000 GPM. Measured in meters AMSL on y-axis. High river stage scenario.

V CONCLUDING REMARKS

The Mississippi River Valley Alluvial Aquifer will continue to see groundwater declines with continued large-scale withdrawals for irrigation. Managed aquifer recharge is a viable to solution to this problem, and using surface water filtered through riverbank sediments as source water for a MAR system is particularly advantageous from an economical and technical standpoint. Investigation of such a system is necessary to quantify the amount of water truly withdrawn from surficial flows versus aquifer storage. Of the most concern to the Groundwater Transfer and Injection Project is the overall source of the withdrawal water, whether it is induced from the river or drawn from storage, and the resulting storage and head decreases around the withdrawal well.

In all scenarios modeled, the reduction in storage and maximum head decline is relatively small compared to the total storage and saturated thickness of the MRVAA. While lowering aquifer conductivity increases steady state groundwater levels considerably, it also causes the lowest resulting heads due to excessive drawdown. It is also the only situation that causes a net outflow to river leakage. Higher aquifer conductivity around the withdrawal well will thus be favorable for the project as it decreases both the maximum head decline and the total reduction in storage.

Also favorable for increasing the amount of water withdrawn from surficial flows is increased pumping duration. As table 9 shows, extended pumping duration causes significantly more water to begin being pulled from the river as the zone of capture is enlarged until an

equilibrium between storage reductions and river leakage is reached. Increasing river conductivity also has a significant impact on the amount of river leakage into the model domain, although this is a less practical variable to control without significant expenditure to dredge or otherwise increase the conductance of the river bottom at the project site. The increase in water from river leakage into the model domain also increases disproportionately with higher pumping rates, suggesting that a higher pumping rate for an extended period of time will maximize the amount of water induced from the river, if the head declines and losses in storage associated with it can be deemed acceptable.

REFERENCES

Ackerman, D. J. (1996). *Hydrology of the Mississippi River Valley Alluvial Aquifer, South-Central United States.* Washington: United States Government Printing Office.

Arthur, K. J. (2001). *Hydrogeology, Model Description, and Flow Analysis of the Mississippi River Alluvial Aquifer in Northwestern Mississippi.* Reston, VA: U.S. Geological Survey.

Barlow, J. R., & Clark, B. R. (2011). *Simulation of Water-Use Conservation Scenarios for the Mississippi Delta Using an Existing Regional Groundwater Flow Model.* Reston, VA: U.S. Geological Survey.

Barlow, P. M., & Harbaugh, A. W. (2006). USGS Directions in MODFLOW Development. *Groundwater*, 771-774 Vol. 44 No. 6.

Bouwer, H. (2002). Artifical recharge of groundwater: hydrogeology and engineering. *Hydrogeology Journal*, 121-142.

Clark, B. R., & Hart, R. M. (2009). *The Mississippi Embayment Regional Aquifer Study (MERAS): Documentation of a Groundwater-Flow Model Constructed to Assess Water Availability in the Mississippi Embayment.* Reston, VA: U.S. Geological Survey.

Clark, B. R., Hart, R. M., & Gurdak, J. J. (2011). *Groundwater Availability of the Mississippi Embayment.* Reston, VA: U.S. Geological Survey.

Cox, R. T., & Van Arsdale, R. B. (2002). The Mississippi Embayment, North America: a first order continental structure generated by the Cretaceous superplume mantle event. *Journal of Geodynamics*, 163-176 Vol. 34.

Fisk, H. N. (1951). Loess and Quaternary Geology of the Lower Mississippi Valley. *The Journal of Geology, Vol. 59, No. 4*, 333-356.

Freeze, A. (1971). Three-Dimensional, Transient, Saturated-Unsaturated Flow in a Groundwater Basin. *Water Resources Research*, 347-366 Vol. 7 No. 2.

Freeze, R. A., & Witherspoon, P. (1966). Theoretical Analysis of Regional Groundwater Flow: 1. Analytical and Numerical Solutions to the Mathematical Model. *Water Resources Research*, 641-656 Vol. 2 No. 4.

Freeze, R. A., & Witherspoon, P. (1967). Theoretical Analysis of Regional Groundwater Flow: 2. Effect of Water-Table Configuration and Subsurface Permeability Variation. *Water Resources Research*, 623-634 Vol. 3 No. 2.

Freeze, R. A., & Witherspoon, P. (1968). Theoretical Analysis of Regional Ground Water Flow 3. Quantitative Interpretations. *Water Resources Research*, 581-590 Vol. 4 No. 3.

Gelhar, L. W., & Wilson, J. L. (1974). Ground-Water Quality Modeling. *Ground water*, Vol 12 p. 399-408.

Harbaugh, A. W. (2005). *Modflow-2005, The U.S. Geological Survey Modular Ground-Water Model-the Ground-Water Flow Process.* Reston, VA: U.S. Geological Survey.

Hiscock, K., & Grischek, T. (2002). Attenuation of groundwater pollution by bank filtration. *Journal of Hydrology*, 139-144 Issue 266.

Maliva, R. G. (2014). Economics of Managed Aquifer Recharge. *Water*, 1257-1279.

Maupin, M. A., & Barber, N. L. (2005). *Estimated Withdrawals from Principal Aquifers in the United States, 2000.* Reston, VA: United States Geological Survey.

McDonald, M. G., & Harbaugh, A. W. (1984). *A Modular Three-Dimensional Finite-Difference Ground-Water Flow Model. Open-File Report 83-875.* Reston, VA: U.S. Geological Survey.

Prathapar, S., Dhar, S., Rao, G. T., & Maheshwari, B. (2015). Performance and impacts of managed aquifer recharge interventions for agricultural water security: A framework for evaluation. *Agricultural Water Management*, 165-175.

Renken, R. A. (1998). *Ground Water Atlas of the United States Segment 5.* Reston, VA: U.S. Geological Survey.

Slack, L. J., & Darden, D. (1991). *Summary of Aquifer Tests in Mississippi, June 1942 through May 1988.* Reston, VA: U.S. Geological Survey.

Sprenger, C., Hartog, N., Hernandez, M., Vilanova, E., Grutzmacher, G., Scheibler, F., & Hannappel, S. (2017). Inventory of managed aquifer recharge sites in Europe; historical development, current situation and perspectives. *Hydrogeology Journal*, 1909-1922.

Sumner, D., & Wasson, B. (1984). *Summary of Results of an Investigation to Define the Geohydrology and Simulate the Effects of Large Ground-Water Withdrawals on the Mississippi River Alluvial Aquifer in Northwestern Mississippi.* Reston, VA: U.S. Geological Survey.

Sumner, D., & Wasson, B. (1990). *Geohydrology and Simulated Effects of Large Ground-Water Withdrawals on the Mississippi River Alluvial Aquifer in Northwestern Mississippi.* Washington, D.C.: United States Government Printing Office.

Toth, J. (1970). A Conceptual Model of the Groundwater Regime and the Hydrogeologic Environment. *Journal of Hydrology*, 164-176 Vol. 10.

VITA

Wesley Bluvstein previously graduated from Westerville South High School in Westerville, Ohio, in 2009. In May of 2013, he graduated from Tulane University after studying Geology and Environmental Science. Following a professional career in the petroleum industry and working as a hydrogeologic consultant, he was admitted to the University of Mississippi graduate program in Geological Engineering in 2017. He studied under Robert Holt and served as a Teaching Assistant in both classroom and field settings.